$2 (m_1 x)$

NGL 19-001-024

LUMPED PARAMETER ANALYSIS OF A STRINGER REINFORCED PLATE EXCITED BY BAND LIMITED NOISE

Dennis J. Bilyeu
Gerald D. Whitehouse
Charles A. Whitehurst

Louisiana State University
Division of Engineering Research
Baton Rouge, Louisiana 70803

November 1972

Contractor Report

TABLE OF CONTENTS

LIST OF TABLES

LIST OF FIGURES (Continued)

LIST OF SYMBOLS

SYMBOL	UNITS	DESCRIPTION
T	Inch-pounds force	Kinetic energy
U	Inch-pounds force	Potential energy
D	Inch-pounds force	Dissipated energy
W	Inch-pounds force	Work done
m_i	Pounds mass $= \dfrac{\text{pounds force}}{386.4}$	Lumped mass at location i
K_{ij}	Pounds force/inch	The i, j component of the spring stiffness matrix
C_{ij}	Pounds force-second/inch	The i, j component of the damping matrix
F_j	Pounds force	Force applied to the ith mass
$\dot{x}_k$	Inches	Displacement of the ith mass
X_k	Inches	Displacement of the kth mode in the normalized coordinate system
t	Seconds	time
V_{ij}	Dimensionless	Component of the eigenvector associated with the ith mass in the jth mode
ω_k	Radians/second	Eigenvalue of the kth mode
ω	Radians/second	Frequency of vibration
Z_k	Dimensionless	Damping ratio in the kth mode

SYMBOLS	UNITS	DESCRIPTION
ω_d	Radians/second	Damped natural frequency = $\omega_k\sqrt{1 - z_k^2}$
δ_k	Dimensionless	$z_k/\sqrt{1 - z_k^2}$
τ	Seconds	$t_2 - t_1$
$R_{xx}(t_1, t_2)$	Same as x^2	Autocorrelation function = $E[x(t_1) \; x(t_2)]$
$E[x(t)]$	Same as x	Expected value (mean value) of $x(t)$
Φ_{xx}	$\dfrac{\text{(Units of } x)^2}{\text{Radians/second}}$	Power spectral density of $x(t)$
Φ_{FF}	$\dfrac{\text{(Units of } F)^2}{\text{Radians/second}}$	Power spectral density of $F(t)$
$H(\omega)$	Inches/pound force	Transfer function
F_k	Pounds force	$\sum\limits_{i=1}^{N} F_i V_{ik}$
F_{ko}	Pounds force	Initial magnitude of F_k
X_{ko}	Inches	Initial magnitude of X_k
a_k	Dimensionless	Modal participation factor of kth mode
A_j	Inches^2	Area of excitation for j^{th} mass
P	Pounds force/inch^2	Uniform excitation pressure
$\bar{x}^2$	(Inches)^2	Mean square value of displacement
A	(Inches)^2	Total surface area

SYMBOLS	UNITS	DESCRIPTION
$J_{rs\tau}$	Dimensionless	Joint acceptance of the pressure field
α_r, α_s	Dimensionless	Normal mode amplitudes
r, r	Inches	Coordinates of a point on the structure
r_1, r_2	Inches	Coordinates of the response point
ρ_1, ρ_2	Inches	Coordinates of the excitation point
H	$\dfrac{\text{seconds}^2}{\text{Pound mass (radians)}^2}$	Transfer function
H^*	$\dfrac{\text{seconds}^2}{\text{Pound mass (radians)}^2}$	Complex conjugate of H
ω_c	Radians/second	Upper cut-off frequency of the excitation
ω_n	Radians/second	Natural frequency
M_k	Pounds mass	$\sum\limits_{i=1}^{N} m_i V_{ik}^2$
C_k	Pound force-Second/inch	$\sum\limits_{i=1}^{N} \sum\limits_{j=1}^{N} C_{ij} V_{ik} V_{jk}$
K_k	Pounds force/inch	$\sum\limits_{i=1}^{N} \sum\limits_{j=1}^{N} K_{ij} V_{ik} V_{jk}$
$\bar{A}_k$	Inches^2	$\sum\limits_{j=1}^{N} A_j V_{jk}$

1. INTRODUCTION

Many engineers have been focusing their attention in the past few years on the problems encountered when a random force is applied to structural materials. The advent of these problems was brought about by the development of jet engines for aircraft and rocket engines for spacecraft. It was found that the panels in the fuselage and wing structures of aircraft in the vicinity of the jet engines fail due to the random acoustical excitation they receive from the jet engine noise. A similar situation exists in the neighborhood of the nozzles on rockets engines. The basic reason this random excitation is so damaging is that it excites materials at all frequencies over the frequency range (bandwidth) of its power spectrum. If a natural frequency of the structure happens to exist in the bandwidth and the structure itself dissipates little or no energy (light damping), the resulting amplitude of vibration would become very large and failure should occur in a reasonably short time.

This type of response occurs in lightly damped systems because the system behaves as a narrow-band filter and absorbs energy primarily at its own natural frequency; this absorption of energy is in phase with the vibration of the system, causing the amplitude of vibration to increase with each successive cycle of vibration. The amplitude of a system with zero damping will tend to increase without bound; the amplitude of systems with damping will tend to increase until it reaches the limiting amplitude defined by the parameters of the system, the limiting amplitude being larger with the lesser amount of damping.

The stringer reinforced plate shown in Figure 1 is a configuration commonly found in aircraft, spaceships, and many other structures. The plate and each of the inner panel areas are square with the outer edges of the plate assumed to be fixed. The stringer reinforcements are an integral part of the plate, the panel areas being created by milling the plate into its present configuration from one sheet of metal (aluminum). The fixed edge condition was imposed by bolting an angle

1
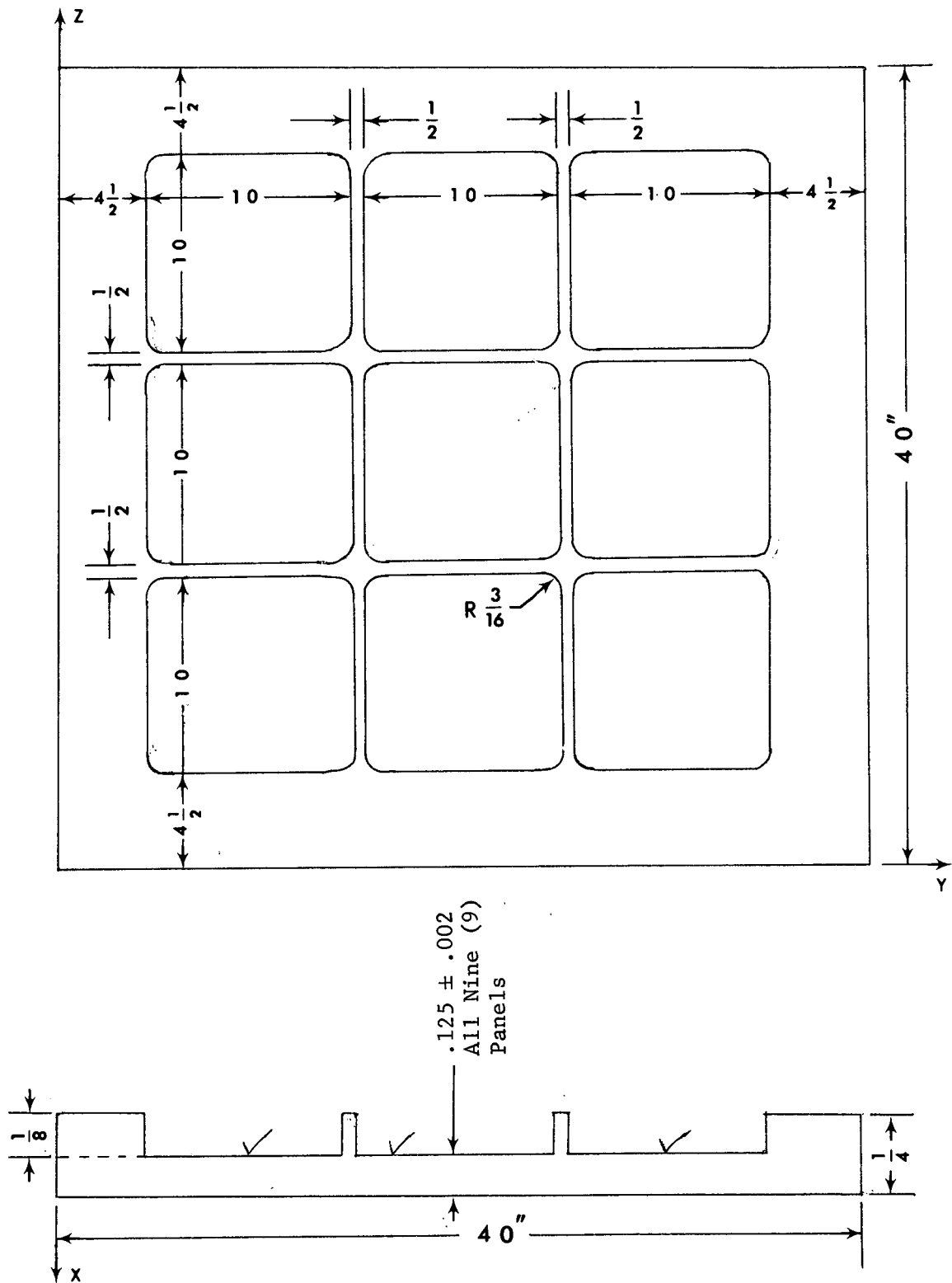
FIGURE 1: Geometric Representation of Test Plate

iron frame to the outer four inches of the plate and connecting the top and bottom frames with plates bolted into the frames. The latter plates were used to support the system during testing.

The problem is: given this plate and this excitation (Figure 2), predict the response of the plate. The problem is solved in two parts: a mathematical model using a lumped parameter analysis; and an experimental test on the particular plate shown in Figure 1.

It was decided that the form of the response should be the response power spectral density and the maximum root mean square displacements of the plate. The plate was excited by a large exponential horn measuring twelve feet square at its mouth and producing a wave front which was approximately plane with normal incidence to the plate and perfectly correlated in the horizontal and vertical directions. The random excitation was band limited from 25 to 500 Hz. This bandwidth contains all the frequencies of interest for this particular problem and allows the attaining of a much higher root mean square power level than that attained by a wider bandwidth. A root mean square square power level of approximately 149 decibels referenced to .0002 bars was attained by the horn. Figure 2 shows the power spectral density of the acoustical force exciting the plate.

FIGURE 2.
EXCITATION POWER SPECTRAL DENSITY
OF THE RANDOM PRESSURE FIELD
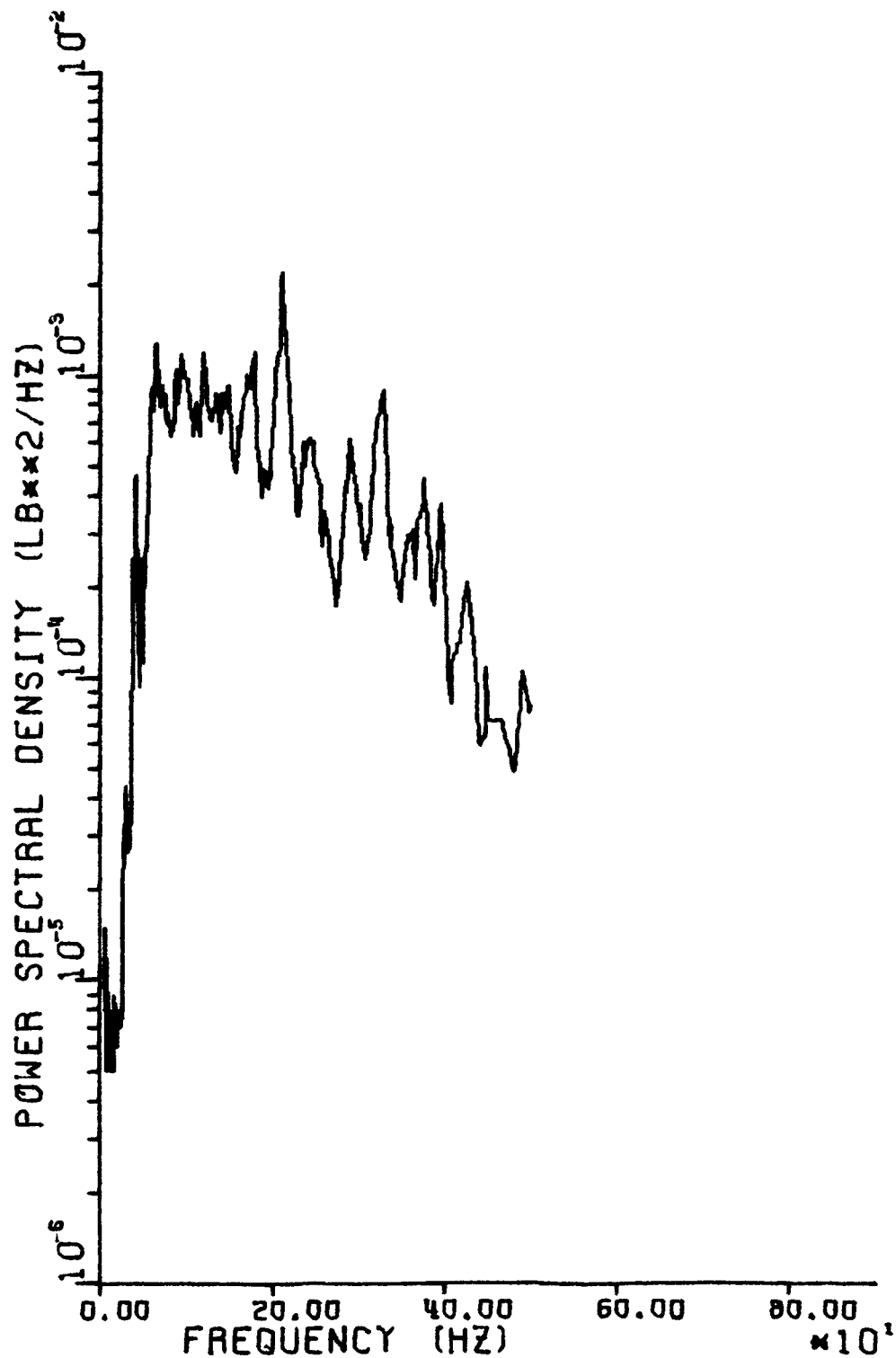
2. PREVIOUS WORK

The purpose of this section is to give credit to the authors whose work was utilized as a guide in performing this investigation. The two common methods of analysis in this type of investigation are the normal mode lumped parameter analysis and the transfer matrix technique, previously known as the Holzer-Myklestad method. Although extensive literature related to this problem was surveyed, the scope of this section is limited to the particular investigations which are similar to this investigation. These particular investigations are also selected because of their practicality.

The normal mode approach in the study of the response of continuous structures under random loading began with the work by Van Lear and Uhlenbeck (1) in 1931. Recent authors using this approach includes Miles in 1954 (14), Lyon in 1956 (2), Eringen in 1957 (3), Thompson and Barton in 1957 (4), Powell in 1958 (5), Samuels in 1958 (6), Dyer in 1958, 1959 (7), (8), Bagdanoff and Goldberg in 1960 (9), Lin in 1963-1965 (10), (11), (26), Barnoski in 1967 (12), and Seireg in 1969 (13).

The work of Miles (14), Powell (5), and Lin (10), (11), (26) is the basis for the lumped parameter analysis performed by Barnoski (12) and Seireg (13). The particular method developed by Seireg is most like the analysis used in this investigation.

In the initial work in this area, Miles (14) assumed that the response of a panel is dominated by one (fundamental) mode. Consequently, he also assumed that the system can be represented by an oscillator with a single degree of freedom. His assumption leads to a simple expression for the output power spectrum of the panel response:

$$\Phi_{xx}(\omega) = |H(\omega)|^2 \Phi_{FF}(\omega) \qquad (2\text{-}1)$$

where Φ_{FF} is the input power spectrum and H is the transfer function. Substituting this expression into the standard mean square value equation,

5

$$\overline{x}^2 = \int_0^\infty \Phi_{xx}(\omega) \, d\omega \qquad (2\text{-}2)$$

one obtains the mean square value of the response. Miles considered only an excitation pressure which is uniformly distributed over the panel in order that the assumption of fundamental-mode predominancy would hold. If the pressure is not uniformly distributed, a more general investigation is warranted. The work by Miles, later extended by Powell (5), was eventually utilized to evaluate the response of aircraft panels to jet-engine noise. In many respects this work is similar to the analysis used in this investigation.

Powell (5) extended Miles' work to consider several modes of vibration and obtained a general expression for the output power spectrum:

$$\Phi_{xx}(\omega) = \sum_r \sum_s |H_r(\omega)| \cdot |H_s(\omega)| \quad \Phi_{FF_0}(\omega) A^2 \, J_{rs_T}^2 \qquad (2\text{-}3)$$

where, Φ_{FF_0} = excitation power spectrum at a reference point

A = overall area of the structure

J_{rs_T} = joint acceptance of the pressure field

$$J_{rs_T} = \frac{1}{A^2} \int_A R_{FF}(\omega; r, r' : T) \, \alpha_r(r) \, \alpha_s(r') \, dr dr' \qquad (2\text{-}4)$$

where α_r and α_s = normal mode amplitudes

r, r' = coordinates of a point on the structure

$dr dr'$ = differential area

R_{FF} = autocorrelation function of the excitation pressure

T = difference in response lags for two modes, r and s when excited at frequency ω.

Lin (10) (11) (26) later simplified Powell's results for the case of light damping and well separated resonant frequencies to

6

$$\Phi_{xx}(\omega) = \sum_r |H_r(\omega)|^2 \; \Phi_{FF_o}(\omega) A^2 \; J_{rr}^2(\omega) \qquad (2\text{-}5)$$

Lin (11) eventually derived what is considered the most general form of the normal mode approach to determining the response of a linear continuous structure subjected to a random pressure. He also proved that the general results (Equation 2-3) arrived at by Powell can be deduced from a more general equation (2-6) by assuming the excitation pressure field to be weakly stationary.

$$\Phi_{xx}(r_1,r_2;\omega) = \int_A \Phi_{FF}(\rho_1,\rho_2;\omega) \; H(r_1,\rho_1;\omega) \; H^*(r_2,\rho_2;\omega) d\rho_1 d\rho_2 \qquad (2\text{-}6)$$

where r_1,r_2 = coordinates of the response point

ρ_1,ρ_2 = coordinates of the excitation pressure

H^* = complex conjugate of H

Barnoski (12) applied the results determined by Lin (11) with the help of work by Crandall (28) and Roberts (29) to predict the mean square displacements and velocity response of rectangular plates subjected to a random excitation. Barnoski developed two dimensionless coefficients, I and II, whose values, ranging from zero to one, are to be multiplied respectively by the results of Lin for the root mean square displacement and velocity. These coefficients are determined by the particular damping ratio (Z) of the system and the ratio of the cut-off frequency (upper bandwidth limit) (ω_c) of the input spectrum to the natural frequency of the system (ω_n). For damping ratios (Z) less than 0.01, both the dimensionless coefficients I and II are nearly zero; for ω_c/ω_n somewhat less than one. They rapidly approach unity as ω_c/ω_n approaches infinity. Barnoski's results converge to the results given by Lin (11) for an excitation spectrum with a cut-off frequency which encompasses the natural frequencies of the system.

Seireg and Howard (30) developed an approximate normal mode method of analysis which permits any linear non-conservative system to be

7

solved by superposition of uncoupled coordinates. The normal mode method does not generally apply to damped systems. Only a particular class of damped systems, originally defined by Rayleigh (31) and later generalized by Caughey (32), can be uncoupled by the same transforformation which uncouples conservative systems. Foss (33) and O'Kelly (34) later described the complex transformations that are required to uncouple certain damped systems. These results, although technically uncoupled, are so complicated that the primary objective of using normal modes is defeated.

Seireg and Howard (30) developed an approximate method which allows any lumped parameter linear system subjected to an arbitrary forcing function to be approximately represented by equations uncoupled by the same transformation which uncouple the conservative systems. Their method utilizes experimental response curves determined by exciting the systems with pure tones. These response curves are utilized to determine the damping ratios (Z_{ik}) as described by Bruel and Kjaer (17). The amplitude ratios at each natural frequency are used to approximate the eigenvectors of the system. Knowing the relation between the eigenvectors (V_{ik}) and the modal participation factors (a_k) to be by definition,

$$\sum_k V_{ik} a_k = 1 \qquad (2\text{-}7)$$

the system of simultaneous equations may be solved for the modal participation factors a_k. The single-resonance assumption that the nonresonant components of the damping are to have negligible effect at the natural frequencies, produce what are called the fictitious damping ratios (ξ_{ik}). They are defined by,

$$\xi_{ik} = \frac{V_{ik} a_k}{Z_{ik}} \qquad (2\text{-}8)$$

These fictitious damping ratios are used to evaluate the fictitious displacements in each mode of vibration. The summation of the independent modal displacements produces the total displacement at each point on the plate. The fictitious damping ratios reduce to modal damping ratios

when the damping of the system is small. This method produces resulting displacements which vary from the expected values by less than ten per cent when the damping ratio is less than 0.10.

The method of analysis utilized in this investigation is similar to that used by Seireg and Howard (30). The essential difference is that the damping ratios in this investigation are sufficiently small (Figure 21) to justify utilizing modal damping ratios rather than fictitious damping ratios. In this investigation, the eigenvectors, eigenvalues, and modal participation factors are determined analytically rather than by the use of the experimental data.

The method of transfer matrices described by Lin (11), (26), McDaniel and Donaldson (27) is also a method of analysis for plates subjected to a random excitation. Dokanish (35) later expanded the transfer matrix method by combining it with the finite element technique. The general technique for applying this method of analysis is to assume the plate is composed of several rows of panels; each row of panels is assumed to be separated by inflexible stringers. The panels in each row are separated by flexible stringers which are perpendicular to the inflexible stringers. The response of this system is assumed to be harmonic in the direction normal to the inflexible stringers and to be random in the direction parallel to the inflexible stringer. Each panel may then be subdivided into strips which have their edges parallel to the stringers. The stiffness and mass matrices for each strip are then calculated. The equilibrium equations are determined to obtain the relation between the right and left edges of each strip. Requirements of displacement continuity and force equilibrium at the edges common to two adjacent strips gives the transfer matrix relation. Successive matrix multiplication finally relates the variables of the left and right boundary of each panel and eventually of the entire plate. Boundary conditions require the determinant of a portion of the overall transfer matrix to vanish at the natural frequencies of the system. By substituting values of frequency until the determinant vanishes, the natural frequencies are determined. The method also produces the mode shapes

of the system.

Another method of analyzing the random response of plates in the utilization of an analog computer to model and solve the problem. Murphy and Swift (37) and Barnoski (12) are some of the authors who have utilized this method of analysis. Through the use of analog computers and control system techniques, a deterministic function is generated which has the correct statistical properties of the random excitation. This function is used to solve in a deterministic fashion for the response, which is described statistically in terms of displacement of stress.

For this method of analysis the kinetic and strain energies are calculated and the equations of motion are derived by using Lagrange's equation. A gaussian noise generator supplies the "white noise" which is passed through additional shaping filters to produce voltates which have the statistical representation of the forcing function. The differential equations are then solved by the analog computer.

The selected investigations discussed in this section indicate that a great deal of work has been done on this problem. The primary development in this area has been in the realm of analysis. Although more work needs to be done analytically, the primary concern now is to develop techniques applicable to practical structures. With all the analytical work accomplished, very little experimental work has been performed to verify the results of the analyses. A spectacular example of the additional work needed in this area is the unexpected fatigue cracks which developed on the Air Force's huge C5-A transport aircraft. These cracks are believed to be caused by the same type of random excitation which is the motivation of this investigation. Although this problem originated with modern flight vehicle structures excited by jet or rocket engine noise, it has been found to apply to many other systems.

10

3. ANALYTICAL EQUATIONS OF MOTION

This section covers a derivation for the mean square response of the panel structure by using an approximate normal-mode method for a damped, lumped parameter system. A scaled drawing of the actual plate is shown in Figure 1. This structure is represented by the lumped mass system shown in Figure 3. The displacements of the masses, $x(I)$, $I = 1, 2, 3, \ldots, 14$, are perpendicular to the plane of the plate and referenced to inertial coordinates. Energy expressions for the system are:

$$\text{Kinetic energy} = T = \tfrac{1}{2} \sum_{i=1}^{N} m_i \, \dot{x}_i^2$$

$$\text{Potential energy} = U = \tfrac{1}{2} \sum_{i=1}^{N} \sum_{j=1}^{N} K_{ij} \, x_i \, x_j$$

$$\text{Dissipated energy} = D = \tfrac{1}{2} \sum_{i=1}^{N} \sum_{j=1}^{N} C_{ij} \, \dot{x}_i \, \dot{x}_j$$

$$\text{Work done} = W = \sum_{i=1}^{N} f_i \, x_i$$

Lagrange's equation in normalized coordinates for a multidegree of freedom system can be written

$$\frac{d}{dt} \left(\frac{\partial T}{\partial \dot{X}_k} \right) - \frac{\partial T}{\partial X_k} + \frac{\partial U}{\partial X_k} + \frac{\partial D}{\partial \dot{X}_k} = \frac{\partial W}{\partial X_k} \tag{3-1}$$

where the coordinate transformation is defined as

$$x_i = \sum_{k=1}^{N} V_{ik} \, X_k$$

$$\dot{x}_i = \sum_{k=1}^{N} V_{ik} \, \dot{X}_k \tag{3-2}$$

11
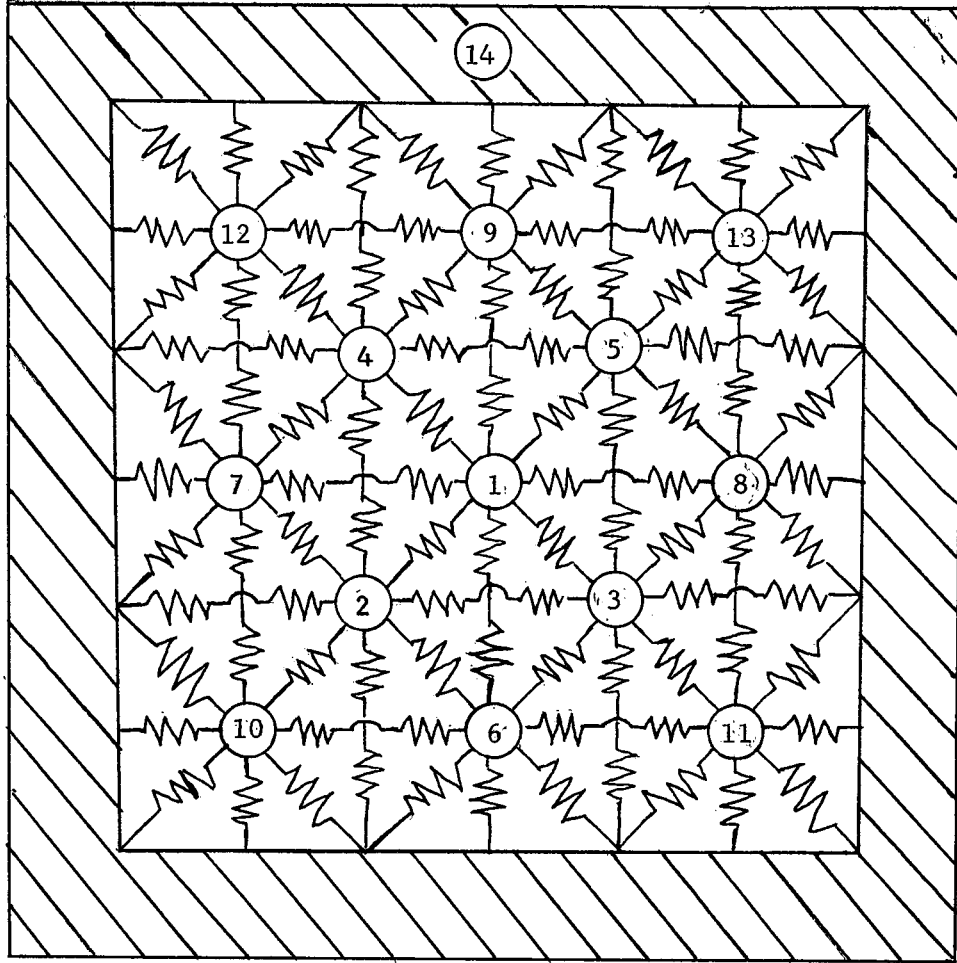
m_1 = .000791 m_6 = .000791 m_{11} = .000791

m_2 = .003022 m_7 = .000791 m_{12} = .000791

m_3 = .003022 m_8 = .000791 m_{13} = .000791

m_4 = .003022 m_9 = .000791 m_{14} = .595238

m_5 = .003022 m_{10} = .000791

FIGURE 3:   Lumped Mass Model of Test Plate

This transformation is necessary in order to uncouple the equations of motion for the system. It is shown in Appendix A that the V_{ik}'s necessary to perform this transformation are the eigenvectors which describe the normal modes of the free, undamped vibration system. The eigenvalues associated with each of the eigenvectors are the undamped natural frequencies of the system and can be obtained along with the eigenvectors by solving the differential equation of motion for the free undamped vibration system.

Substitution of the transformations into the work and energy terms, and utilization of the orthogonality relationship given below,

$$\sum_{i=1}^{N} m_i V_{ik} V_{im} = \begin{cases} 0, & \text{for } k \neq m \\ \\ \sum_{i=1}^{N} m_i V_{ik}^2, & \text{for } k = m \end{cases}$$

$$\sum_{i=1}^{N} \sum_{j=1}^{N} K_{ij} V_{ik} V_{jm} = \begin{cases} 0, & \text{for } k \neq m \\ \\ \sum_{i=1}^{N} \sum_{j=1}^{N} K_{ij} V_{ik} V_{jk}, & \text{for } k = m \end{cases}$$

with the frequency equation for the undamped free vibration system,

$$\sum_{i=1}^{N} \sum_{j=1}^{N} K_{ij} V_{ik} V_{jk} = \sum_{i=1}^{N} m_i V_{ik}^2 \omega_k^2$$

and making the substitutions,

$$\sum_{i=1}^{N} \sum_{j=1}^{N} K_{ij} V_{ik} V_{jk} = M_k \omega_k^2 \qquad (3\text{-}3)$$

13

$$M_k = \sum_{i=1}^{N} m_i \, V_{ik}^2$$

$$K_k = \sum_{i=1}^{N} \sum_{j=1}^{N} K_{ij} \, V_{ik} \, V_{jk} \qquad\qquad (3\text{-}3a)$$

$$C_k = \sum_{i=1}^{N} \sum_{j=1}^{N} C_{ij} \, V_{ik} \, V_{jk}$$

one obtains:

$$T = \tfrac{1}{2} \sum_{i=1}^{N} \sum_{k=1}^{N} m_i \, V_{ik} \, V_k \, \dot{X}_k^2 = \tfrac{1}{2} \sum_{k=1}^{N} M_k \, \dot{X}_k^2$$

$$U = \tfrac{1}{2} \sum_{k=1}^{N} \sum_{i=1}^{N} \sum_{j=1}^{N} K_{ij} \, V_{ik} \, V_{jk} \, X_k \, X_k = \tfrac{1}{2} \sum_{k=1}^{N} M_k \, \omega_k^2 \, X_k^2$$

$$D = \tfrac{1}{2} \sum_{k=1}^{N} \sum_{i=1}^{N} \sum_{j=1}^{N} C_{ij} \, V_{ik} \, V_{jk} \, \dot{X}_k \, \dot{X}_k = \tfrac{1}{2} \sum_{k=1}^{N} \sum_{i=1}^{N} \sum_{j=1}^{N} C_{ij} \, V_{ik} \, V_{jk} \, \dot{X}_k^2$$

By substitution of these relations into Lagrange's equation, the following set of equations are obtained:

$$\ddot{X}_k + \omega_k^2 \, X_k + \frac{C_k}{M_k} \, \dot{X}_k = \frac{F_k}{M_k} \qquad\qquad (3\text{-}4)$$

where

$$F_k = \sum_{i=1}^{N} f_i \, V_{ik} \qquad\qquad (3\text{-}4a)$$

Equation 3-4 is converted to the form which represents uniform

14

viscous damping by using Equation 3-3.

$$\ddot{X}_k + \omega_k^2 X_k + \frac{C_k}{K_k} \omega_k^2 \dot{X}_k = \frac{F_k}{M_k} \qquad (3-5)$$

If C_k/K_k is constant for each value of K_k in Equation 3-5, the system has uniform viscous damping. This is a good approximation for systems in which the damping is an inherent property of the spring material (13). Since the physical structure utilized in the experimental work was constructed of aluminum and the inherent damping of the aluminum was the only damping considered, the above assumption of C_k/K_k equal to a constant is valid for this system. It is shown below that this constant C_k/K_k equals $2Z_k/\omega_k$, where Z_k is the modal damping ratio.

By definition

$$Cc_k = 2\sqrt{K_k M_k} \quad , \text{ critical damping coefficient}$$

$$Z_k = \frac{C_k}{Cc_k}$$

$$\omega_k = \sqrt{\frac{K_k}{M_k}}$$

Substituting into the above expression, one obtains

$$\frac{C_k}{K_k} = \frac{Z_k Cc_k}{\omega_k^2 M_k}$$

$$\frac{C_k}{K_k} = \frac{2Z_k \sqrt{K_k M_k}}{\omega_k^2 M_k}$$

$$\frac{C_k}{K_k} = \frac{2Z_k \omega_k}{\omega_k^2}$$

$$\frac{C_k}{K_k} = \frac{2Z_k}{\omega_k}$$

Equation 3-5 with the above substitutions now becomes

$$\ddot{X}_k + \omega_k^2 X_k + 2Z_k \omega_k \dot{X}_k = \frac{F_k}{M_k} \qquad (3\text{-}6)$$

The solution of Equation 3-6 may be determined by the well-known method of convolution (13) to be

$$X_k = \frac{1}{M_k \omega_d} \int_0^\infty F_k(\tau) \exp\left[-\zeta_k \omega_d (t-\tau)\right] \sin \omega_d(t-\tau) \ d\tau \qquad (3\text{-}7)$$

where

$$\omega_d = \omega_k \sqrt{1 - z_k^2}$$

$$\zeta_k = z_k \Big/ \sqrt{1 - z_k^2}$$

$$t = \text{time}$$

$$\tau = t_2 - t_1$$

Since a function to adequately represent the forcing function $F_k(\tau)$ cannot be written explicitly, a probabilistic representation must be utilized. This representation essentially transforms the deterministic problem from an explicit forcing function and a resulting definite value for the response to the probabilistic problem with the input forcing function given as a power spectral density and the output, as the mean square value of the response.

It is assumed that the excitation is at least weakly stationary, which defines its expected value (mean value) to be a constant and its

autocorrelation function to depend only on $\tau = t_2 - t$. The auto-correlation, R_{xx}, is defined by

$$R_{xx}(t_1, t_2) = E\left[x(t_1) \, x(t_2)\right]$$

where the E denotes expected value.

$$E[x] = \int_{-\infty}^{\infty} x \, f_x(x) \, dx$$

where $f_x(x)$ is the probability density function. In equation form, the above definition of a weakly stationary force F is

$$E\left[F(t)\right] = \text{constant}$$

$$R_{FF}(t_1, t_2) = R_{FF}(t_2 - t_1) = R_{FF}(\tau)$$

From the statistical analysis of the actual random excitation that was used as an input to the structure, it was found that the excitation was indeed weakly stationary (Section 6). The response to a weakly stationary excitation is nonstationary for small values of time (t). The response becomes weakly stationary after the system has been exposed to the weakly stationary excitation for a sufficiently long period of time. Lin (11) states, for example, that a sufficiently long period of time is four natural periods if the damping ratio $Z = 0.1$, or about twenty natural periods if $Z = 0.02$. These times are required for the effects of configuration of the system at $t = 0$ and the resultant transient response to die out. The resulting weakly stationary response is analogous to the steady-state response in the deterministic vibration theory.

The power spectral density $\left(\Phi_{xx}\right)$ is defined as the Fourier transform of the autocorrelation function $\left(R_{xx}\right)$ of the weakly stationary random variable $\left(x(t)\right)$

$$\Phi_{xx}(\omega) = \frac{1}{2\pi} \int_{-\infty}^{\infty} R_{xx}(\tau) \, \exp\left(-i\omega\tau\right) d\tau$$

The inversion formula can also be written as

$$R_{xx}(\tau) = \int_{-\infty}^{\infty} \Phi_{xx}(\omega) \exp(-i\omega\tau) d\omega$$

where, i, as used in the exponential term here and in the appropriate equations to follow, is equal to $\sqrt{-1}$.

The significance of this expression is apparent where τ is allowed to approach zero for large values of time (t).

$$R_{xx}(0) = \int_{-\infty}^{\infty} \Phi_{xx}(\omega) d\omega$$

$$R_{xx}(0) = E\Big[x(t_1), x(t_1)\Big] = E\Big[x^2(t_1)\Big] = \bar{x}^2(t)$$

$$\bar{x}^2(t) = \int_{-\infty}^{\infty} \Phi_{xx}(\omega) d\omega \qquad (3-8)$$

This last equation equates the mean-square response to the integral of the response spectral density. From the work done by Lin (11), the relationship between the spectral densities of the excitation and the response is obtained.

$$\Phi_{xx}(\omega) = \Phi_{FF}(\omega) |H(\omega)|^2 \qquad (3-9)$$

Substituting Equation 3-9 into Equation 3-8, one obtains

$$\bar{x}^2(t) = \int_{-\infty}^{\infty} \Phi_{FF}(\omega) |H(\omega)|^2 d\omega \qquad (3-10)$$

The analysis will be accomplished in two parts: one, assuming that the power spectral density is a constant; and two, assuming that it is not a constant. The results of these two parts will be compared in Section 6.

If the spectral density of the excitation changes very slowly in the vicinity of the natural frequency of the system, it can be assumed that this spectral density is a constant for all values of frequency and that the value of the constant is the value of the spectral density

18

evaluated at the natural frequency. This implies that $\Phi_{FF}(\omega)$ is a constant and is equal to $\Phi_{FF}(\omega_k)$.

$$\overline{x}^2(t) = \Phi_{FF}(\omega_k) \int_{-\infty}^{\infty} |H(\omega)|^2 \, d\omega$$

The transfer function $H(\omega)$ is determined by exciting the system with a sinusoidial forcing function f and arranging the resulting response x in the form

$$x_i(t) = H(\omega) \, f_i(t)$$

Utilizing Equation 3-6

$$\ddot{X}_k + 2Z_k \, \omega_k \, \dot{X}_k + \omega_k^2 \, X_k = \frac{F_k}{M_k}$$

where

$$F_k = F_{ko} \, \exp(i\omega t)$$

and X_k is assumed to be

$$X_k = X_{ko} \, \exp(i\omega t)$$

$$\dot{X}_k = X_{ko} \, \exp(i\omega t) \, (i\omega)$$

$$\ddot{X}_k = X_{ko} \, \exp(i\omega t) \, (i\omega)^2 = -\omega^2 \, X_{ko} \, \exp(i\omega t)$$

Equation 3-6 then becomes

$$-X_{ko} \, \omega^2 \, \exp(i\omega t) + 2Z_k \omega_k \, X_{ko}(i\omega) \, \exp(i\omega t)$$

$$+ \omega_k^2 \, X_{ko} \, \exp(i\omega t) = \frac{F_{ko}}{M_k} \, \exp(i\omega t)$$

$$X_{ko} \, (\omega_k^2 - \omega^2 + 2i \, Z_k \, \omega_k \, \omega) = \frac{F_{ko}}{M_k}$$

$$X_{ko} = \frac{F_{ko}}{M_k \left[\omega_k^2 - \omega^2 + 2i \, Z_k \, \omega_k \, \omega \right]}$$

$$X_k = \frac{F_{ko} \exp(i\omega t)}{M_k \left[\omega_k^2 - \omega^2 + 2i\, Z_k\, \omega_k\, \omega\right]} = \frac{F_k}{M_k \left[\omega_k^2 - \omega^2 + 2i\% Z_k\, \omega_k\, \omega\right]}$$

Substituting X_k into Equation 3-2 and substituting Equation 3-3a and 3-4a into the resulting equation, one obtains

$$x_i = \sum_{k=1}^{N} \frac{V_{ik} \sum\limits_{j=1}^{N} f_j\, V_{jk}}{\sum\limits_{j=1}^{N} m_j\, V_{jk}^2 \left[\omega_k^2 - \omega^2 + 2i\, Z_k\, \omega_k\, \omega\right]}$$

$$x_i = \sum_{k=1}^{N} \frac{1}{\sum\limits_{j=1}^{N} m_j\, V_{jk}^2} \cdot \frac{V_{ik} \sum\limits_{j=1}^{N} P\, A_j\, V_{jk}}{\left[\omega_k^2 - \omega^2 + 2i\, Z_k\, \omega_k\, \omega\right]}$$

Define

$$a_k = \frac{1}{\sum\limits_{j=1}^{N} m_j\, V_{jk}^2}$$

(3-11)

$$\sum_{j=1}^{N} f_j\, V_{jk} = \sum_{j=1}^{N} P\, A_j\, V_{jk} = P \sum_{j=1}^{N} A_j\, V_{jk} = P\, \overline{A}_k$$

where   P = uniform pressure applied to all masses

A_j = area of each mass

$$\overline{A}_k = \sum_{j=1}^{N} A_j\, V_{jk}$$

$$x_i = \sum_{k=1}^{N} \frac{a_k\, V_{ik}\, \overline{A}_k}{\left[\omega_k^2 - \omega^2 + 2i\, Z_k\, \omega_k\, \omega\right]}\, P$$

20

It can now be seen that $H(\omega)$ is determined to be

$$H(\omega) = \sum_{k=1}^{N} \frac{a_k \, V_{ik} \, \overline{A}_k}{\omega_k^2 \left[1 - \dfrac{\omega^2}{\omega^2} + 2i \, Z_k \dfrac{\omega}{\omega_k} \right]}$$

$$\left| H(\omega) \right|^2 = \sum_{k=1}^{N} \frac{a_k^2 \, V_{ik}^2 \, \overline{A}_k^2}{\omega_k^4 \left[\left(1 - \dfrac{\omega^2}{\omega_k^2} \right)^2 + \left(2Z_k \dfrac{\omega}{\omega_k} \right)^2 \right]}$$

Substituting $\left| H(\omega) \right|^2$ into Equation 3-10, one obtains the general equation for the steady-state mean-square response at the ith location for a lumped parameter system.

$$\overline{x}_i^2(t) = \sum_{k=1}^{N} \int_{-\infty}^{\infty} \Phi_{FF}(\omega) \; \frac{a_k^2 \, V_{ik}^2 \, \overline{A}_k^2}{\omega_k^4 \left[\left(1 - \dfrac{\omega^2}{\omega_k^2} \right)^2 + \left(2Z_k \dfrac{\omega}{\omega_k} \right)^2 \right]} \; d\omega \qquad (3\text{-}12)$$

If the power spectral density can be assumed to be a constant with respect to frequency, Equation 3-12 becomes

$$\overline{x}_i^2(t) = \sum_{k=1}^{N} \Phi_{FF}(\omega) \int_{-\infty}^{\infty} \frac{a_k^2 \, V_{ik}^2 \, \overline{A}_k^2}{\omega_k^4 \left[\left(1 - \dfrac{\omega^2}{\omega_k^2} \right)^2 + \left(2Z_k \dfrac{\omega}{\omega_k} \right)^2 \right]} \; d\omega \qquad (3\text{-}13)$$

The integral in Equation 3-13 may be evaluated by the theorem of residues as given in references (11) and (15). (See Appendix B)

$$\int_{-\infty}^{\infty} \frac{a_k^2 \, V_{ik}^2 \, \overline{A}_k^2 \; d\omega}{\omega_k^4 \left[\left(1 - \dfrac{\omega^2}{\omega_k^2} \right)^2 + \left(2Z_k \dfrac{\omega}{\omega_k} \right)^2 \right]} = \frac{\pi a_k^2 \, V_{ik}^2 \, \overline{A}_k^2}{2Z_k \, \omega_k^3}$$

Considering only the physically realizable part of the frequency spectrum, the above equation becomes

$$\int_0^\infty \frac{a_k^2 \, V_{ik}^2 \, \overline{A}_k^2 \, d\omega}{\omega_k^4 \left[\left(1 - \frac{\omega^2}{\omega^2}\right)^2 + \left(2Z_k \frac{\omega}{\omega_k}\right)^2 \right]} = \frac{\pi a_k^2 \, V_{ik}^2 \, \overline{A}_k^2}{4Z_k \, \omega_k^3}$$

The integrated form of Equation 3-13 becomes

$$\overline{x}_i^2(t) = \sum_{k=1}^N \Phi_{FF}(\omega) \frac{\pi a_k^2 \, V_{ik}^2 \, \overline{A}_k^2}{4Z_k \, \omega_k^3} \qquad\qquad (3\text{-}14)$$

Utilizing Equation 3-14, one can obtain the steady state mean-square response for a system excited by a nearly constant random force. The random force in this case must be nearly constant in the neighborhood of the natural frequencies. If this latter condition is not met by the system being analyzed, Equation 3-12 must be utilized. In Section 4, the physical plate will be modeled in a lumped parameter format. The appropriate lumped parameter will be calculated and substituted into Equations 3-12 and 3-14 respectively. These two outputs will be compared with the intention of determining the error involved in assuming a constant power spectrum in the neighborhood of the natural frequencies for a particular input power spectrum.

4. LUMPED PARAMETER MODEL OF THE PLATE

In this section, the particular plate shown in Figure 1 will be
modeled as a lumped parameter system. The physical quantities such as
mass, damping, and stiffness will be lumped at fourteen different lo-
cations on the plate (Figure 3). The methods used to apportion values
for the lumped parameters will subsequently be discussed. Equations
3-12 and 3-14 will be evaluated using the derived values for the
lumped parameters will subsequently be discussed. Equations 3-12 and
3-14 will be evaluated using the derived values for the lumped para-
meters. The final results will be given in terms of the power spectral
density of the output response and the root mean square maximum dis-
placements at the fourteen locations and will be calculated by the two
analytical methods discussed in Section 3.

The experimental plate was square for fabrication convenience; how-
ever, the analysis is general for any plate configuration. Since the
plate was square, it would have been possible to model only one-eighth
of the plate and maintain geometrical symmetry and obtain the deflec-
tions of the remainder of the plate through geometrical considerations;
however, the small variations in the dimensions of the physical system
(plate plus frame) from the dimensions which would make the system per-
fectly symmetrical caused some concern as to how the response may be
affected, and accordingly, it was decided to model the entire plate and
structure.

The number and location of the lumped masses were arbitrary, but
once selected, became fixed and the distribution of the total mass to
each of the selected lumped mass points was determined by the rule of
pleasing proportions. This rule of pleasing proportions is based on
knowledge obtained from numerous lumped parameter investigations of
beam vibrations. One investigation (21) indicated that a beam which is
proportioned such that one-half the total mass is lumped at the center
and one-quarter at each of the ends, will produce analytical results
which compare very favorably with the predicted values for the natural

frequencies of the beam considering the beam as a continuous structure. The central area of the plate is partitioned into thirteen masses and a fourteenth mass is used to represent the outer edge of the plate and the fixed frame (Figure 3). Each of the nine panels (Figure 1) is proportioned such that half the mass of each panel is lumped at the panel's center and one-eighth of the mass lumped at each of the four outer edges of each panel. The masses lumped at the center of each panel are the ones shown in Figure 3 with the associated numbers: 1, 6, 7, 8, 9, 10, 11, 12, 13. The lumped masses numbered 2, 3, 4, and 5 in Figure 3 are comprised of the mass of the adjoining stringers and the edge mass of the adjoining panels. The edge mass of the panels which are in direct contact with the outer frame are lumped with the mass of the frame as the mass numbered 14 in Figure 3.

The influence coefficient matrix, which is the inverse of the stiffness matrix, for the fourteen mass system is determined by two methods. Analytically, the influence coefficients are determined by using Weaver's structural analysis programs named FR1 and FR3 (16). Experimentally, the influence coefficients are determined by measuring deflections of the lumped mass points with a dial indicator when loads are applied at the various mass points. Loads ranging from five to thirty pounds when required in increments of five pounds were applied at each point, and deflections at all mass points were measured for each of the applied loads (Table 1). The value of the influence coefficients are then determined by dividing the measured value of the deflections in inches by the applied load in pounds force. An average value over all the applied loads is then calculated for each lumped mass point. For

TABLE 2a

Loads (Pounds)	5	10	15	20
Deflections (Inches)	.007	.018	.028	.038

TABLE 1

Root Mean Square Amplitudes of Vibration (Inches)

Mass Points	Equation 3-14	Equation 3-12	Experimental	Error Between Exp. and Eq 3-12
1	.0340	.0175	.01418	23.2%
2	.0227	.0117	.00824	41.0%
3	.0255	.0131	.01097	19.1%
4	.0250	.0129	.01059	21.7%
5	.0248	.0128	.00915	39.1%
6	.0130	.0067	_*	
7	.0128	.0067	_	
8	.0134	.0069	_	
9	.0130	.0067	_	
10	.0057	.0029	_	
11	.0062	.0031	_	
12	.0056	.0029	_	
13	.0059	.0030	_	
14	.0000	.0000	_	

*Experimental Data not available

example, shown in Table 2a preceding are typical values of load and deflection at the center of the plate. These values are then used to fill the 14 x 14 matrix of influence coefficients. See Table 2.

In order to utilize FR1 and FR3 in determining the analytical coefficients, the plate is represented by a dense network of beams. These beams are represented in Figure 3 by the symbol for a spring ($-\wedge\!\!\wedge\!\!\wedge-$). The results indicate, as was expected, that the more dense the network of beams used to represent the plate, the better the correlation between the analytical and the experimentally measured values of the influence coefficients. Table 3 shows the analytically determined influence coefficients using the network of beams shown in Figure 3. This network of beams represents the most dense network of beams as applied to the solution of this problem, and Table 3 represents the best analytical approximation to the experimental data in Table 2. The effect on the natural frequencies of the system is the most important factor to be considered when analyzing the difference between the two sets of influence coefficients in Table 2 and Table 3. A comparison of the natural frequencies of the system when calculated by using the experimental and the analytical values of the influence coefficients is shown in Table 4. The final results presented in this investigation are the results determined by utilizing the experimentally measured values of the influence coefficients.

As mentioned in Section 3, the damping associated with this system is assumed to be an inherent property of the spring material, aluminum. In this investigation, the total damping of the system was measured indirectly from forced vibration traces and assumed to conform to the restrictions imposed upon the system in Section 3, particularly modal damping. This assumption proved to be valid for the particular system being modeled because of the relatively low values which were measured for the damping ratios (Figure 21). Authors Lin (11) and Seireg (13) give 0.04 as a sufficiently low value for the damping ratio in order order that this assumption be valid. Since all measured values of the damping ratios in the frequency range of interest are below the 0.04

26

TABLE 2

Experimental Influence Coefficients

Value Shown $\times 10^{-3} = A_{ij}$

(Inches/Pound)

A_{ij}	j=1	j=2	j=3	j=4	j=5	j=6	j=7	j=8	j=9	j=10	j=11	j=12	j=13	j=14
i=1	1.270	0.660	0.680	0.730	0.690	0.320	0.320	0.320	0.320	0.152	0.140	0.140	0.145	0.030
i=2	0.660	0.830	0.460	0.380	0.300	0.400	0.360	0.150	0.130	0.279	0.110	0.085	0.069	0.030
i=3	0.680	0.460	1.020	0.300	0.380	0.420	0.190	0.430	0.135	0.105	0.310	0.069	0.100	0.030
i=4	0.730	0.380	0.300	1.000	0.430	0.160	0.415	0.150	0.450	0.105	0.070	0.295	0.100	0.030
i=5	0.690	0.300	0.380	0.430	0.982	0.160	0.160	0.430	0.430	0.070	0.100	0.100	0.295	0.030
i=6	0.320	0.400	0.420	0.160	0.160	0.680	0.123	0.123	0.062	0.145	0.145	0.045	0.045	0.030
i=7	0.320	0.360	0.190	0.415	0.160	0.123	0.690	0.062	0.117	0.120	0.050	0.125	0.045	0.030
i=8	0.320	0.150	0.430	0.150	0.430	0.123	0.062	0.670	0.123	0.045	0.135	0.045	0.135	0.030
i=9	0.320	0.130	0.135	0.450	0.430	0.062	0.117	0.123	0.605	0.045	0.045	0.145	0.135	0.030
i=10	0.152	0.279	0.105	0.105	0.070	0.145	0.120	0.045	0.045	0.520	0.055	0.044	0.035	0.030
i=11	0.140	0.110	0.310	0.070	0.100	0.145	0.050	0.135	0.045	0.055	0.473	0.035	0.050	0.030
i=12	0.140	0.085	0.069	0.295	0.100	0.045	0.125	0.045	0.145	0.044	0.035	0.450	0.050	0.030
i=13	0.145	0.069	0.100	0.100	0.286	0.045	0.045	0.135	0.135	0.035	0.050	0.050	0.488	0.030
i=14	0.030	0.030	0.030	0.030	0.030	0.030	0.030	0.030	0.030	0.030	0.030	0.030	0.030	0.030

TABLE 3

Theoretical Influence Coefficients

Value Shown x10^{-3} = A$_{ij}$

(Inches/Pound)

A$_{ij}$	j=1	j=2	j=3	j=4	j=5	j=6	j=7	j=8	j=9	j=10	j=11	j=12	j=13	j=14
i=1	1.550	0.747	0.747	0.747	0.747	0.379	0.379	0.379	0.379	0.113	0.113	0.113	0.113	0.030
i=2	0.747	0.978	0.430	0.430	0.296	0.396	0.396	0.170	0.170	0.227	0.075	0.075	0.055	0.030
i=3	0.747	0.430	0.978	0.296	0.430	0.396	0.170	0.396	0.170	0.075	0.227	0.055	0.075	0.030
i=4	0.747	0.430	0.296	0.978	0.430	0.170	0.396	0.170	0.396	0.075	0.055	0.050	0.075	0.030
i=5	0.747	0.296	0.430	0.430	0.978	0.170	0.170	0.396	0.396	0.055	0.075	0.075	0.227	0.030
i=6	0.379	0.396	0.396	0.170	0.170	0.644	0.130	0.130	0.089	0.088	0.088	0.043	0.043	0.030
i=7	0.379	0.396	0.170	0.396	0.170	0.130	0.644	0.087	0.130	0.088	0.043	0.088	0.043	0.030
i=8	0.379	0.170	0.396	0.170	0.396	0.130	0.087	0.644	0.149	0.043	0.088	0.043	0.088	0.030
i=9	0.379	0.170	0.170	0.396	0.396	0.087	0.130	0.149	0.644	0.043	0.043	0.088	0.088	0.030
i=10	0.113	0.227	0.075	0.075	0.055	0.088	0.088	0.043	0.043	0.442	0.034	0.034	0.032	0.030
i=11	0.113	0.075	0.227	0.055	0.075	0.088	0.043	0.088	0.043	0.034	0.442	0.032	0.034	0.030
i=12	0.113	0.075	0.055	0.227	0.075	0.043	0.088	0.043	0.088	0.034	0.032	0.442	0.034	0.030
i=13	0.113	0.055	0.075	0.075	0.227	0.043	0.043	0.088	0.088	0.032	0.034	0.034	0.442	0.030
i=14	0.030	0.030	0.030	0.030	0.030	0.030	0.030	0.030	0.030	0.030	0.030	0.030	0.030	0.030

TABLE 4

NATURAL FREQUENCIES(HZ) DETERMINED BY USING
EXPERIMENTAL AND ANALYTICAL INFLUENCE COEFFICIENTS

EXPERIMENTAL	ANALYTICAL
36.7620544	36.7590637
60.7374878	59.8366852
100.591385	106.387955
111.057571	106.861526
138.671692	140.428879
253.736816	255.540680
256.553955	262.554687
280.063965	268.186768
293.056885	279.673096
298.084961	287.891357
310.320068	301.017578
313.791260	305.689697
322.051758	311.158936
438.847412	331.779785

value (Figure 21), the assumption is substantiated.

The damping ratios were determined from the typical experimental response curves shown in Figures 17, 18, 19, and 20. Actually, 19 curves were utilized in the investigation. The damping ratios were calculated at each natural frequency for each location on the plate. The curves showing the results of these calculations, Figure 21, indicate that the damping ratio is a function of frequency and not a strong function of location on the plate as noted by the relatively close grouping of the data points at each frequency. The particular values for the damping ratios (Z) at each frequency are determined by the functional relationship,

$$Z = \frac{\Delta f}{2f}$$

where f is the damped natural frequency or the value of the frequency associated with each major peak in the power spectral density plots. Δf is defined as the half power bandwidth or as the frequency range spanned by the response curve at the point on the curve which has half the power as does the peak value at the damped natural frequency (12), (17).

The particular shape of the excitation power spectral density with regard to the location in the frequency spectrum of the natural frequencies of the system will determine which equation, 3-12 or 3-14, should be used to calculate the root mean square response of the system (11). If the excitation power spectral density is constant over the range of frequencies spanned by the natural frequencies of the system, Equation 3-14 can be used; if the excitation power spectral density is anything other than a constant over the frequency range of interest, Equation 3-12 should be used to obtain best results. For camparison purposes, the excitation shown in Figure 2 is used as the input for both Equations 3-12 and 3-14. The resulting root mean square displacements are shown in Table 1, along with the corresponding values measured experimentally. In the course of evaluating Equation 3-12 the necessary

30

data for plotting the analytical power spectral density was calculated as described in the computer solution of the problem and eventually plotted (Figures 4 through 16).

FIGURE 4.
THEORETICAL RESPONSE POWER SPECTRAL
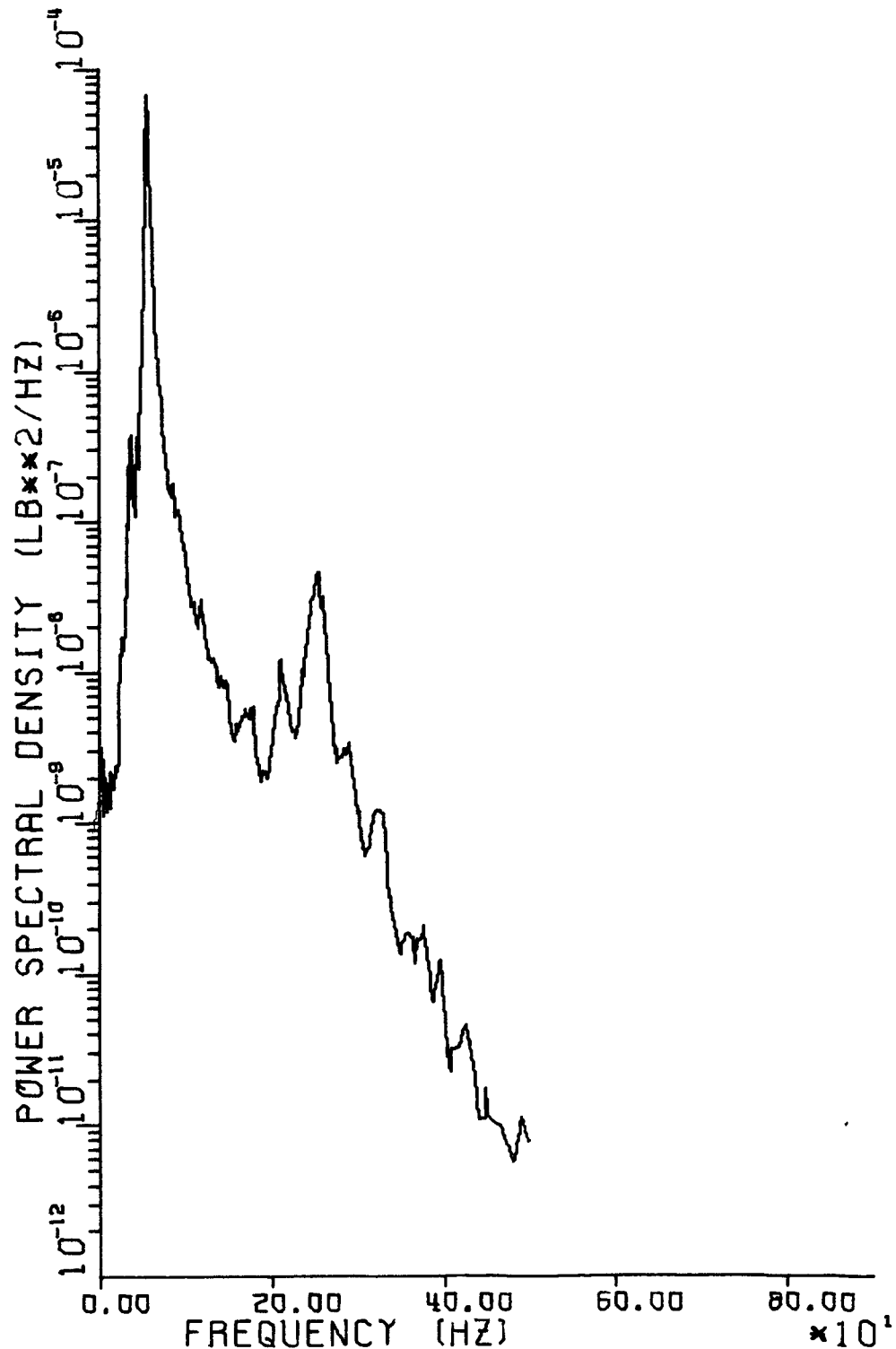DENSITY AT LUMPED MASS NUMBER 1

FIGURE 5.
THEORETICAL RESPONSE POWER SPECTRAL
DENSITY AT LUMPED MASS NUMBER 2

FIGURE 6.
THEORETICAL RESPONSE POWER SPECTRAL
DENSITY AT LUMPED MASS NUMBER 3

FIGURE 7.
THEORETICAL RESPONSE POWER SPECTRAL
DENSITY AT LUMPED MASS NUMBER 4
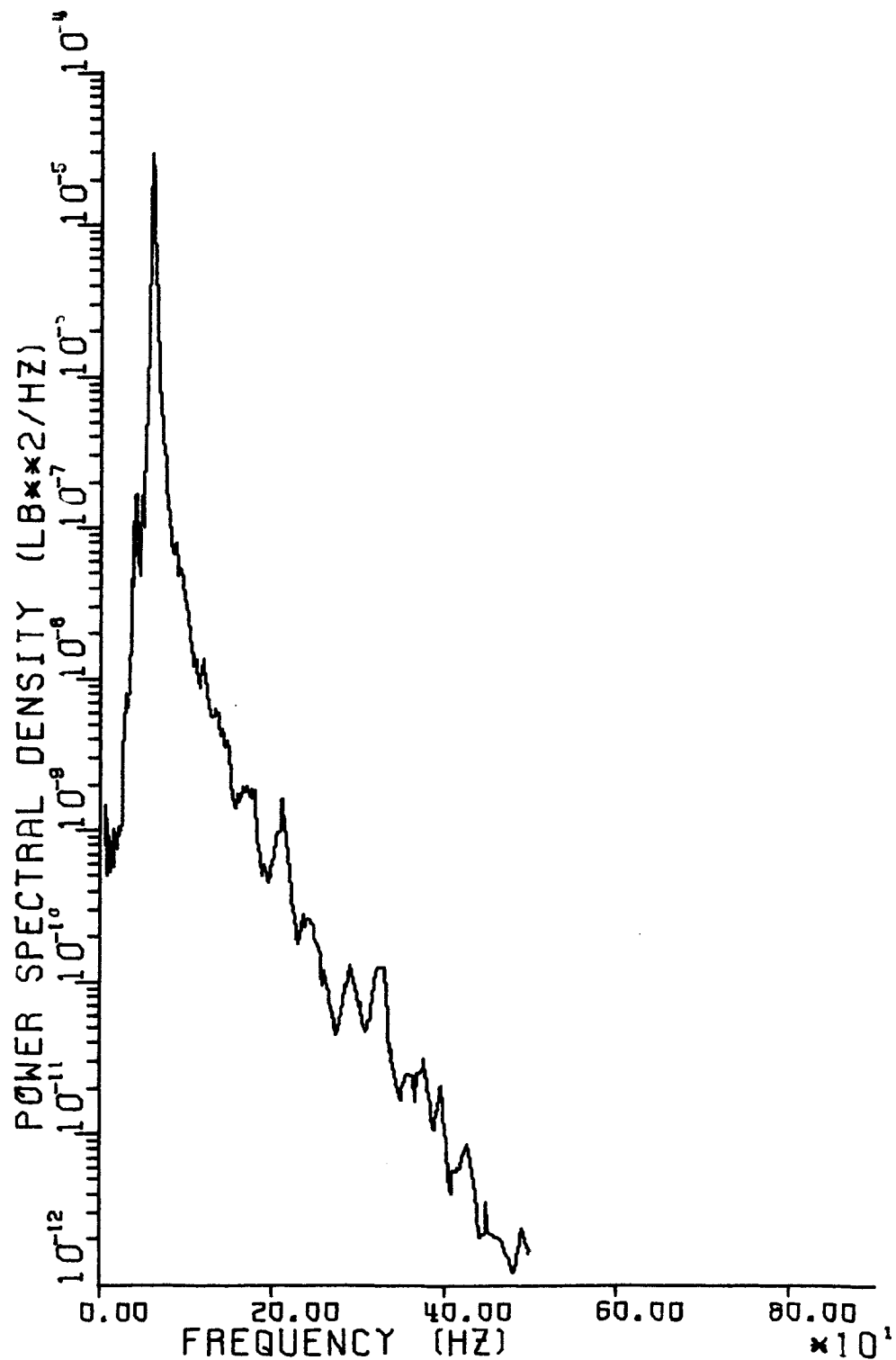
FIGURE 8.
THEORETICAL RESPONSE POWER SPECTRAL
DENSITY AT LUMPED MASS NUMBER 5

FIGURE 9.
THEORETICAL RESPONSE POWER SPECTRAL
DENSITY AT LUMPED MASS NUMBER 6

FIGURE 10.
THEORETICAL RESPONSE POWER SPECTRAL
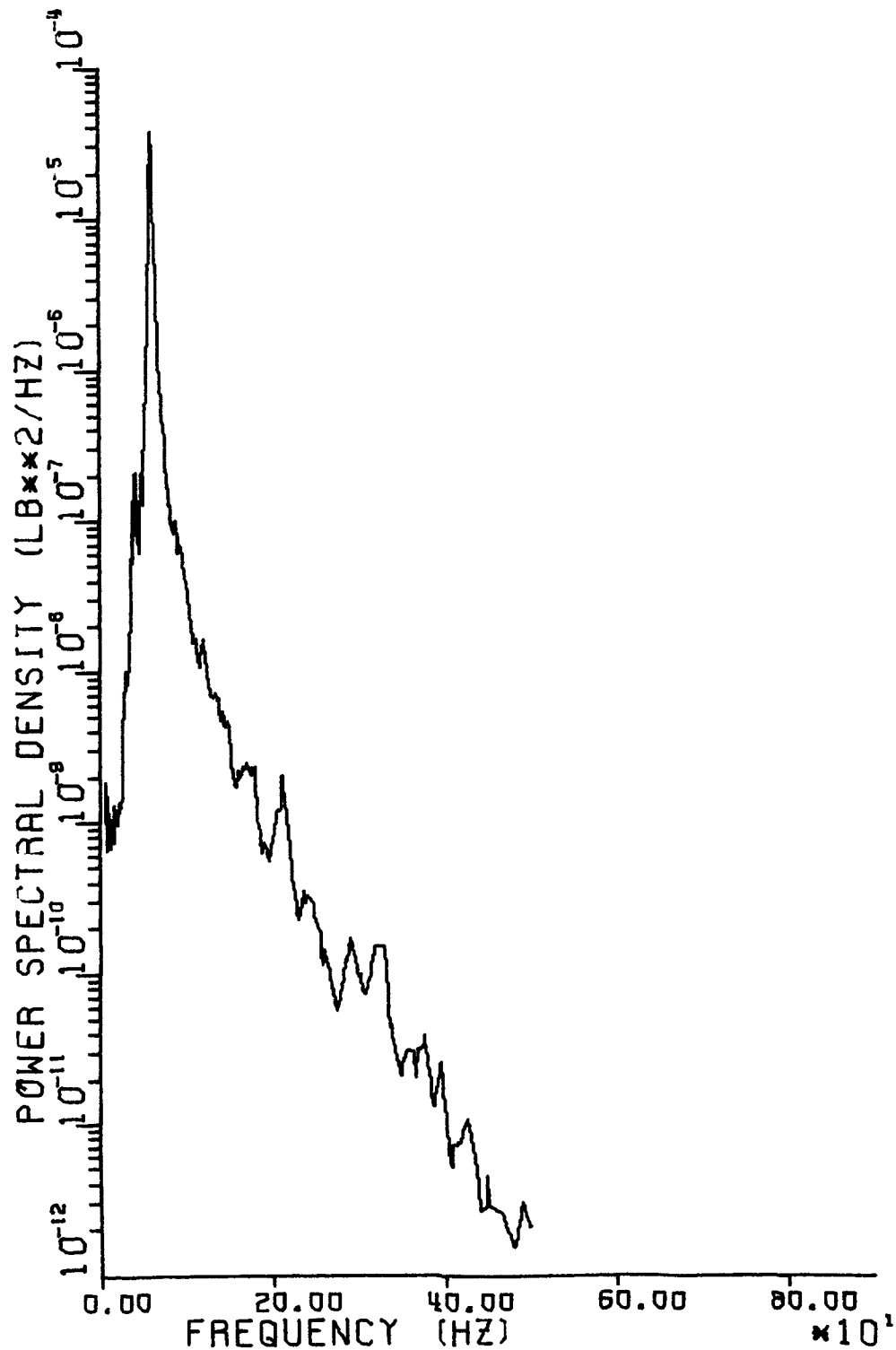DENSITY AT LUMPED MASS NUMBER 7

38
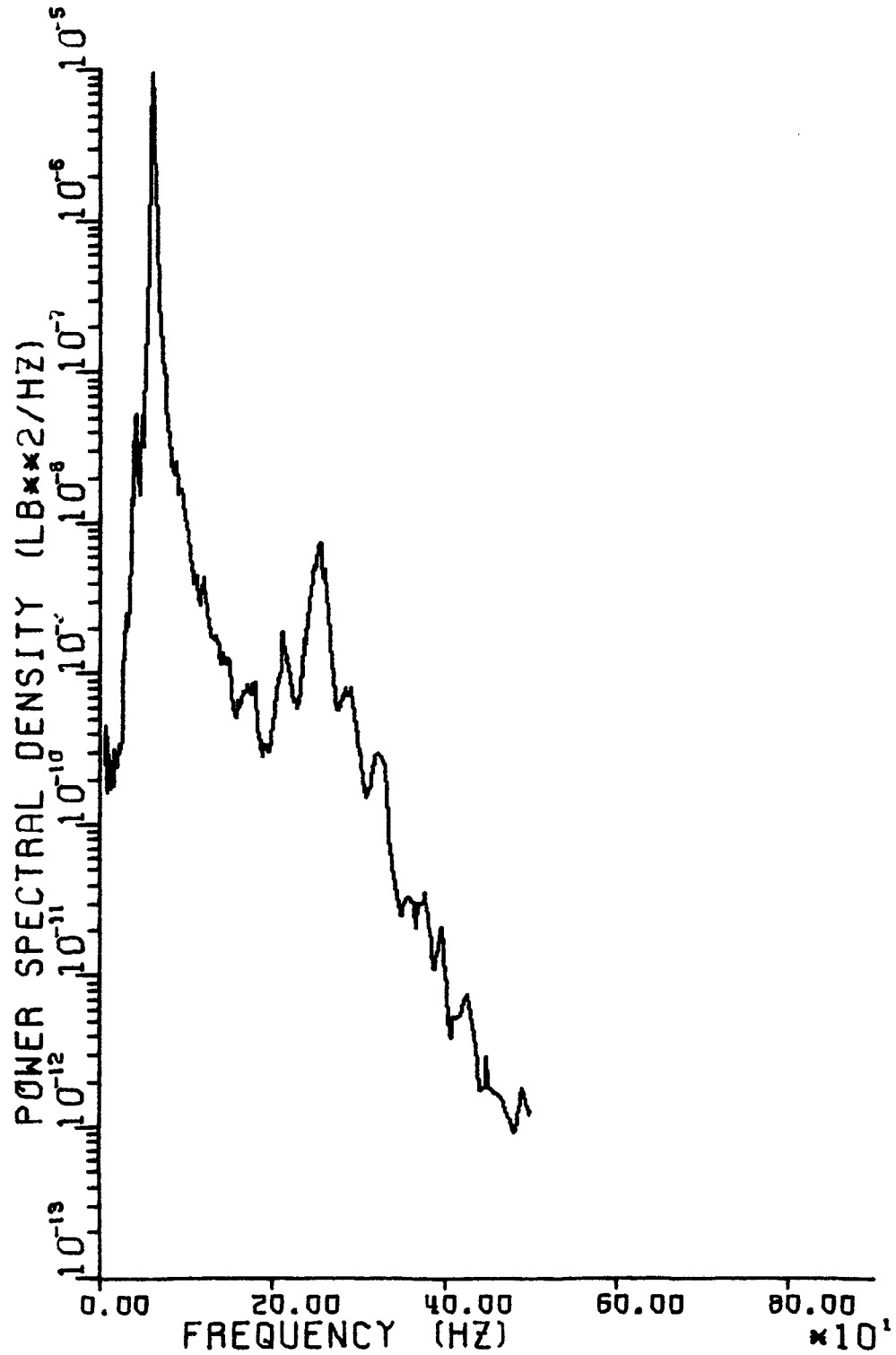
FIGURE 11.
THEORETICAL RESPONSE POWER SPECTRAL
DENSITY AT LUMPED MASS NUMBER 8
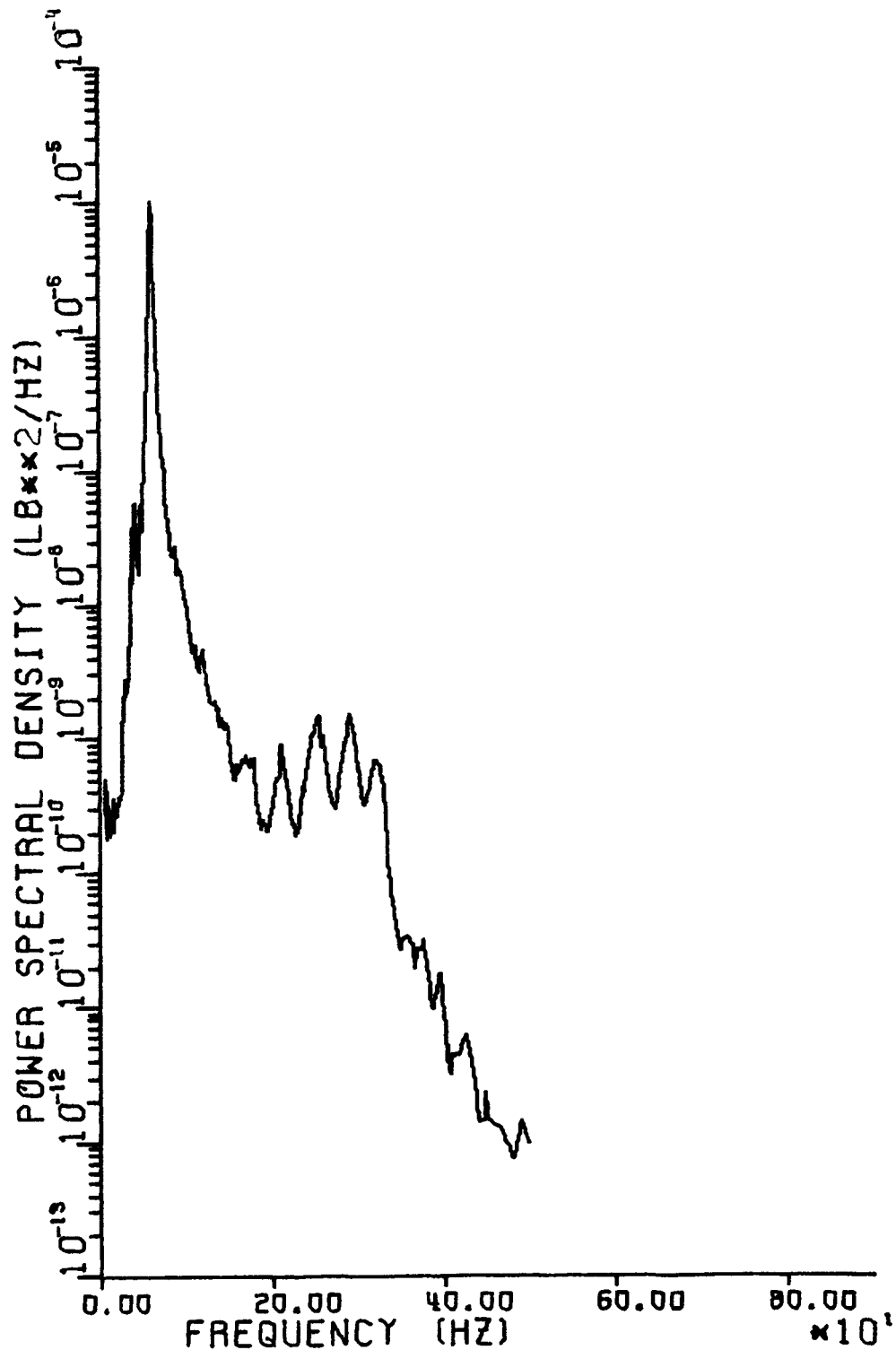
FIGURE 12.
THEORETICAL RESPONSE POWER SPECTRAL
DENSITY AT LUMPED MASS NUMBER 9
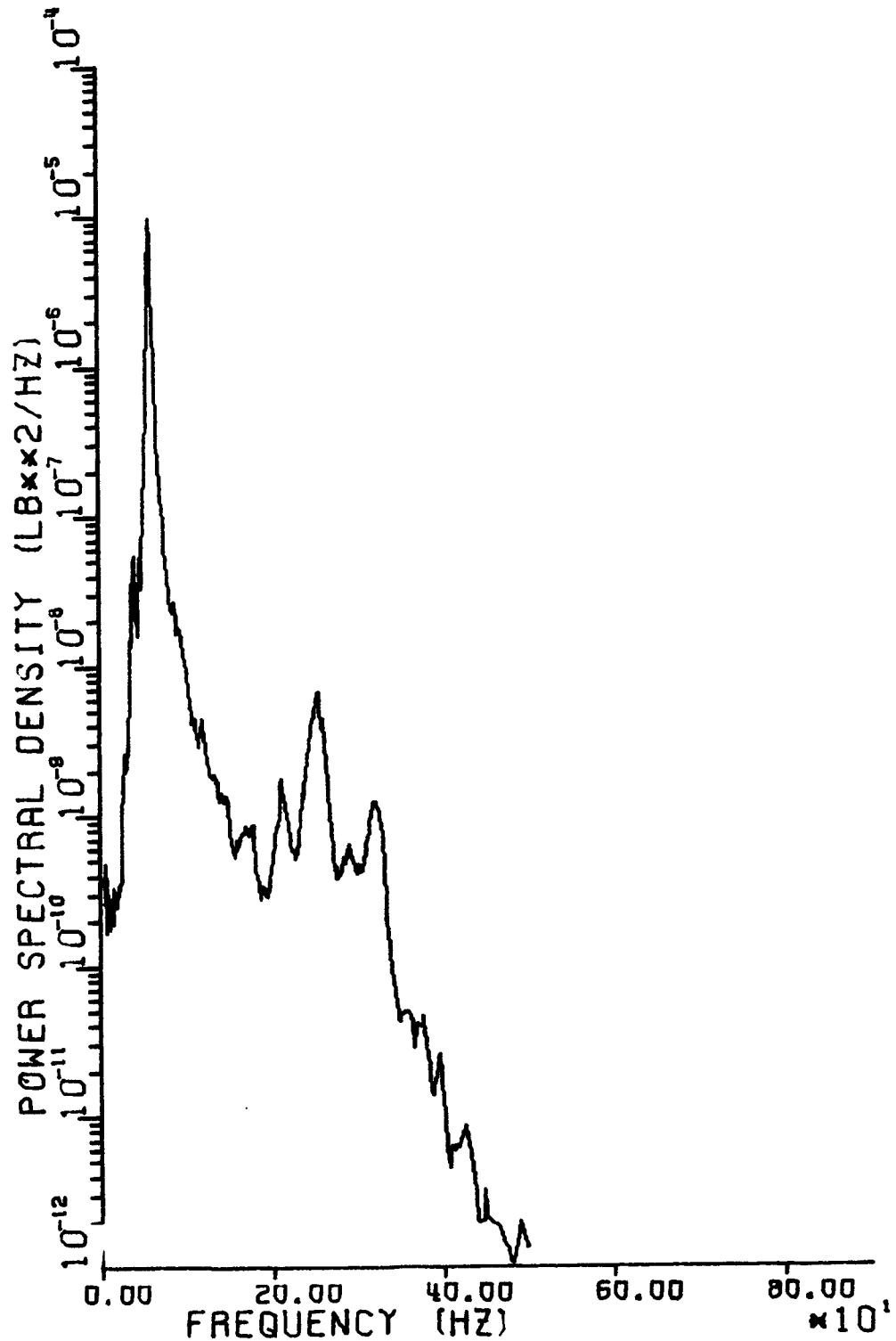
FIGURE 13.
THEORETICAL RESPONSE POWER SPECTRAL
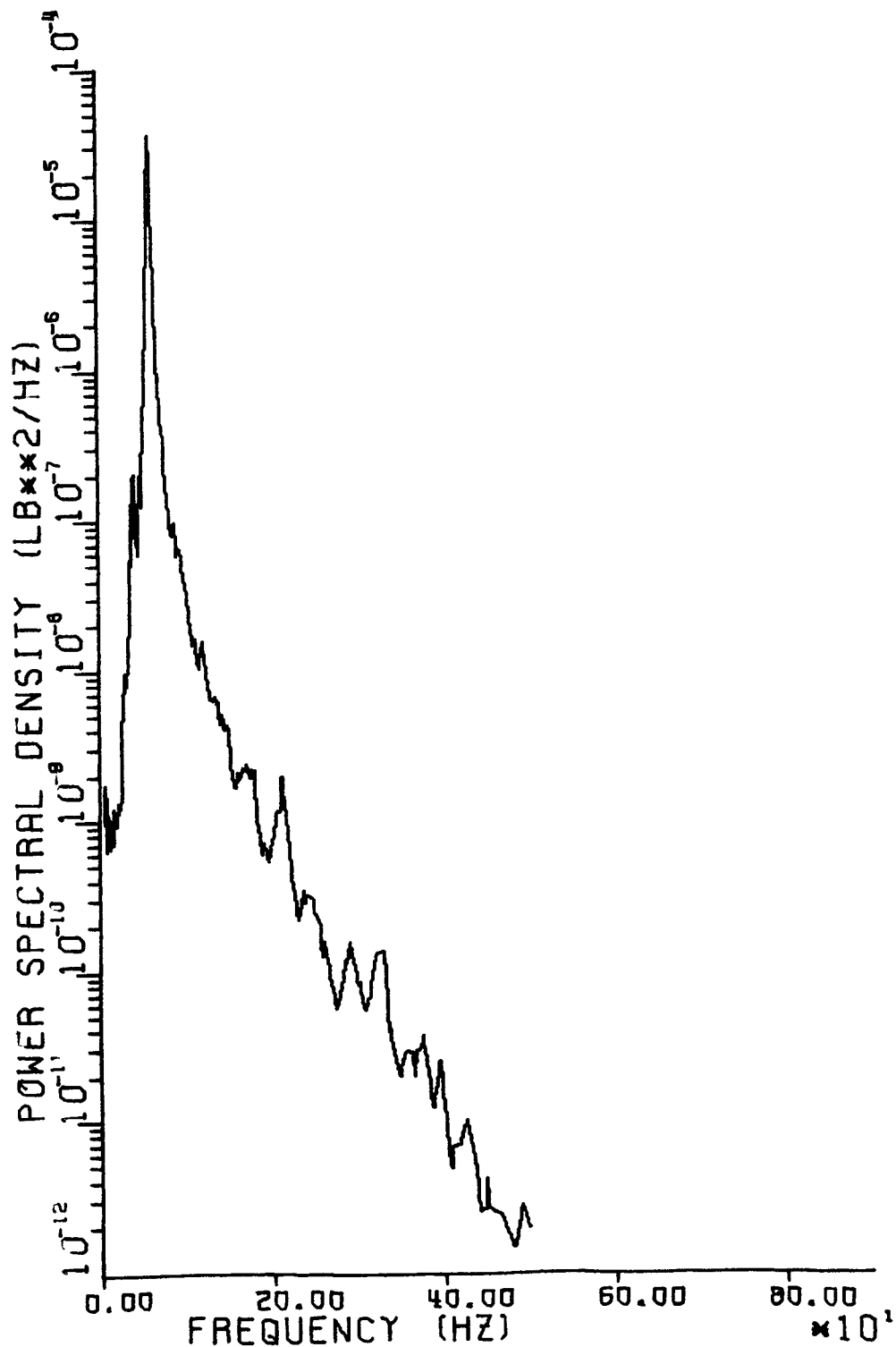DENSITY AT LUMPED MASS NUMBER 10
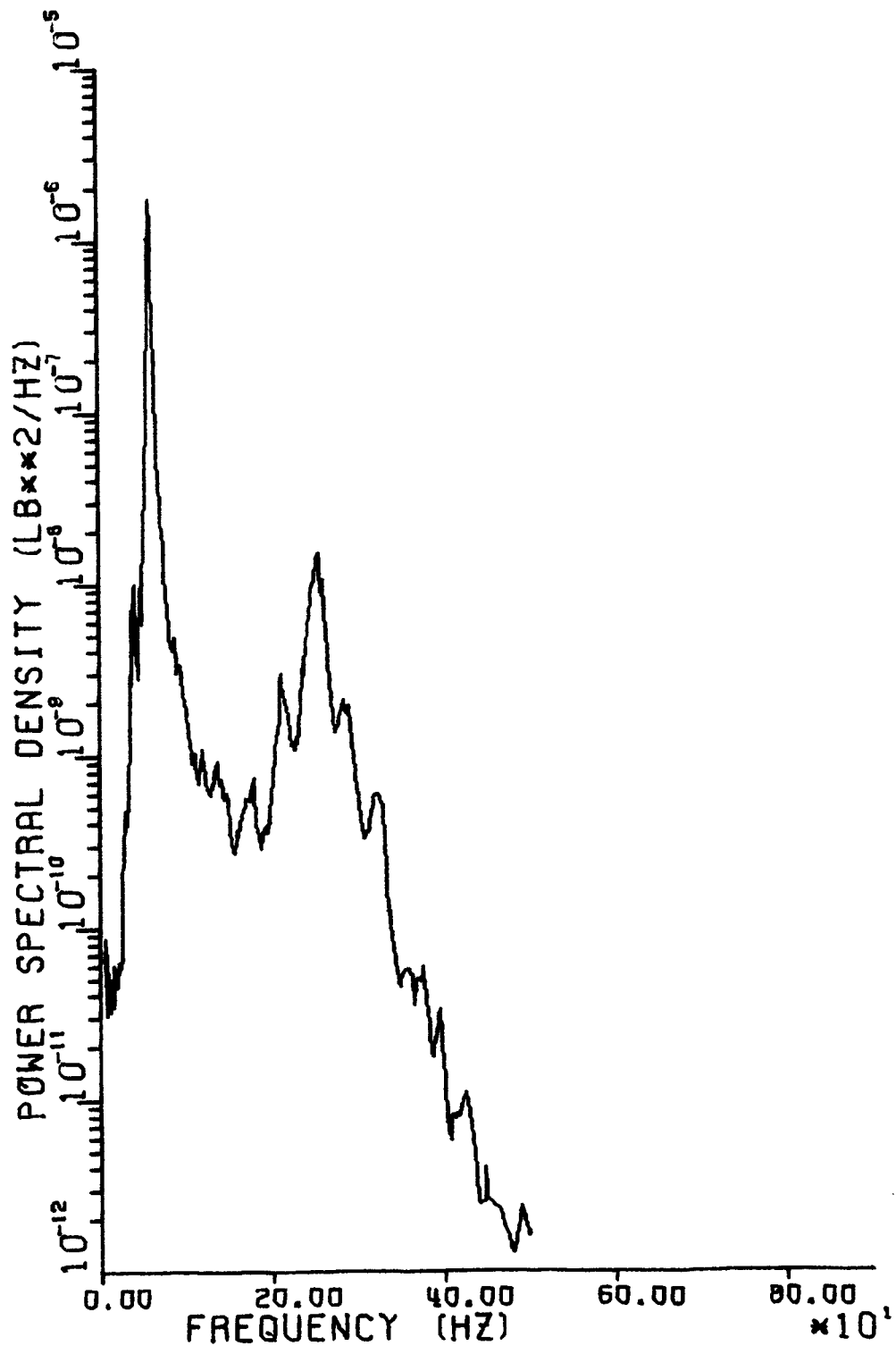
FIGURE 14.
THEORETICAL RESPONSE POWER SPECTRAL
DENSITY AT LUMPED MASS NUMBER 11
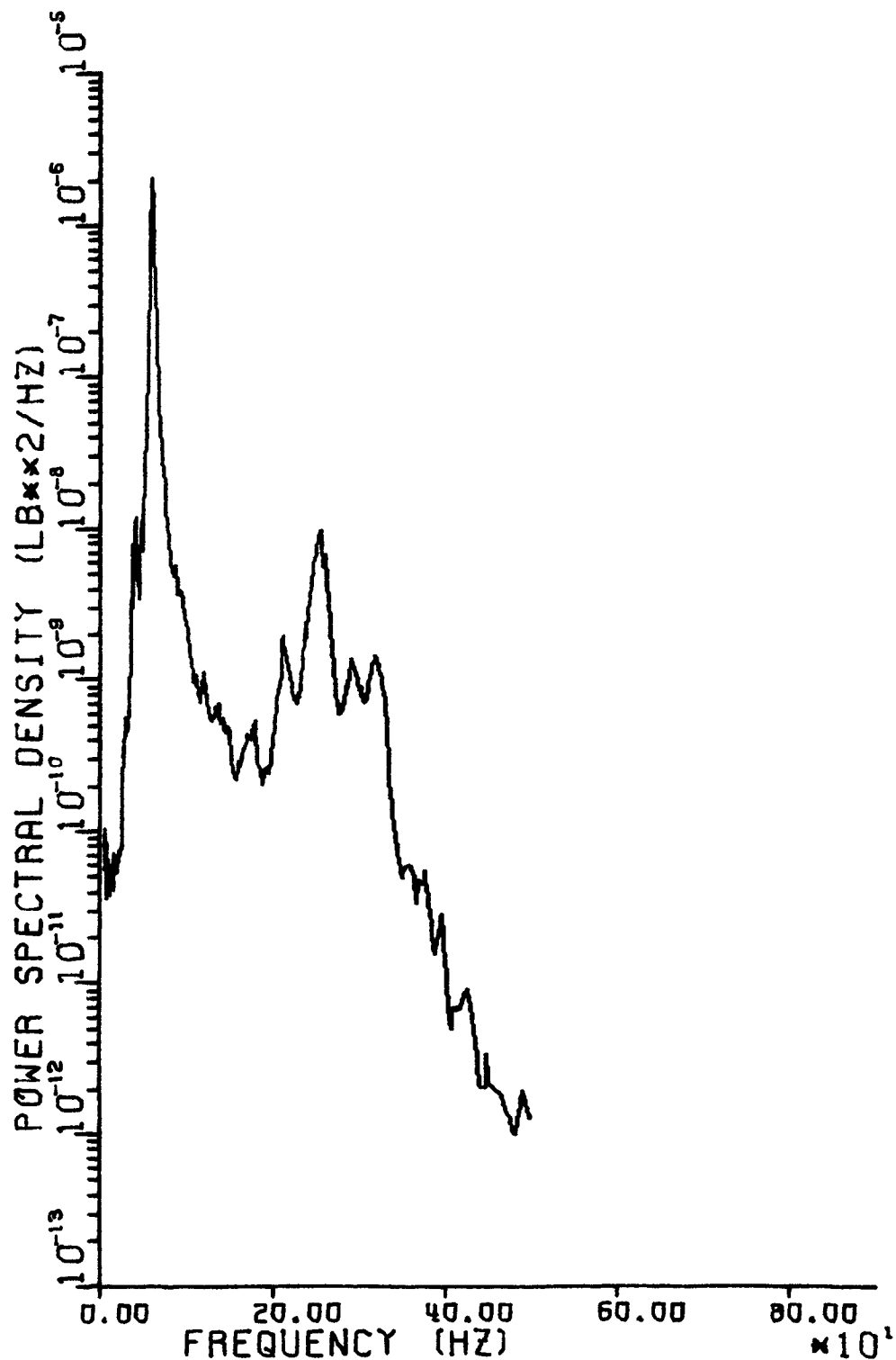
FIGURE 15.
THEORETICAL RESPONSE POWER SPECTRAL
DENSITY AT LUMPED MASS NUMBER 12

43
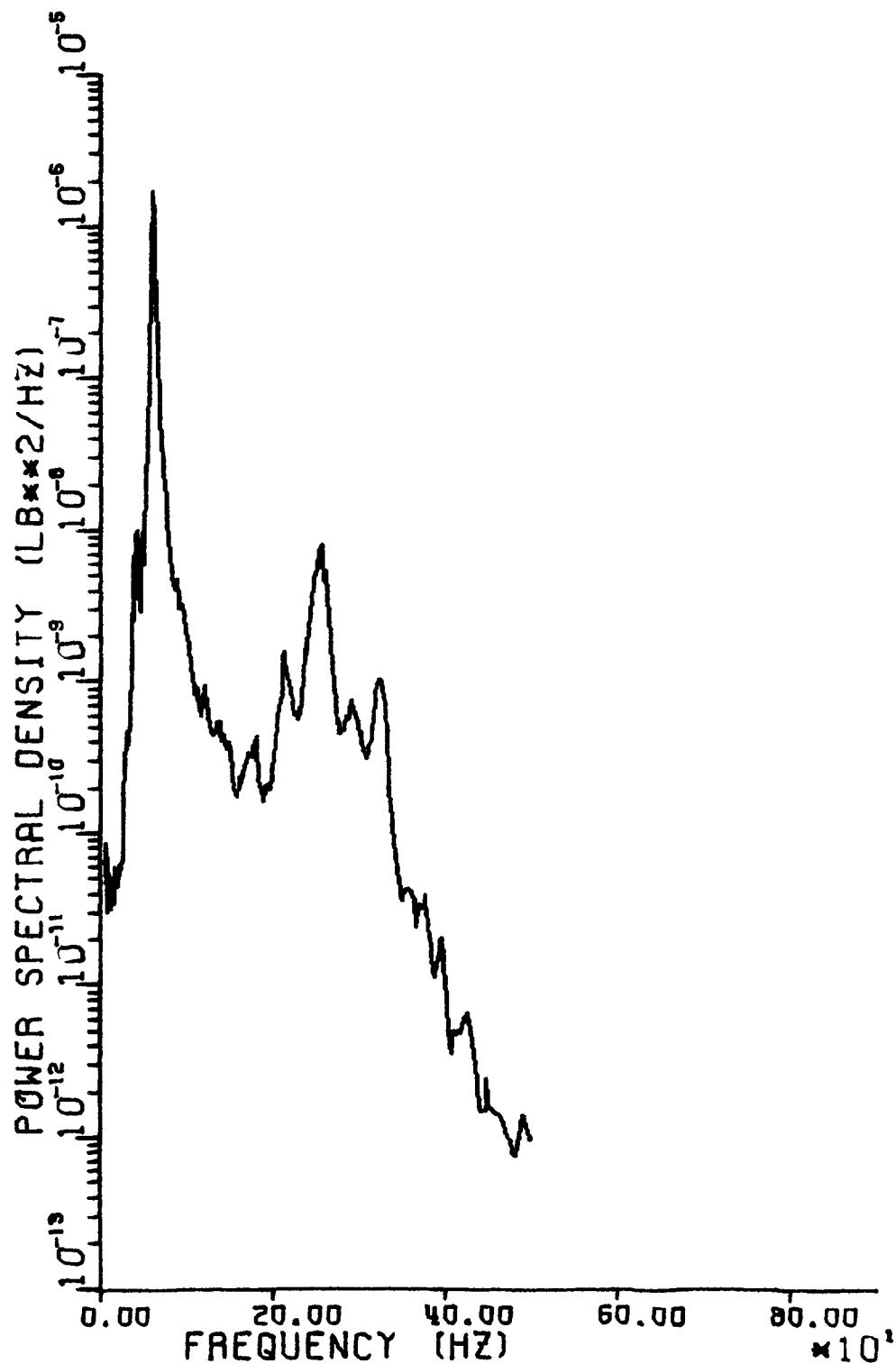
FIGURE 16.
THEORETICAL RESPONSE POWER SPECTRAL
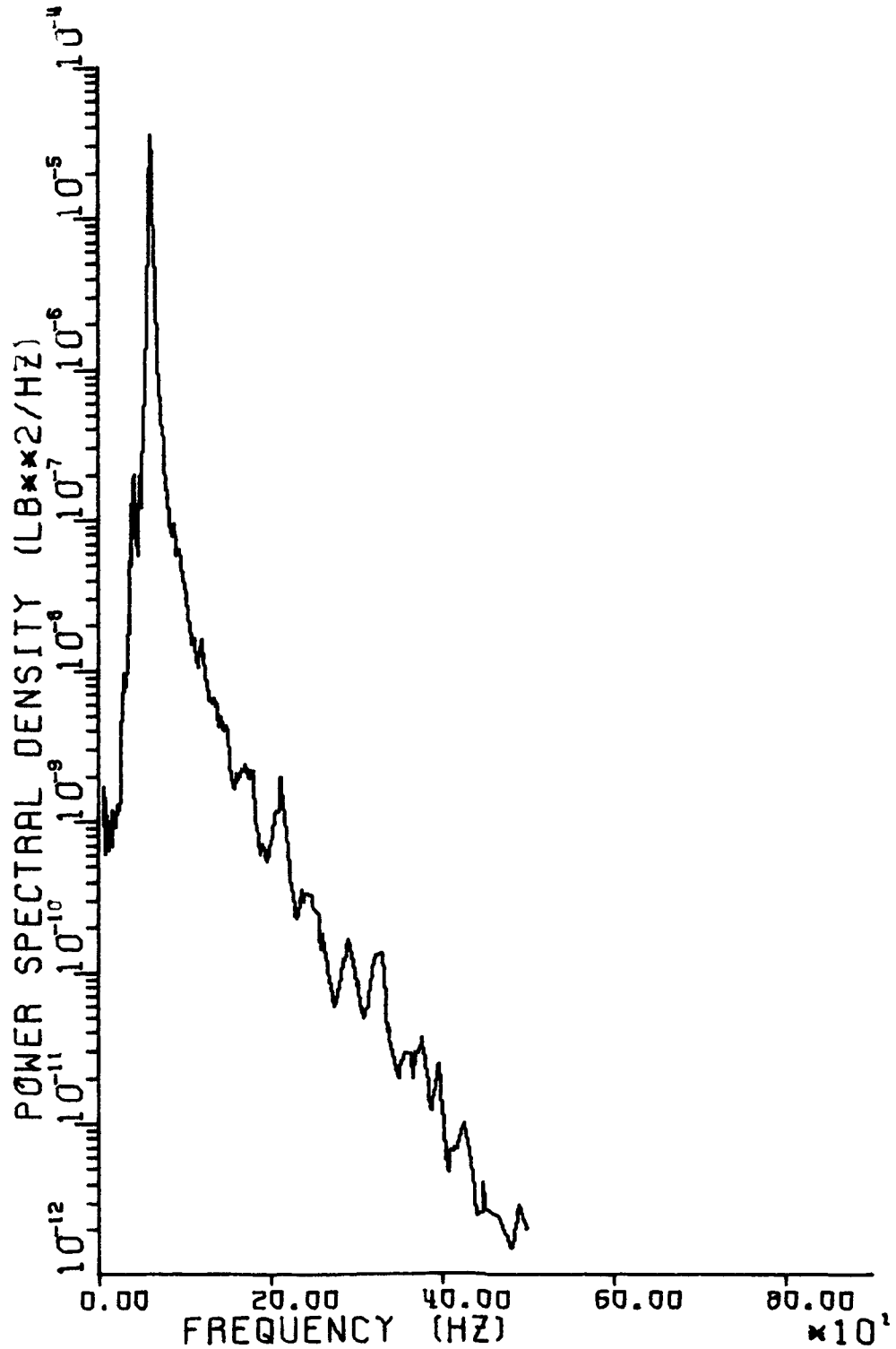DENSITY AT LUMPED MASS NUMBER 13

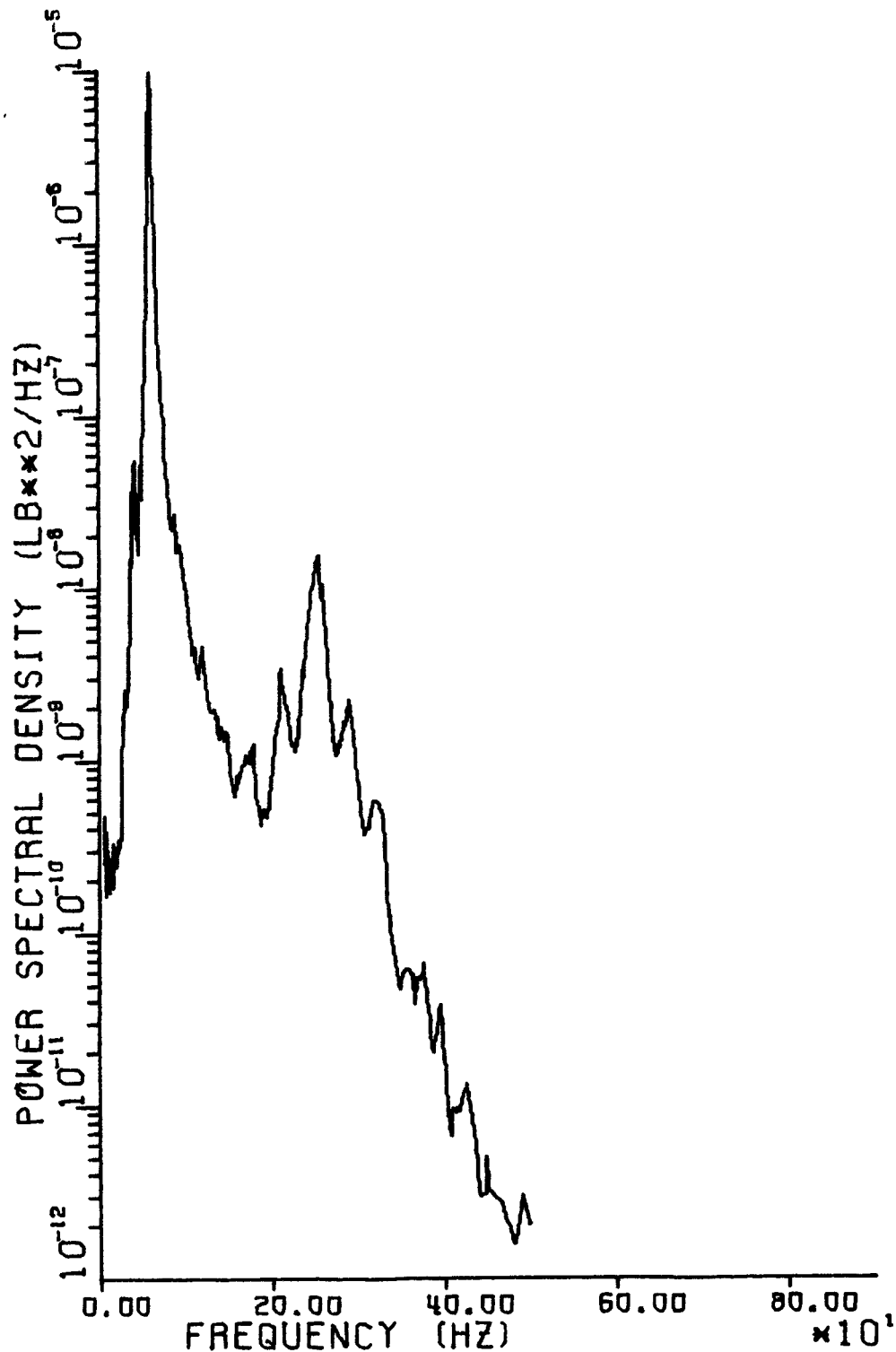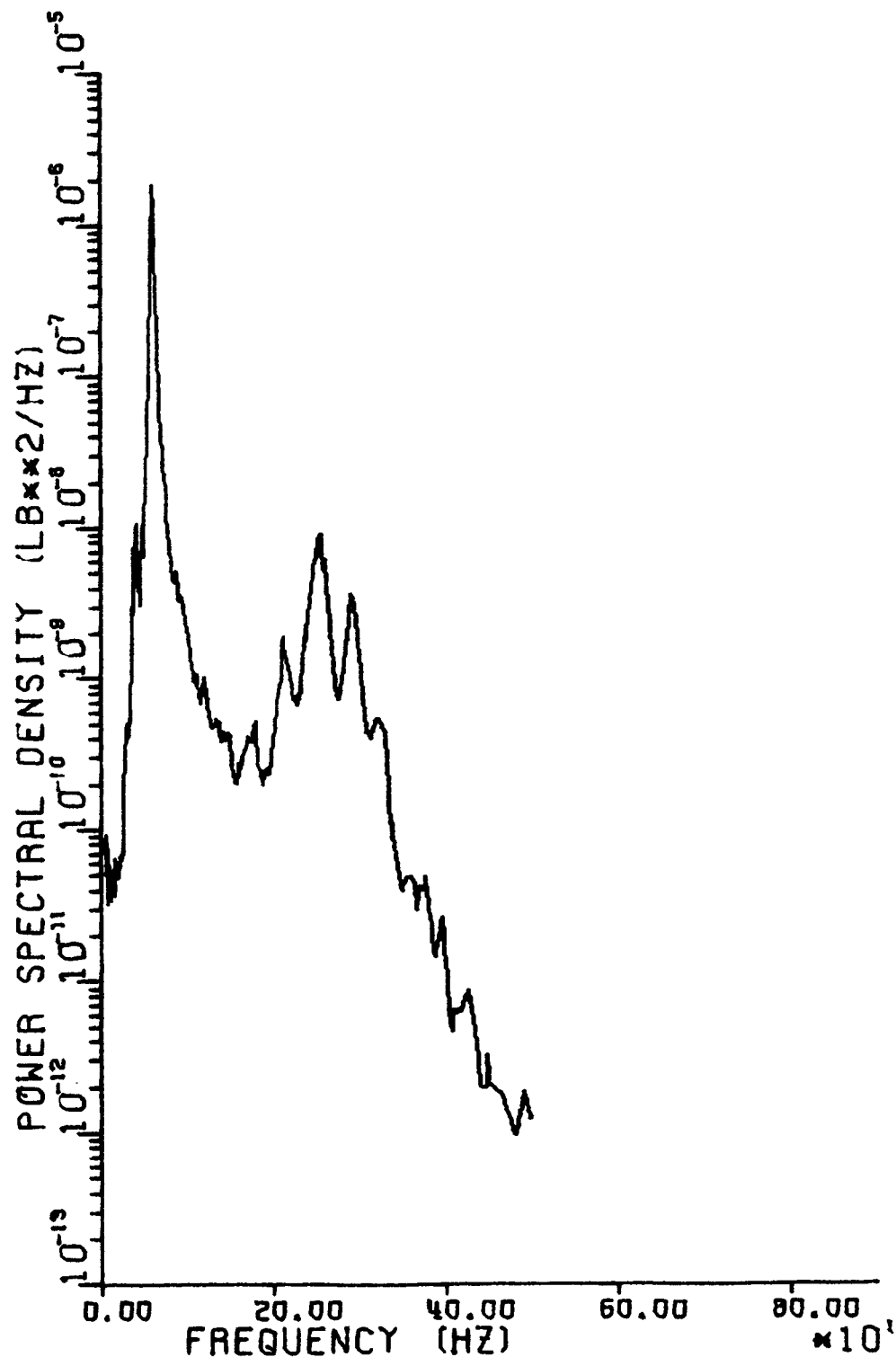FIGURE 17.
EXPERIMENTAL RESPONSE POWER SPECTRAL
DENSITY CORRESPONDING TO MASS 1
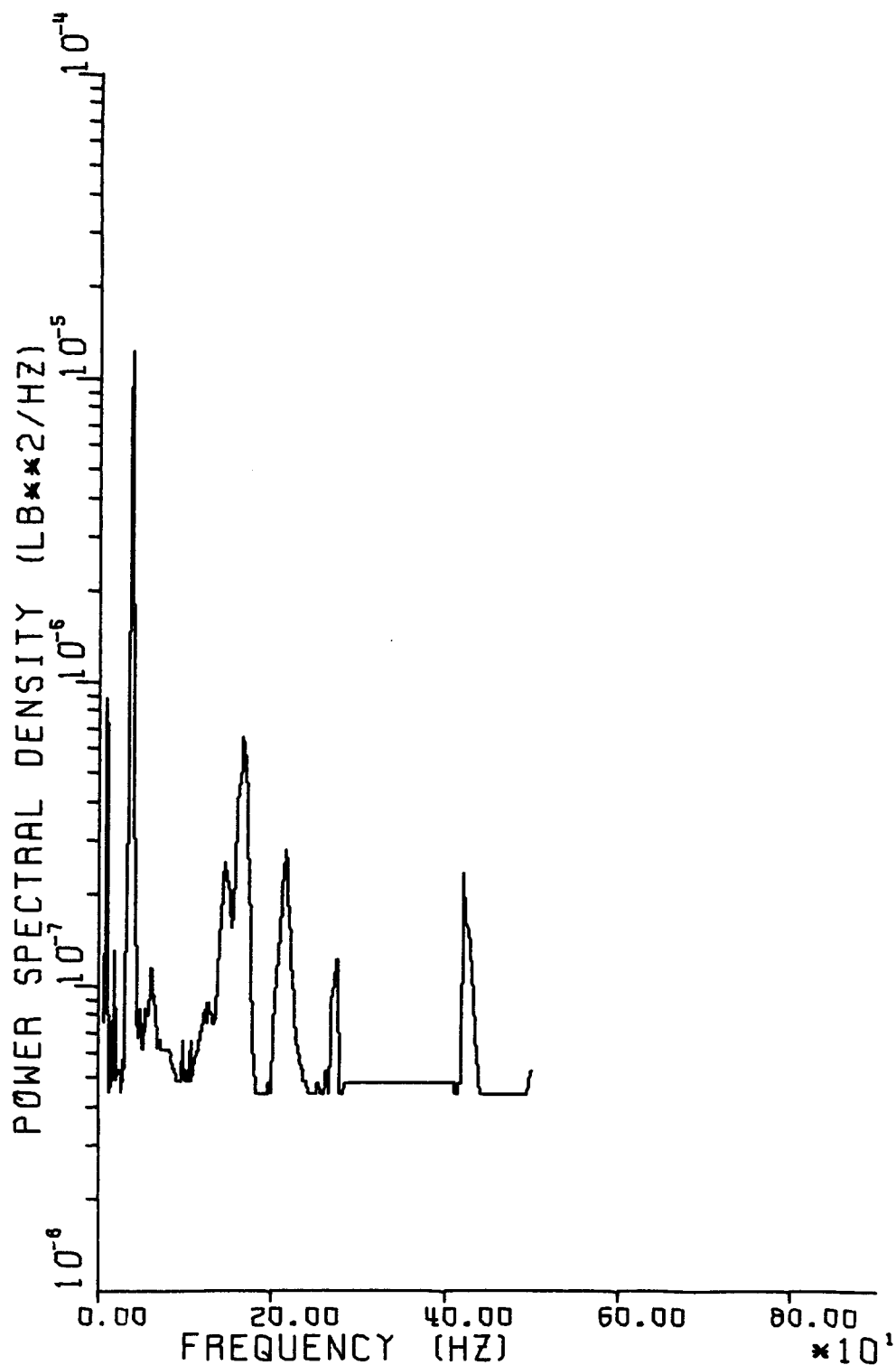
FIGURE 18.
EXPERIMENTAL RESPONSE POWER SPECTRAL
DENSITY CORRESPONDING TO MASS 2

46
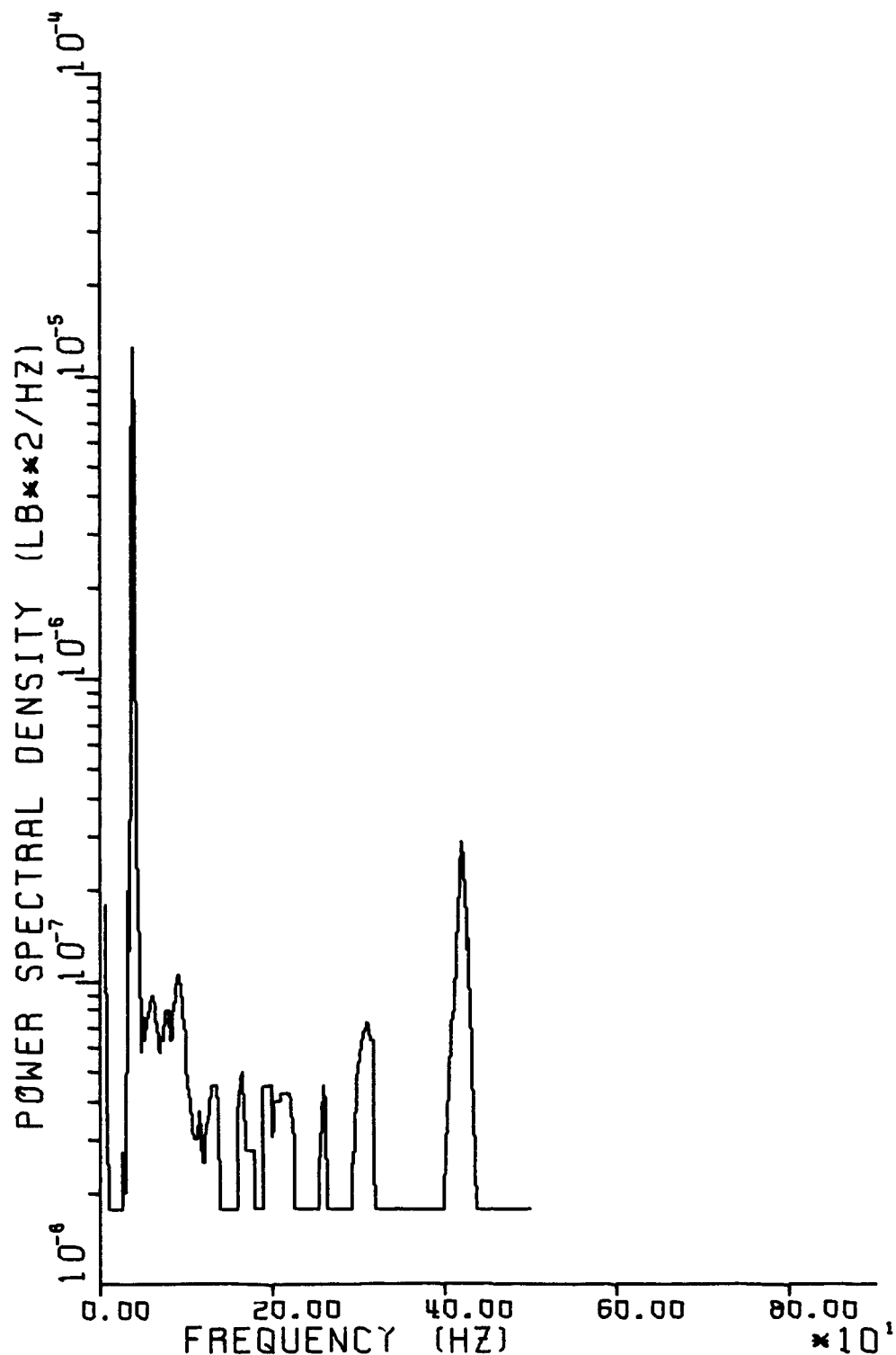
FIGURE 19.
EXPERIMENTAL RESPONSE POWER SPECTRAL
DENSITY CORRESPONDING TO MASS 3

47
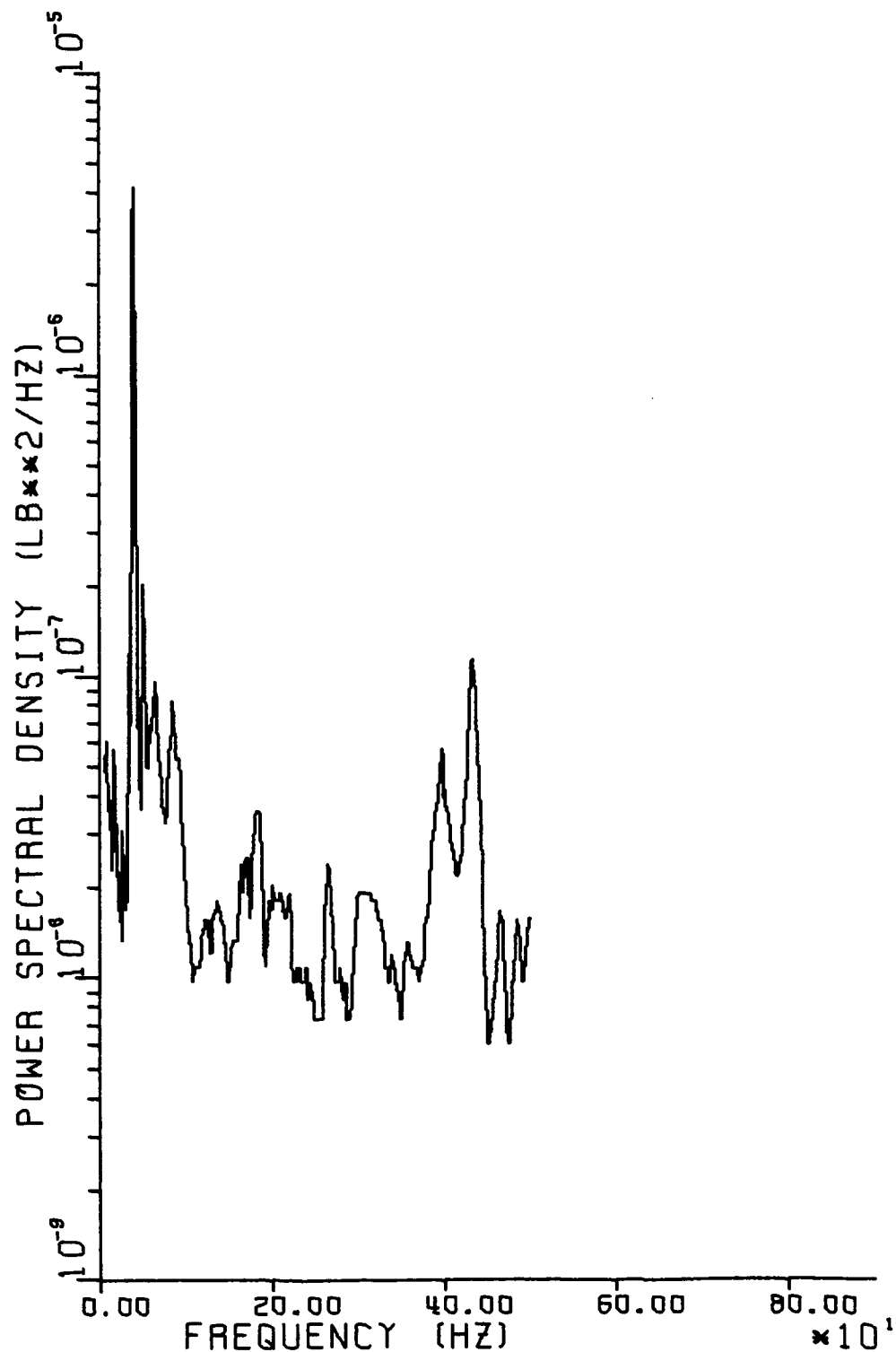
FIGURE 20.
EXPERIMENTAL RESPONSE POWER SPECTRAL
DENSITY CORRESPONDING TO MASS 8

POWER SPECTRAL DENSITY (LB**2/HZ)

10^5 10^{-6} 10^7 10^8 10^8

FREQUENCY (HZ)

0.00   20.00   40.00   60.00   80.00 $*10^1$

48

FIGURE 21: EXPERIMENTAL VALUES
— OF DAMPING RATIOS

□ — MASS 1
△ — MASS 3
⊙ — MASS 6

FREQUENCY (HZ)

DAMPING RATIO (Z)

49
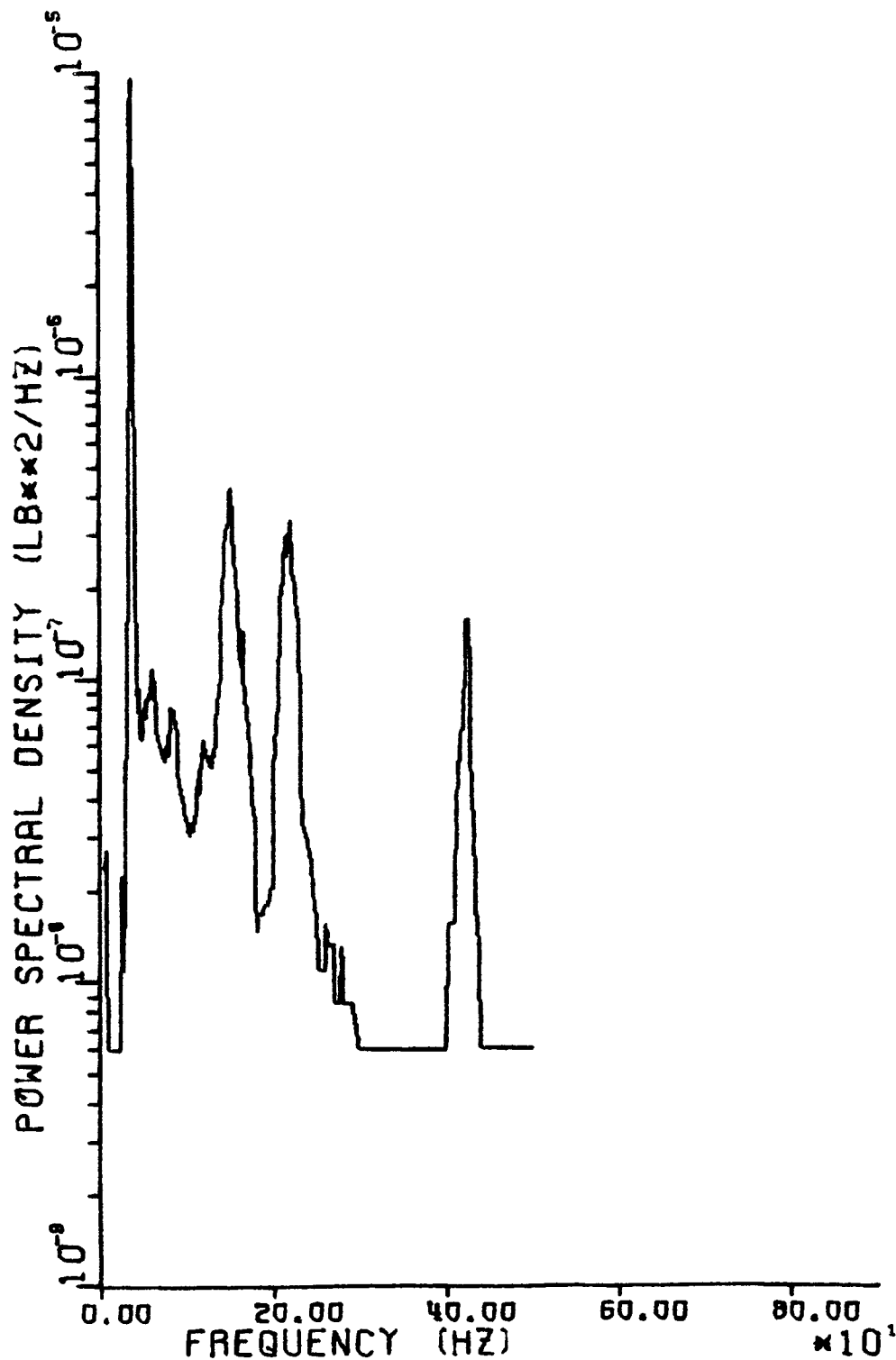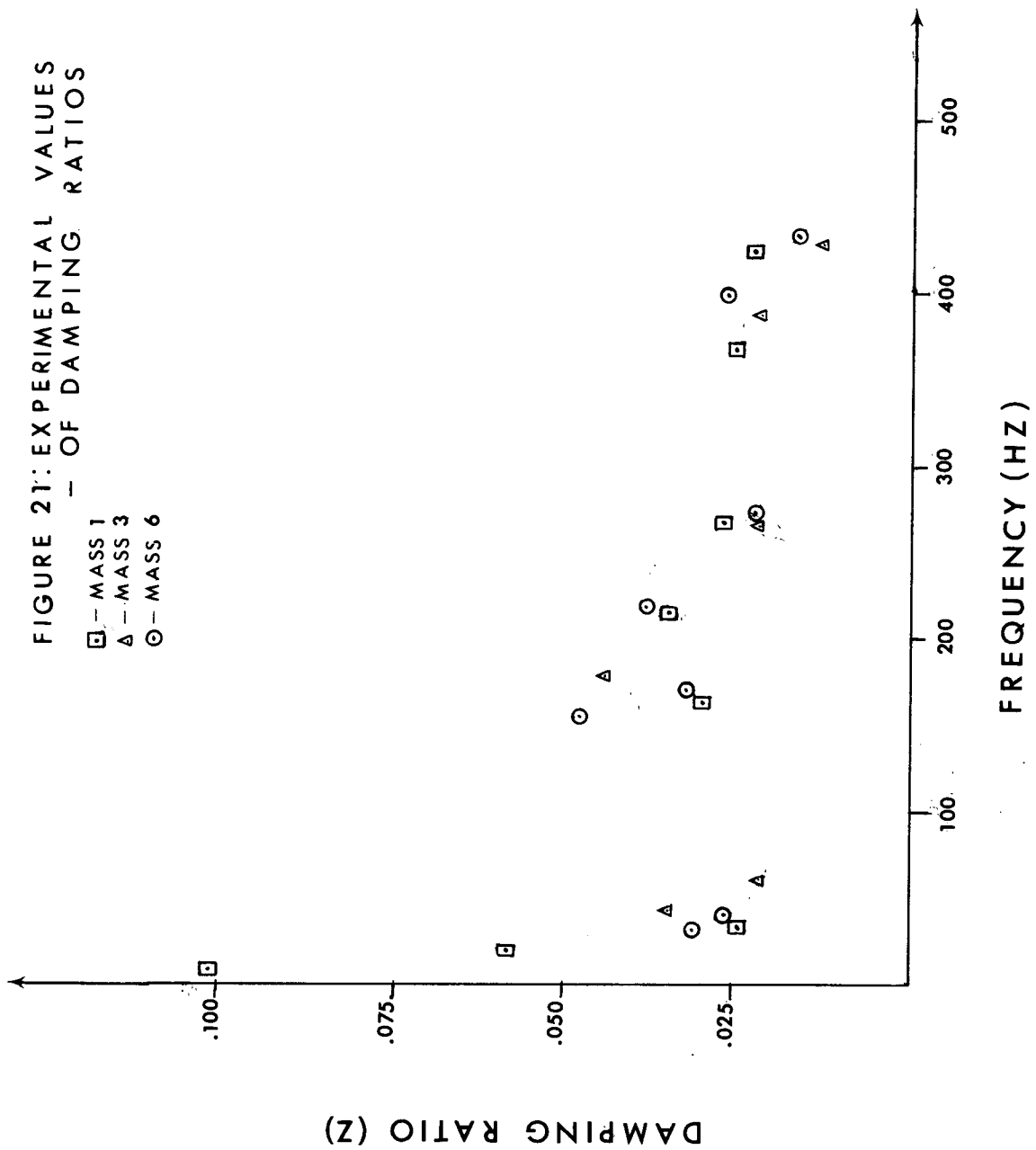
5. COMPUTER EVALUATION OF THE EQUATIONS OF MOTION

In this section, the computer program which was developed to perform the calculations necessary for evaluating Equations 3-12 and 3-14 will be discussed. (This program is listed in Appendix B.) The necessary inputs to this program are: (1) the mass matrix, (2) the influence coefficient matrix, (3) the modal damping ratio matrix, (4) the power spectral density of the excitation and (5) the operational parameters (Figure 22). With these inputs, the computer will calculate the stiffness matrix, the natural frequencies of the structure, the mode shapes of vibration, the modal participation factors, the power spectral density of the response, and the root mean square displacements of the system. The program is also capable of generating the necessary data for plotting the power spectral density of both the excitation and the response.

Before the progression of calculations performed by the computer program and the methods employed to perform these calculations are discussed in detail, a very basic breakdown of the program is given. The basic format on which the program is structured can be seen from these major steps: (1) the input of the appropriate data, (2) the calculation of necessary parameters, (3) substitution of the necessary parameters into Equations 3-12 and 3-14, and (4) printing the desired results. These four divisions are indicated in Figure 21 by the corresponding Roman numerals. Steps in the flow diagram which are located between the horizontal dash lines are the ones associated with each of the four major steps numbered between these lines.

The first major division of the program is devoted to reading the appropriate data necessary for calculating the parameters of the problem. The flow diagram (Figure 22) lists the particular items which are read into the computer program. The particular order and format for inputing the data is shown in the program listing in Appendix C. The first set of six 'A' format read statements are the common titles which will be printed on the power spectral density plots. Particular titles will be read in the same DØ Loops performing the particular calculations. The

FIGURE 22: FLOW DIAGRAM

I

READ

Titles, Cases, Dimension, Degrees of freedom, Mass
Influence Coefficients, Damping Ratios, Excitation

CALL DECOMP

A =
Real Symmetric
Matrix

NO → STOP

YES

CALL INVERT

Combine Mass and
Stiffness Matrix

II

CALL JACOB

Transform Eigenvalues
And Eigenvectors into
Real System

Print Eigenvalues
And Eigenvectors

Calculate Modal Participation
Factors by Equation (III-11)

CALL GRAND

2

1

3

FIGURE 22 (Continued)

2

1

3

III

W>0

NO

W=EXIC

YES

Evaluate
Equation III-14

Print X

NO

WI<0 —YES→ L = K

NO

YES

Evaluate
Equation (III-12)

STOP

Print WO

CALL GRAND

IV

Print XI

CALL WEBAL

Plot WO, WI

NO

L=K

YES

STOP
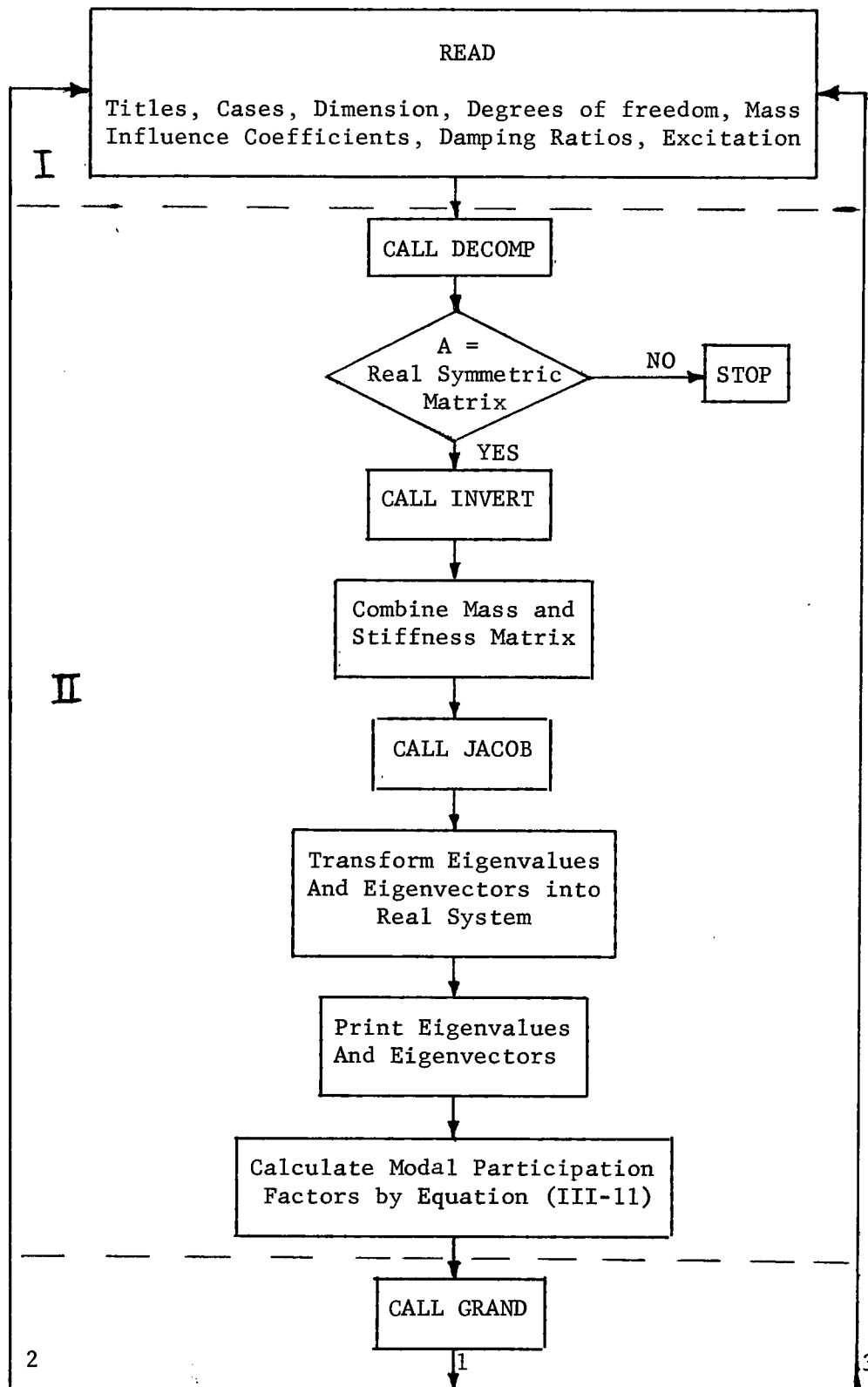
next read statement identifies the number of data sets (K) and the actual dimension size of the influence coefficient matrix (NA). The number of degrees of freedom (N) is read in next. The mass (AMASS), area of excitation for each mass (FA), the damping ratio (Z), the constant value of the excitation power spectral density (W), the variable values of the excitation power spectral density (WI), and the influence coefficients (A) are inputed in this same order. The mass, being read in, in units of pounds force, is converted to the proper inch-pound-seconds system of units by dividing it by 386.4. The values of WI are also converted back to their actual values by multiplying by 10^{-5}. If the excitation power spectral density is not a constant, one inputs a zero for W in the data deck. If the excitation power spectral density is a constant, one inputs a minus one for WI in the data deck.

The second major division in the program begins by calling subroutine DECOMP. This subroutine decomposes the influence coefficient matrix into an upper tri-diagonal matrix and tests the matrix to determine if it is a real symmetric matrix (18). If it is not a real symmetric matrix, the next step cannot be performed and the program is sent to stop. If it is a real symmetric matrix, the program then calls subroutine INVERT, which inverts the influence coefficient matrix and produces the stiffness matrix. The stiffness matrix (A) is then transformed by the inverse of the mass matrix in such a fashion that the resulting matrix (A) is still symmetrical. This matrix is now in the proper form for substitution into subroutine JACOB. This subroutine calculates the eigenvalues and eigenvectors of the system by using the Jacobi Method for real symmetric matrices (20). The resulting eigenvalues are converted into units of hertz and the eigenvectors are transformed back into the real system by multiplying them by the inverse square root of the mass matrix. The total area over which the excitation is applied and the generalized area are calculated. The mass matrix and the eigenvectors are then used to calculate the modal participation factors as described by Equation 3-11. At this point, the displacements of the plate are referenced to the fixed frame (fourteenth mass) by subtracting the eigenvector component

associated with the fourteenth mass in all the modes of vibration, [V(14,J)], from the other eigenvector components.

It can be seen in Figure 2 that the excitation power spectral density is not a constant in the particular case being investigated, but evaluation of Equation 3-14 was performed for comparison purposes by approximating the curve in Figure 2 with an average value. Subroutine GRAND is called to integrate the curve in Figure 2 from 6 to 500 Hz. The average value of the curve is then obtained by dividing the integrated value by 495, which is the total frequency range.

The third major division of the program, the evaluation of Equations 3-12 and 3-14 is initiated by testing the value of W. If W is equal to zero, W is set equal to EXIC which is the average value calculated by subroutine GRAND. At this point, the other quantities necessary for substitution into Equation 3-14 have already been stored in the computer, and determination of the root mean square displacements (x) is merely a matter of performing the required mathematical operations. The factor 2π is used to convert the frequency units from Hz (cycles per second) to radians per second. The constant 165.5 determined by calibration procedures discussed in Section 5, effectively converts the excitation from volts to pounds force. The output (x) is now printed as the response displacement of each lumped mass in inches.

A test is performed on WI to determine if the evaluation of Equation 3-12 is necessary in this case. If this evaluation is not necessary, (WI = -1) control is shifted to the next test, (L = K), which determines whether or not any more cases are to be calculated. If no more cases are to be evaluated the program stops. If more cases are to be evaluated, the control is sent to the beginning of the program, and the cycle is started again by reading new data for the next case. If WI is not equal to a minus one, the sequence of calculations continues. The power spectral density of the response is calculated using Equation 3-9, or equivalently the integrand of equation 3-12. The calculation is performed in 1-Hz increments over the frequency range of 6 to 500 Hz. The response power spectral density (WO) is multiplied by the same conversion

factors (2π and 165.5) as applied in the displacement calculations of
Equation 3-14. The resulting power spectral density of the response is
now in terms of pounds force squared per hertz.

The fourth major division of the program is begun by printing the
response power spectral density (WO). Subroutine GRAND, which utilizes
a Simpson's rule integration technique, is called to integrate WO over
its range of frequencies to produce the mean square values of the dis-
placements. The square roots of these values produce the root mean
square values of the displacements (XI) in inches; XI is then printed.
The particular titles for each data set are read in as 'A' format data.
The subroutine WEBAL is called twice to plot the necessary power spectral
density curves. The first time WEBAL is called, the power spectral den-
sity of the response at each lumped mass point (WO) is plotted (Figures
4 through 16). The second time WEBAL is called, it plots the power spec-
tral density of the excitation (WI). See Figure 2. The number of cases
is tested (L = K). If more cases are to be calculated the program re-
turns to the appropriate read statement and the cycle of calculations is
again performed. If all the cases have been completed the program stops.

6. EXPERIMENTAL TEST

The object of the experimental test was a determination of the root
mean square values of the displacements and the response power spectral
density of a plate (Figure 1) subjected to the random acoustical pres-
sure (Figure 2). The experimental tests were performed at Mississippi
Test Facility and financially supported by NASA through the Division of
Engineering Research at Louisiana State University.

The particular shape of this plate was chosen because its shape is
a simple geometric form and generally found in areas where the acous-
tical noise may be at a sufficiently high level as to cause damage to
the surrounding structures. As noted in Section 2, other investigations
in this area were made on the assumption that the stringers were suffi-
ciently stiff in at least one direction as to give the adjoining edge
of the panels a fixed boundary condition in that direction. See Lin
(26) and McDaniel and Donaldson (27). This particular plate has no such
restrictions and differs from other plates subjected to a random excit-
ation in that it resists analysis by the method of transfer matrices (26),
(27). The only fixed condition imposed on this plate are the fixed outer
edges.

The plate is constructed of sheet aluminum alloy 6061-T6 with a
modulus of elasticity of 1×10^7 lb-ft/in^2 and a shear modulus of 4×10^6
lb-ft/in^2. (These properties are standard handbook values.) The maxi-
mum thickness of the plate is 0.25 inch at the boundaries and stringers.
The panel thickness is 0.125 inch. The plate was constructed from a solid
sheet of aluminum with the panel areas formed by milling away the unwanted
metal. The radius of curvature at the corners where the panels and the
stringers intersect is no longer than 3/16 of an inch, and the surface
finish is specified as a standard 63 smooth. All tolerances were held
to ± 1/64 of an inch. The plate is shown in the foreground of Figure 23
fixed on all four edges by a 4x1/4 angle iron frame which is bolted to
the edge of the plate by 36 half inch bolts. The top and bottom frames
are also joined by two 1/2 inch thick plates which were attached on

Figure 23

Half-tone negative
with caption

NOT Reproducible

opposite edges of the plate and used to support the entire system of frame
and plate during the experimental test.

The plate was clamped before the strain gages were attached. Biaxial
and rosette type strain gages were mounted on the surface of the plate
primarily around the centrally located panel. Two strain gages were also
mounted on the frame. Figure 26 shows the location and alignment of the
strain gages. The strain gages were calibrated in the laboratory with the
use of the equipment shown in Figure 23. The dynamic part of the cali-
bration procedure was performed in the Mobile Instrumentation Unit; this
trailer is shown in Figure 24. The equipment inside the Mobile Instrumen-
tation Unit is shown in Figure 25. The laboratory calibration was per-
formed by attaching weights to the particular points designated as lumped
mass points on the plate and measuring the strains and deflections at all
points of interest. See Table 6 for results of the strain measurements
and Table 2 for results of deflection measurements. It is noted that
strain gages are not located at all fourteen points designated as lumped
mass points in the analysis. This caused some concern until calibration
was completed on the five points shown in Table 1 which coincided both
experimentally and analytically. The five calibrated points produced
the same conversion constants and gave credence to the assumption that
these conversion constants were uniform for all points on the plate as
shown in the calibration calculations which follow.

Two conversion constants are necessary; one to convert the volts
representing the excitation power to pounds force, and a second factor to
convert the root mean square volts to displacement in inches.

The conversion of volts to pounds force is accomplished through the
set of linear equations.

$\Delta R = A(\Delta V)$, $\varepsilon = B(\Delta R)$, and $L = C\varepsilon$, where

ΔR = Change in resistance (ohms)

ΔV = Change in voltage

ε = Strain in inches/inch   (6-1)

A,B, and C are constants to be determined through calibration procedures.
The desired relationship is determined by combining the above equations to

58

Figure 24
Halftone negative
w/caption

NOT Reproducible

59

Figure 25

Halftone negative w/caption

NOT REPRODUCIBLE

60
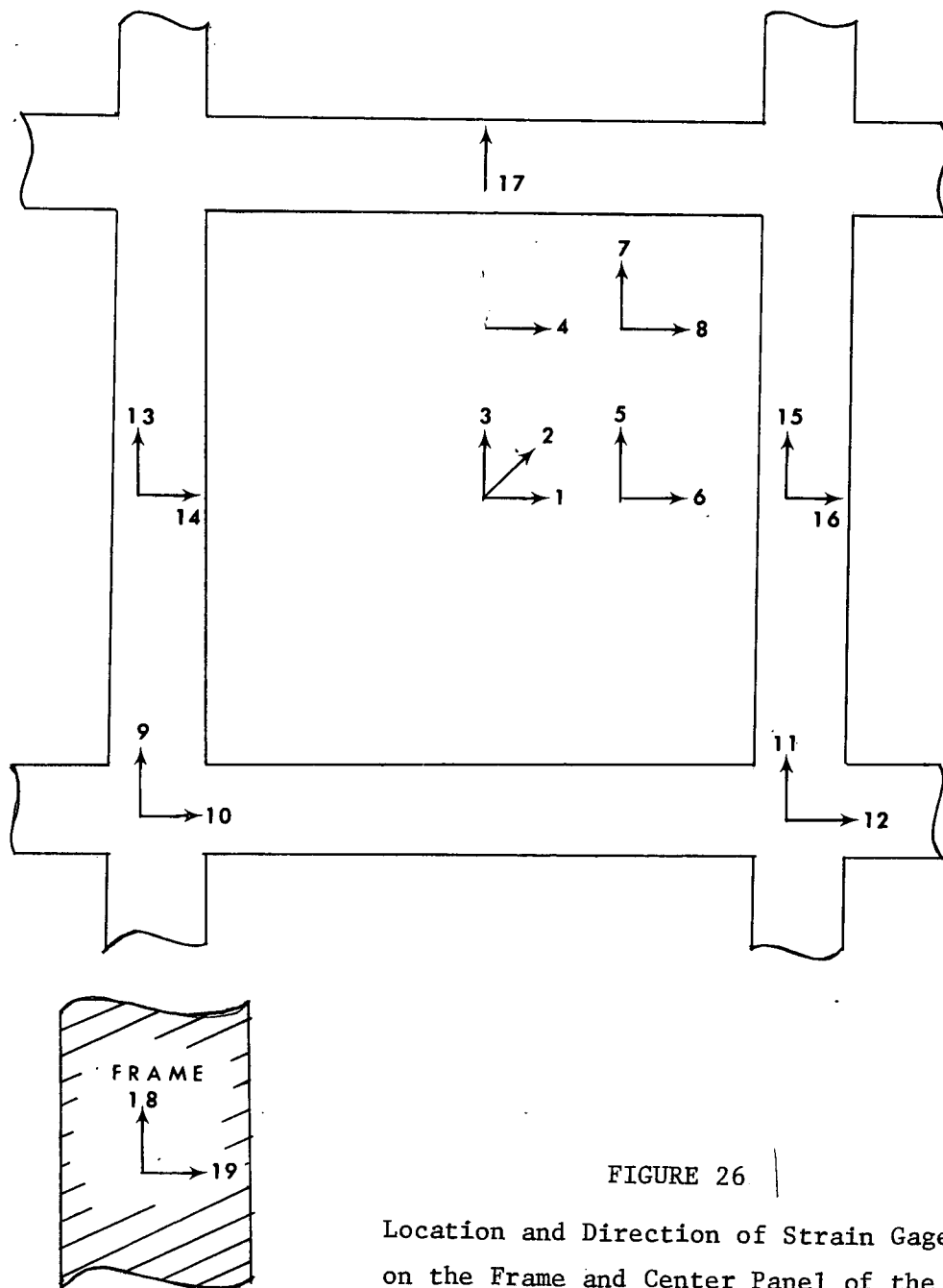
FIGURE 26

Location and Direction of Strain Gages
on the Frame and Center Panel of the Plate

produce L = ABC (ΔV), where L is the load in pounds force and ΔV is the change in voltage in volts.

The calibration constant A is determined by placing 50,000 and 220,000 hom calibration resistors (R_p) in parallel with the 120 ohm (R_G) strain gages. The ΔR is calculated from the equation (36),

$$R = R_G - \frac{R_G R_p}{R_G + R_p} \qquad (6-2)$$

in which the second term on the right hand side is the effective value of resistance created by the two resistors R_G and R_p acting in paralle. The two values of ΔR_5 = .29 ohms and ΔR_{20} = .07 ohms. See Appendix D for sample calculations. ΔR_5 is determined by using the 50,000 ohm calibration resistor in Equation (6-2), and ΔR_{20} is determined by using the 220,000 ohm calibration resistor. Values of voltage were recorded on a digital volt meter by switching the calibration resistors in and out of the circuit until the change in voltage (ΔV) was stabilized. (See Table 5.) An average value for ΔV was then determined. This procedure was repeated for both of the calibration resistors at each strain gage location. The calibration constant A is then calculated by the equation, A = ΔR/ΔV. The constant A is expected to be uniform for all the strain gages. since the initial value of resistance is the same for all gages. The experimental data substantiates this statement. A, equal to 0.274, represents an average value calculated for all strain gages shown in Figure 27. (See Appendix D for sample calculation.)

The calibration constant B is determined for the equation which defines the Gage Factor (F) in terms of resistance (R), change in resistance (ΔR), and strain (ε).

$$F = \frac{\Delta R/R}{\varepsilon} \quad \text{or} \quad \varepsilon = \frac{1}{RF} \Delta R$$

comparing the above equation with ε = BΔR, B is seen to be defined as 1/RF; R and F are given by the strain gage manufacturers (Micro-Measurement, Inc.) to be R = 120.8 ohms and F - 1.98. B is then calculated to be equal to .00418.

62

TABLE 5

Change in Voltage (ΔV) for Each Calibration Resistor at all Strain Gage Locations

Strain Gage Number	Initial D. C. Voltage	Final D. C. Voltage	120.8 Ohms in Parallel with
1	-.047	+1.000	50,000 Ohms
	-.020	+1.030	" "
	-.013	+1.037	" "
	-.036	+0.2050	220,000 Ohms
1	-.020	+0.1987	" "
	-.050	+0.190	" "
	-.057	+0.187	" "
	-.054	+0.190	" "
2	-.065	+0.997	50,000 Ohms
	-.066	+0.996	" "
	-.068	+0.995	" "
	-.070	+0.993	" "
	-.074	+0.988	" "
	-.072	+0.989	" "
2	-.065	+0.175	220,000 Ohms
	-.063	+0.178	" "
	-.063	+0.178	" "
	-.066	+0.175	" "
3	-.254	+0.698	50,000 Ohms
	-.240	+0.741	" "
	-.43	+0.62	" "
	-.41	+0.63	" "
	-.40	+0.65	" "
3	-.36	-0.13	220,000 Ohms
	-.34	-0.100	" "
	-.33	-0.099	" "
	-.121	+0.118	" "
	-.121	+0.933	50,000 Ohms
4	+.120	+1.162	50,000 Ohms
	+.111	+1.160	" "
	+.104	+1.148	" "
4	+.090	+0.313	220,000 Ohms
	+.070	+0.298	" "
	+.077	+0.301	" "
	+.072	+0.306	" "
5	+.010	+0.251	220,000 Ohms
	+.009	+0.250	" "

TABLE 5 (Continued)

Strain Gage Number	Initial D. C. Voltage	Final D. C. Voltage	120.8 Ohms in Parallel with
5	+.009	+1.067	50,000 Ohms
	+.010	+1.069	" "
6	+.064	+1.145	50,000 Ohms
	+.068	+1.150	" "
	+.068	+0.314	220,000 Ohms
	+.070	+0.319	" "
7	+.156	+0.400	220,000 Ohms
	+.153	+0.398	" "
	+.152	+1.220	" "
	+.147	+1.218	" "
8	..000	+1.050	50,000 Ohms
	..000	+1.060	" "
	..000	+0.227	220,000 Ohms
	-.016	+0.225	" "
	-.018	+0.222	" "
9	.000	+0.227	220,000 Ohms
	-.008	+0.264	" "
	-.003	+0.260	" "
	.000	+1.070	50,000 Ohms
	+.029	+1.075	" "
	+.050	+1.095	" "
	+.065	+1.108	" "
10	..030	+1.036	50,000 Ohms
	+.002	+1.040	" "
	+.008	+1.072	" "
	+.015	+1.077	" "
	+.035	+1.100	" "
	+.035	+0.284	220,000 Ohms
	+.040	+0.284	" "
	+.037	+0.283	" "
11	+.368	+0.564	220,000 Ohms
	+.365	+0.567	" "
	+.367	+0.570	" "
	+.370	+1.260	50,000 Ohms
	+.378	+1.270	" "

TABLE 5 (Continued)

Strain Gage Number	Initial D. C. Voltage	Final D. C. Voltage	120.8 Ohms in Parallel with
12	+.125	+1.165	50,000 Ohms
	+.126	+1.168	" "
	+.126	+0.360	220,000 Ohms
	+.130	+0.363	220,000 Ohms
13	+.025	+0.262	220,000 Ohms
	+.024	+0.261	" "
	+.027	+1.071	50,000 Ohms
	+.024	+1.070	" "
14	+.114	+1.184	50,000 Ohms
	+.120	+1.183	" "
	+.120	+0.364	200,000 Ohms
	+.122	+0.363	" "
15	+.068	+0.312	200,000 Ohms
	+.070	+0.312	" "
	+.074	+0.319	" "
	+.076	+0.318	" "
	+.078	+1.139	" "
	+.079	+1.140	" "
16	+.110	+1.160	50,000 Ohms
	+.117	+1.165	" "
	+.128	+0.365	220,000 Ohms
	+.110	+0.355	" "
17	-.001	+0.237	220,000 Ohms
	-.028	+0.236	" "
	-.024	+1.053	50,000 Ohms
	-.008	+1.053	" "
18	+.021	+1.070	50,000 Ohms
	+.010	+1.072	" "
	+.016	+0.240	220,000 Ohms
	+.009	+0.243	" "
19	+.048	-0.316	220,000 Ohms
	+.045	-0.316	" "
	+.045	+1.117	50,000 Ohms
	+.043	+1.120	" "

TABLE 6

Values of Strain in Micro-Inches per Inch for
Various Loads at Selected Strain Gage Locations

Strain Gage Number	Loads at Corresponding Strain Gage Number (Pounds Force)							
	0	1	5	10	15	20	25	30
1	10,000	9,993	9,966	9,935	9,905	9,876	9,848	9,820
2	10,000	9,993	9,964	9,927	9,890	9,859	9,822	9,790
3	10,000	9,993	9,967	9,937	9,905	9,875	9,840	9,820
5	5,000	4,990	4,954	4,911	4,869	4,832	4,793	4,758
6	5,000	4,991	4,961	4,924	4,889	4,848	4,818	4,785
7	10,000	9,994	9,966	9,929	9,890	9,859	9,824	9,792
8	5,000	4,994	4,965	4,926	4,889	4,856	4,822	4,790
13	5,000	4,988	4,944	4,888	4,834	4,780	4,726	4,674

The calibration constant C is determined from the data recorded in Table 6. This data was recorded by loading the plate at the desired points of interest and recording the change in strain (ε) due to the applied loads (L). The constant C is then calculated by the equation, $C = L/\varepsilon$. As noted previously, strain gages were not set at all lumped mass points. An average value of the five points was used for all points. (A sample calculation is shown in Appendix D.) The value for C is determined to be equal to $.144 \times 10^6$. The conversion constant relating load (L) and voltage (ΔV) may now be determined by multiplying the three calibration constants A x B x C. This calculation is performed in Appendix D, the resulting conversion constant is equal to 165.5. The equation defining the conversion from volts to pounds force can now be written as $L - 165.5\ \Delta V$.

The second calibration constant, which relates volts to inches, is obtained by adding another linear equation to the set of three equations utilized in the above calibration. This equation, $\delta = DL$, relates deflections (δ) and the (L) through the conversion factor (D), which is seen to be the influence coefficients of the system. Solving this latter equation for $L = \delta/D$ and substituting in the above conversion between volts and pounds force, one obtains $= 165.5\ D\Delta V$. This conversion equation is a function of location on the plate and will be evaluated for each point at which both experimental and analytical data is available. (See Table 7.)

The equipment utilized in performing the experimental test is shown in Figures 23,24,25. Figure 23 shows the plate and frame in the foreground and strain sensing and recording equipment in the background. Figure 25 shows the equipment inside the Mobile Instrumentation Unit which was used to sense and record nineteen channels of dynamic strain and will be further described. Figure 24 shows the control center on the right, the Mobile Instrumentation Unit at right center, the exponential horn with the plate and frame mounted near its mouth at left center, and the pressurized air storage vessels on the left.

The strain sensing equipment seen in the background of Figure 23 consists of two Baldwin-Lima-Hamilton Strain Indicators and balancing units, a Honeywell galvanometer oscillograph, and a Tektronix Memory Oscilloscope.

TABLE 7

Evaluation of $\delta = 165.5D \, \Delta V$

| Mass	D(from table 2)	165.5D	ΔV = Peak Value of rms Response (Volts)	δ = Deflection in Inches
1	.00127	.2100	.0675	.01418
2	.00083	.1372	.060	.00824
3	.00102	.1688	.065	.01097
4	.00100	.1655	.064	.01059
5	.00098	.1620	.0565	.00915

The equipment seen in Figure 25 consists of a bank of signal conditioners
in the upper right hand corner, and a bank of amplifiers in the lower right
center of the figure. A multiplexing unit is located in the lower center
foreground. A nine track Lockheed tape recorder is seen on the table in
the upper left hand corner along with the direct current power source lo-
cated in the left center background. The control center in Figure 24 con-
tains the necessary equipment for operating the exponential horn. Included
in this equipment is a variable frequency signal generator, a bandwidth
limiting noise signal generator, and an amplifier. Switches for con-
trolling the flow of the compressed air from the pressurized air storage
vessels to the vibrator baffles of the horn are also located in the con-
trol center. The exponential horn shown in Figure 24 has a profile which
is described by an exponential function. It was rotated to the position
shown in Figure 24 and the plate was adjusted in the crow's nest in the
position shown such that the plane of the plate and the plane of the mouth
of the horn were parallel. This insured that an acoustical wave impinging
on the plate from the horn would impact the plate with normal incidence.
The radius of curvature of the wave leaving the mouth of the horn is so
much greater than the dimensions of the plate that this wave can be as-
sumed to be plane. A near field test on the acoustical pressure field
impinging on the plate verified this assumption. Figure 32 (a, b, c)
shows the correlation between the amplitude and the phase angle along
three radial lines in the plane of the plate. The four individual curves
represent the four radial distances at which the pressure was recorded.
The radial distances from the center of the plate are 0, 10, 20, and 30
inches. The three radial lines along which these four pressure measure-
ments were recorded are oriented with the horizontal y axis (a), the
vertical z axis (c), and the 45 degree diagonal connecting the corners
of the plate (b). These curves substantiate the assumption that the
acoustical field is uniform over the entire area occupied by the plate.
The curves shown in Figure 32 represent an 80 Hz pure tone. The same
series of test was performed for a 500 Hz pure tone to determine if fre-
quency has an effect on the pressure distribution. The relationship between

69

amplitude and phase angles at the various locations of the 500 Hz pressure field were the same as the ones for the 80 Hz pressure field. This substantiated the assumption that the pressure is uniform over the area occupied by the plate regardless of its frequency. This statement is interpreted to state that a random pressure field emmitted from the horn will produce a uniform pressure field in the plane occupied by the plate.

The block diagram shown in Figure 27 represents the path followed by the experimental data from its generation at the plate in the form of strain to the final results represented by the power spectral density plots and the maximum root mean square deflections. The plate and horn system is composed of the plate instrumented with nineteen strain gages, the frame, the structure supporting the plate and frame, and the exponential horn. The exponential horn generates the random acoustical field which excites the plate, causing the deflections of the plate to change the resistance of the strain gages. Each strain gage is wired into a full Wheatstone bridge circuit located in the signal conditioners. The change in resistance is converted to an equivalent change in voltage as determined by the calibration constant. The resulting change in voltage is directed into amplifiers which increase the voltage from millivolts to volts (a factor of one thousand). The resulting magnified voltage is sent into the multiplexing unit along with a one volt calibration signal. The multiplex system stores the change in voltage on a high frequency carrier. The five different carrier frequencies used to record the different channels of voltage are 200, 300, 400, 500, and 600 KHz. The data was then recorded on the odd numbered (1, 3, 5, 7, 9) tracks of a nine track tape. Five multiplex signals were recorded on each track, except track number nine which contained three channels of excitation data. The calibration signal was recorded on each channel before each test for a period of one minute. The calibration signal was a 1 volt, 80 Hz pure tone generated from a 155 decibel sound source (See Figure 28).

Figure 28 shows the power level and the time duration of the four excitations produced by the exponential horn. The figure shows the last few seconds of the calibration signal starting at time equal zero. The

70

FIGURE 27: Block Diagram of Experimental Test

FIGURE 28: Power Level and Duration of
Excitation Applied to the Plate
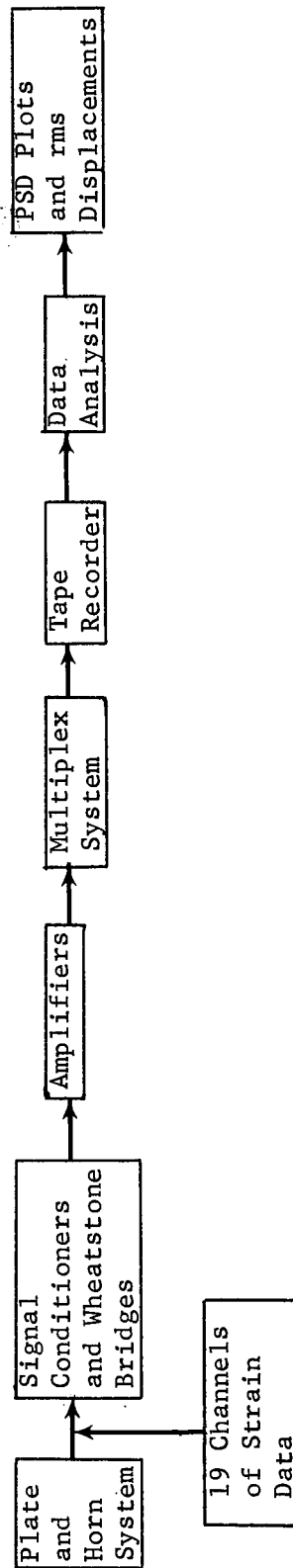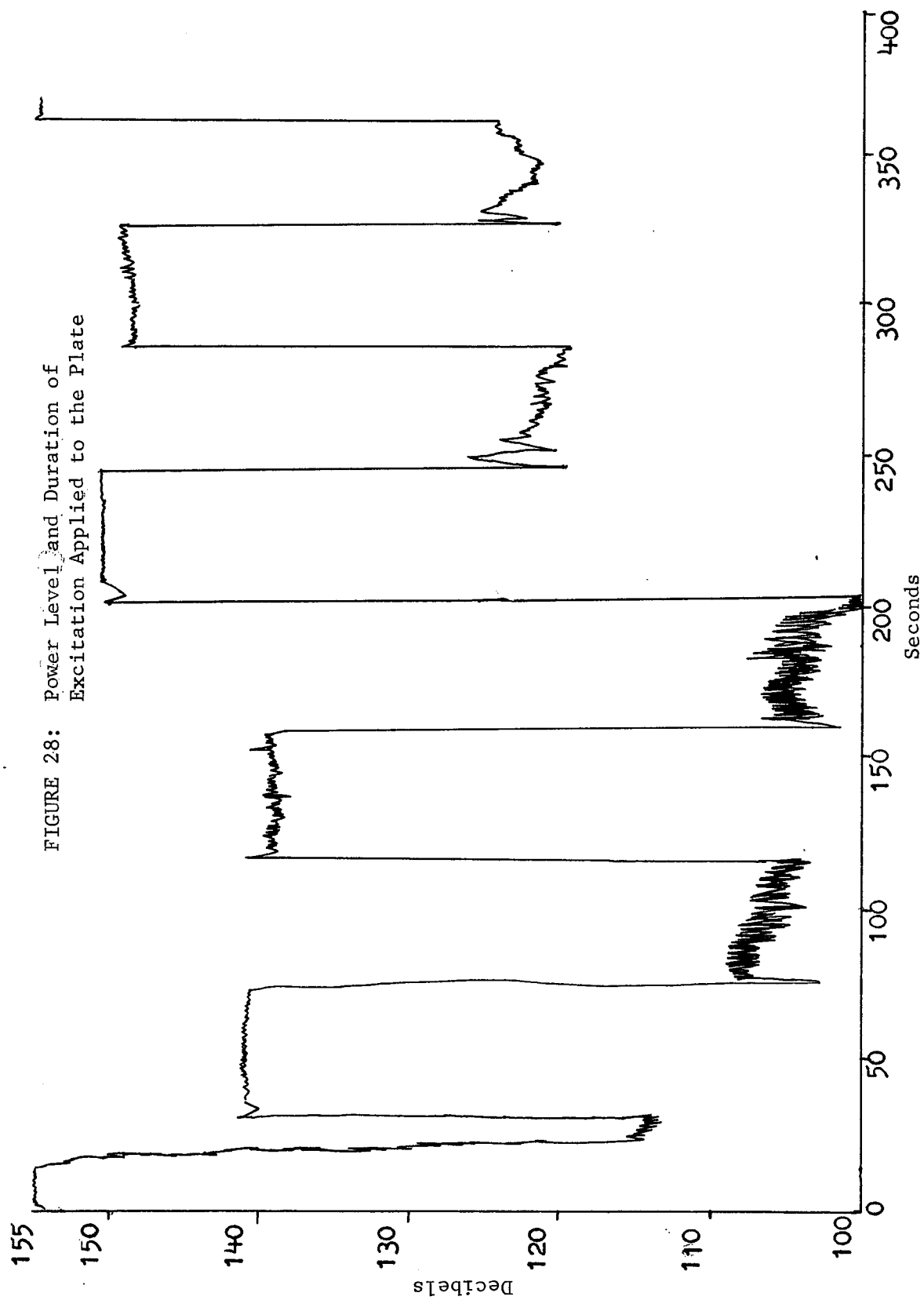
signal drops down to the background level of 80 Hz pure tone excitation. After 45 seconds of 80 Hz excitation, the signal drops down to the noise floor for 45 seconds. The next 45 seconds of excitation consist of 139 decibels of random excitation having the same frequency spectrum as shown in Figure 2. After another 45 seconds of noise floor, the output power of the horn is raised approximately 10 more decibels. The same sequence of excitation described above is repeated at the higher power levels. The sequence of excitations is as follows: 80 Hz excitation for 45 seconds at 151 decibels, 45 seconds of noise floor, and back to the calibration level. The only excitation used in the data analysis is the 149 decibels of random excitation for 45 seconds. The other tests were performed only to check the signal quality generated by the strain gages and the general behavior of the system.

The analysis of the data consists of printing the raw data and determining the root mean square value, the amplitude spectrum of the data (Figure 29), the probability density of the data (Figure 30 and 31), and the power spectral density of the data (Figures 2, 17, 18, 19, and 20).

Figure 29 is a representative slice of the data recorded by strain gage number 2. The amplitude spectrum indicates the location of the natural frequencies in the frequency spectrum and the amount of amplitude associated with each frequency. The plot of the raw data shows the particular section of data being analyzed. The root mean square plot shows the root mean square in volts of the data as a function of time. These root mean square plots are scanned to locate the maximum root mean square values of the data. (See ΔV in Table 7.) These maximum values will be converted through the use of the calibration constants to the maximum root mean square deflections of the plate in inches. (See δ in Table 7.)

Figures 30 and 31 represent the probability density plots of the response at strain gage number 2 and of the excitation respectively. Figure 31 represents a nearly perfect Guassian distribution which, as Lin (11) indicates, determines the excitation to be at least stationary. The probability density of the response (Figure 30) represents a near perfect Guassian distribution, and by Lin (11) determines the response to be

FIGURE 29

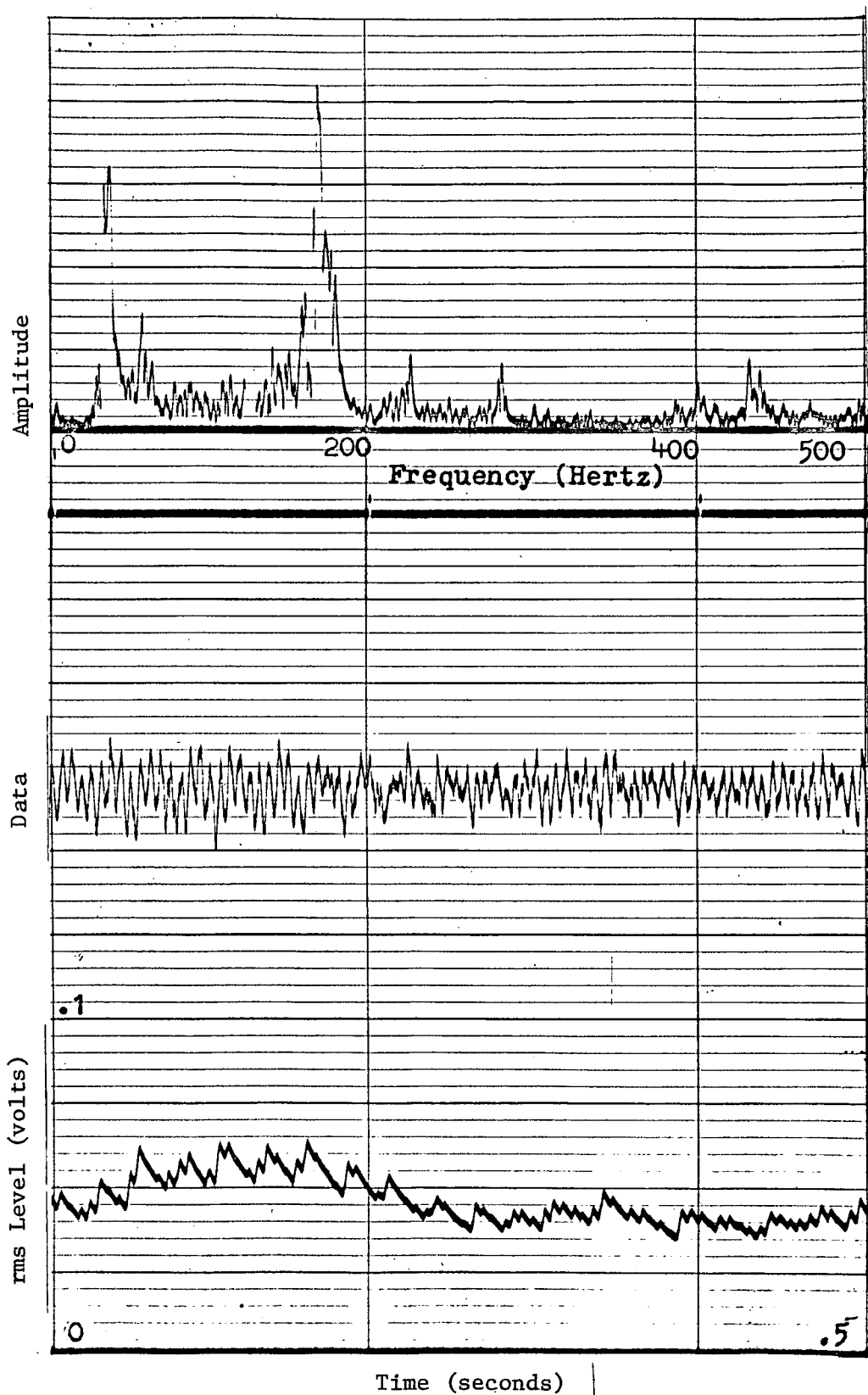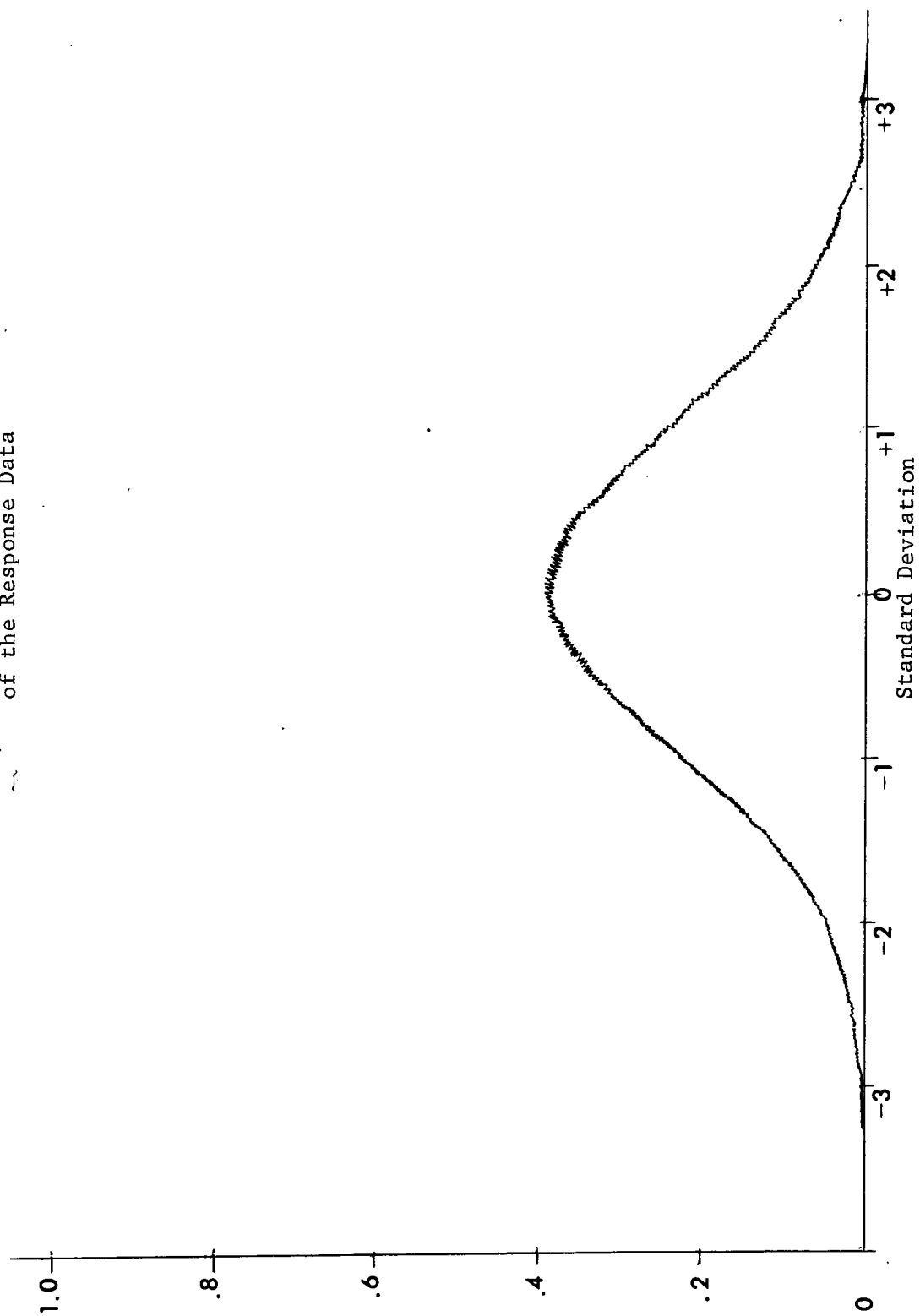Amplitude Spectrum, Data, and rms Level

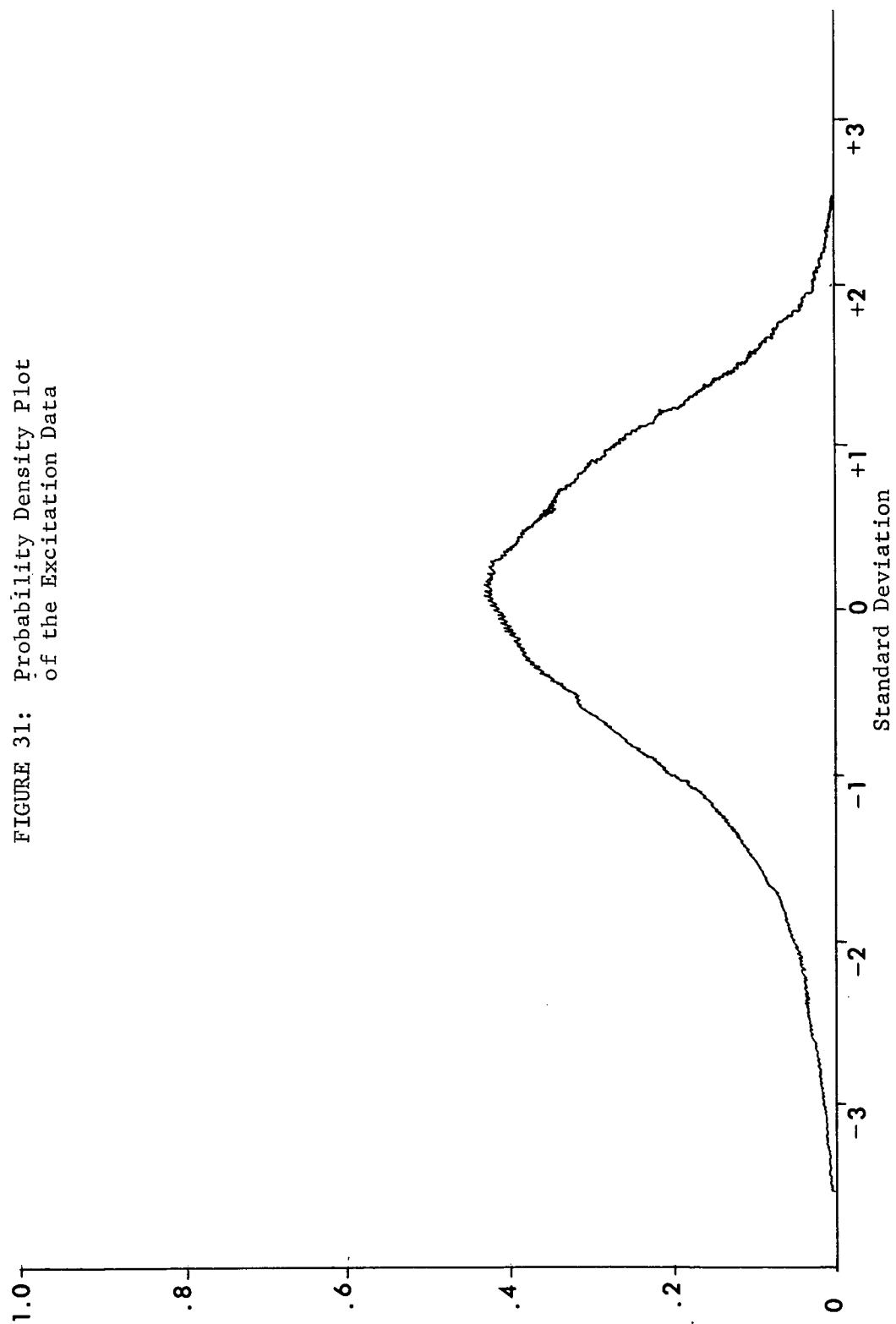FIGURE 30: Probability Density Plot
of the Response Data

FIGURE 31:   Probability Density Plot
             of the Excitation Data

Standard Deviation

Fig. 32

Halftone Neg.

(Captions on separate flat)

NOT REPRODUCIBLE

strongly stationary or analogously the steady state condition of the deterministic theory. Lin also states that given an excitation whose probability density has a Gaussian distribution and a structural system which is linear, the output response of the system will have a probability density which has a Gaussian distribution. Figures 30 and 31 verify this statement and also the assumption made in Section 3 regarding the excitation being at least weakly stationary.

The power spectral density plot of the excitation shown in Figure 2, along with Figure 31, contains all the information required to completely define the random excitation. The power spectral density plots of the response data shown in Figures 17, 18, 19, and 20 contain the necessary information to completely describe the response. These plots can be used to determine the natural frequencies of the system and the power stored at all of these frequencies. Integration of the response power spectral density curves produces the mean square response of the plate. Using the square root of this quantity and converting to the proper units, the root mean square displacements of the plate in inches are obtained. (See δ in Table 7.)

7. COMPARISON OF ANALYTICAL AND EXPERIMENTAL RESULTS

The results obtained from the analytical and experimental work described in Sections 3 through 6 are compared and discussed in this section. Plausible explanations are given for the differences between the analytical and experimental results. The particular results are discussed in terms of the power spectral density plots and the root mean square deflections. The accuracy of approximating this plate with a network of beams is also discussed.

Figures 4 and 17 represent the analytical and experimental power spectral densities of the response at the center of the plate. The general trend followed by both these curves is in good agreement. The magnitude of the peaks tend to decrease with an increase in frequency in both the analytical and experimental cases. The frequency (37 Hz) of the first natural frequency predicted analytically agrees very well with the experimentally measured value of 38 Hz. The magnitude of these two peaks also agree quite well. In this discussion, the peaks in the power spectral density plots imply a natural frequency exists at that frequency. The peak having the greatest amount of power is the first fundamental frequency of the system. The importance of the agreement between experimental and analytical values of magnitude and frequency at the first natural frequency of the system is realized when one applies this analysis to the solution of vibration problems. The magnitude and the frequency of the first natural frequency of a structure is usually the most important information needed to solve vibration problems associated with the structure. Good agreement of the analytical and experimental frequency of the last peak (430 Hz) on the power spectral density plots is also observed. The magnitude of this analytical peak is low as compared to the magnitude of the experimental peak. This trend of low values of magnitude for the analytical peaks is consistent throughout the entire frequency spectrum with the exception of the peaks at or near the first natural frequency of 37 Hz. This trend becomes more pronounced as the frequencies increase. The experimental and analytical frequencies of the system indicated by the peaks in the

power spectrum tend to agree very well through the entire frequency range. The only exception is a peak at 60 Hz in the analytical power spectrum whose magnitude is two orders higher than the peak indicated by the first natural frequency noted above. The trend of the small disagreement between values of frequency for the peaks, particularly in the midband frequencies from 100 to 400 Hz, is for the analytical frequencies to be higher than the experimental frequencies. Located at approximately 10 Hz in the experimental power spectral density plot, a peak is observed which does not show up on the analytical plot. This discrepancy can be explained by realizing also the reason for the shift of natural frequencies to higher values on the analytical plots. One reason the analytical natural frequencies are slightly high is because the entire structure supporting the plate and horn system is not included in the lumped parameter model of the system. Only the crow's nest, shown in Figure 22 as the platform protruding out from under the mouth of the exponential horn is included in the model of the system. The remainder of the supporting structure, including the horn itself, is not accounted for in the analysis. The effect on the natural frequencies of the system of including the entire structure which supports the horn and plate would be to shift the lowest analytical natural frequencies to a lower value and essentially leave the higher natural frequency unchanged except for a small overall shift to lower values of frequency. It is proposed that the value of frequency to which the lowest frequency would be shifted would coincide with the peak at 10 Hz shown on the experimental curve. The shift of the other analytical natural frequencies to lower values would tend to bring these values into bett agreement with the experimental values. The peak at 60 Hz which would be shifted to a lower value would then exist as the only peak on the experimental curve which does not match with a corresponding peak on the experimental curve. A possible remedy for correcting this problem is to distribute the mass in such a manner that more mass is located at the center of the plate. This modification would have the effect of lowering the magnitude and frequency of the response near 60 Hz. This idea will be pursued after a comparison is made of the next two power spectral density plots.

80

Figures 5, 18, and 19 are representative of the analytical and the experimental response power spectral densities of a lumped mass at the intersection of two stringers on the plate. Both the analytical and experimental curves possess the same trend which is the decrease in response power as the frequencies increase. The only exception to this trend is a peak on the experimental curve at approximately 430 Hz which is not predicted on the analytical curve. This indicates that too much mass is allocated to the lumped mass points in the peripheral area of the plate near the frame. Allocating less mass to each lumped mass point near the frame and adding more lumped mass points in this area will cause the magnitude of the response peaks to increase at the higher frequencies. This new distribution of the mass toward the center panel area will also cause the frequency of the lower modes to decrease. If this distribution of the mass is accomplished in an optimum fashion, the two peaks located at 37 and 60 Hz would be shifted to match the experimental peaks at 10 and 37 Hz. The general tendency of the analytically determined magnitude of the peaks, particularly at the higher modes of vibration, to be higher than the corresponding experimental magnitudes would be rectified. The analytical peak at 60 Hz can be diminished by placing several more lumped mass points in the area of the central panel. Inclusion of these mass points at the center of the stringers which surround the center panel and at points on the center panel near the stringers would have the effect of distributing the response over several frequencies in the neighborhood of 60 Hz. These additional natural frequencies could be adjusted by proper allocation of the mass to the new lumped mass points. The net effect would be to reduce the single peak at 60 Hz to a group of smaller peaks, as seen in Figurer 18 and 19 in the frequencies neighboring 60 Hz.

The central portion of the frequency bandwidth from 100 to 400 Hz in Figures 5, 18, and 19 match very well on both the analytical and experimental curves in that no major peaks are observed on either of the curves in this frequency range. This type of response is expected since the lumped mass point is located at the intersection of two stringers, which is the stiffest point in the central area of the plate. The stringers

have a tendency to become node lines for all modes of vibration higher
than the second mode and are exactly node lines for the third, sixth,
ninth and twelfth modes of vibration. This tendency has the effect of
allowing this lumped mass point to respond primarily to only the first
and second modes of vibration. This tendency is observed on the curves
in Figures 5, 6, 7, 8, 18, and 19.

Figures 11 and 20 represent the analytical and experimental response
power spectral densities at two points which are not geometrically equiv-
alent, but are located sufficiently close to one another to observe simi-
larities in their power spectral densities. Figure 11 represents the
response power spectral density of lumped mass number 8 (Figure 3) and
Figure 20 represents the response power spectral density of strain gage
16 (Figure 26). The root mean square displacements of the two points in
question are not expected to compare favorably, but the power spectral
densities do show some similarities in natural frequencies between the
two points. Bascially, the same similarities which were observed for the
two previous sets of response power spectral density plots are observed
for this pair of curves. The decreasing power of the response peaks as
the frequency increases is observed for both these curves. The first and
last natural frequencies at 37 and 430 Hz respectively, match very well
on both curves. The magnitudes of these peaks do not match as is expected.
The correlation between the experimental and analytical peaks in the mid-
bank frequencies of 100 to 400 Hz is good, but has the same shift of
analytical frequencies to higher values. The analytical peak of 60 Hz is
again the only major difference in natural frequencies between the two
curves. Although the two response points being discussed are not equiv-
alent points, the same basic similarities noted in their power spectral
densities as observed at the other points already compared indicate that
the entire plate possesses these similarities between the experimental
and analytical results. Figures 9, 10, 11, 12, and 20 support this
observation. Figures 13, 14, 15, and 16, which represent the power spectral
densities of the lumped masses at the corner panels, possess most of the
same characteristics noted in the comparison between Figures 11 and 20,

82

and, in general, also support the above observation. Correlated with this observation is the observation that the modifications suggested to improve the analytical results would apply over the entire plate.

The modifications needed in the analytical model, as noted above, would redistribute the mass such that more mass is included near the center of the plate. This additional mass near the center of the plate is coupled with a corresponding decrease in the mass at the lumped points near the fixed boundary of the plate. An increase in the number of lumped mass points, particularly at the midpoint of the stringers, is also needed. The entire supporting structure of the plate and horn should be included in the lumped parameter model of the system.

The effect of these analytical modifications would be to shift the analytical natural frequencies associated with each peak in the response power spectral density plots to lower values of frequency. The first and second natural frequencies would be shifted the greatest amount, and the highest natural frequency would be shifted the least amount. The overall level of power associated with the peaks at the higher frequencies would be increased with respect to the power level at the lower frequencies. All these effects on the analytical response power spectral density would tend to make the resulting curves more similar to the experimental curves.

A comparison of the maximum root mean square deflections determined both analytically and experimentally, is displayed in Table 1. The error indicated in this table is the percent deviation of the analytical results obtained by integrating Equation 3-12 from the experimental results. The error between the experimental results and the results of utilizing Equation 3-14 is in every case greater than the error shown for Equation 3-12 . The results obtained by using Equation 3-14 are approximately 100 percent greater than the results of Equation 3-12 and do not predict the experimental results as well as Equation 3-12 . These comparisons indicate that Equation 3-12 is not a very good approximation to Equation 3-12 for the particular excitation power spectral density shown in Figure 2. The maximum deviation between the experimental and analytical (Equation 3-12) amplitudes is only 41.0 percent. Considering the complexity

of the system involved and the fact that by definition a random vibration
defies explicit definition, the 41.0 percent error represents an excellent
analytical prediction. Unfortunately, not enough experimental data points
were recorded to compare with all of the analytical points.

Table 4 lists the fourteen natural frequencies calculated by using
the experimentally measured and the analytically calculated influence
coefficients. The analytical influence coefficients are determined by
approximating the plate with a dense network of beams in which all inter-
sections of beams are made rigid. The experimental influence coefficients
are measured by recording the deflections of the plate due to calibrated
point loads. The two sets of influence coefficients are listed in Tables
2 and 3, but comparing the influence coefficients at each point in the
matrix is not an efficient method of comparison in this case. A better
comparison is to observe the effect these two sets of influence coefficients
have on the results of this problem. The entire effect of the influence
coefficients on this problem is transmitted through the eigenvalues (natural
frequencies) and eigenvectors of the system. The analytical eigenvectors
are altered slightly from the experimental eigenvectors, and the effect
on the eigenvalues is represented in Table 4 by the natural frequencies.
The maximum root mean square values calculated by using the analytical
influence coefficients are altered by a maximum of 6 percent from the
values calculated by using Equation 3-12 and the experimental coefficients.
In most cases, these influence coefficients' root mean square amplitudes
are better approximations to the experimental amplitudes than the ones
given by Equation 3-12 in Table 1. Generally, the influence coefficients
determined by the analytical method described in Section 4 are a good
approximation to the actual values and particularly for the purposes of
this problem produce very good results.

8. CONCLUSIONS AND RECOMMENDATIONS

Conclusions

A lumped parameter analysis of a non-homogeneous plate subjected to a random excitation produced maximum root mean square displacements which compare very well to the results obtained by experimental tests. Results from the experimental work when compared to the analytical show a range of error from 19.1 to 41.0 percent.

The lumped parameter analysis yields its best predictions of the experimental power spectral densities at the lower frequencies of vibration. The error of predicting the power level associated with each peak increases as the frequency increases and ranged from an error of less than one order of magnitude at the lower frequencies to four orders of magnitude at 500 Hz.

For the particular excitation utilized in this investigation, integration of Equation 3-12 with the actual excitation produces values of maximum root mean square displacements which compare much more favorably with the experimental results than the results produced by utilizing the "white noise" approximation of Equation 3-14 and the average value of the excitation.

The accuracy of predicting the peaks in the response power spectral densities of the plate in question is strongly dependent on the proper distribution of mass to the various lumped mass points. The distribution of mass and the insufficient number of lumped mass points utilized in this investigation are the major reasons a peak in the response power spectral density plots at 60 Hz contained an erroneously large amount of power.

An increase in the number of lumped mass points and the proper distribution of mass to these points will also alleviate the problem of predicting low power levels at the higher frequencies.

The influence coefficients of the plate can be predicted sufficiently well for this investigation by representing the plate as a dense network of beams. The error in predicting the natural frequencies is less than 3.5 percent for the first thirteen natural frequencies.

The damping ratio can be regarded as a constant with respect to location on the plate, and as a variable with respect to frequency of vibration. This is veritied by experimentally measuring the damping ratio (Figure 21) as both a function of location and frequency.

This method of analysis for non-homogeneous plates has the basic qualities of simplicity and accuracy, and may be applied to a wide variety of oddly shaped structures with an ease not found among other methods of analysis.

Recommendations

The effect of various distributions of mass to the lumped mass points on the response of plates should be studied. Homogeneous plates subjected to pure tones could be the first phase and the complexity of this study increased until it includes non-homogeneous plates subjected to random excitations. The object of the study would be to determine the optimum proportions for allocating mass to the lumped points in order to predict the response accurately. Hopefully, the study will lead to a set of rules or guidelines which may be used to allocate mass to thellumped points in any lumped parameter analysis of plates.

After the proper allocation of mass to the different areas of the plate have been determined, obtain a relationship between the number of lumped masses used in modeling the plate and the resulting error of the predicted response. This information would be extremely valuable to persons trying to make the most efficient lumped parameter analysis of a plate.

Study the versatility, reliability, and limitations of using a network of beams to approximate the influence coefficients of a variety of oddly shaped plates.

Study the tendency of the damping ratios for a plate to exhibit a sinusoidal variation in magnitude as a function of frequency. Particularly, study the behavior of the damping ratios at very low and very high frequencies.

86

APPENDIX A

DETERMINATION OF THE TRANSFORMATION WHICH
UNCOUPLES THE EQUATIONS OF MOTION

The purpose of this appendix is to determine the conditions under which a damped dynamic system possess classical normal modes. It is shown that a necessary and sufficient condition for a damped dynamic system to possess classical normal modes is that the damping matrix be diagonalized by the same transformation which uncouples the undamped system. This transformation is accomplished by the normalized eigenvectors of the system.

In general, the coupled equations of motion for an N degree of freedom linear dynamic system with lumped parameters may be written in matrix notation as:

$$[m] \{\ddot{g}\} + [c] \{\dot{g}\} + [k] \{g\} = \{f(t)\} \qquad (A-1)$$

where $[m]$, $[c]$, and $[k]$ are positive definite and symmetric. The homogeneous equation is simply,

$$[m] \{\ddot{g}\} + [c] \{\dot{g}\} + [k] \{g\} = 0 \qquad (A-2)$$

The undamped homogeneous equation is determined when $[c]$ and $\{f(t)\}$ are equal to zero.

$$[m] \{\ddot{g}\} + [k] \{g\} = 0 \qquad (A-3)$$

Let $[\theta]$ be the transformation which makes $[m]$ a diagonal matrix when multiplied in this form $[\theta]^T [m] [\theta]$. This transformation necessarily exists because of the symmetry of $[m]$.

Define

$$\{g\} = [\theta]\{x\} \tag{A-4}$$

and substitute into Equation A-2.

$$[m][\theta]\{\ddot{x}\} + [c][\theta]\{\dot{x}\} + [k][\theta]\{x\} = 0 \tag{A-5}$$

Premultiply Equation A-5 by $[\theta]^T$.

$$[\theta]^T[m][\theta]\{\ddot{x}\} + [\theta]^T[c][\theta]\{\dot{x}\}$$
$$+ [\theta]^T[k][\theta]\{x\} = 0 \tag{A-6}$$

Define

$$[\theta]^T[m][\theta] = [\bar{m}] \text{ a diagonal matrix}$$

$$[\theta]^T[c][\theta] = [\bar{c}]$$

$$[\theta]^T[k][\theta] = [\bar{k}] \tag{A-7}$$

Since $[m]$, $[c]$, and $[k]$ are positive definite and symmetric matrices, $[\bar{m}]$, $[\bar{c}]$, and $[\bar{k}]$ will also be positive definite and symmetric. Substituting the terms defined in Equation A-7 into Equation A-6 one obtains

$$[\bar{m}]\{\ddot{x}\} + [\bar{c}]\{\dot{x}\} + [\bar{k}]\{x\} = 0 \tag{A-8}$$

The $[\bar{m}]$ matrix in Equation A-8 is reduced to the identity matrix by defining

$$\{p\} = [R]\{x\} \tag{A-9}$$

where

$$[R] - [\sqrt{\bar{m}}] \tag{A-10}$$

88

and substituting in Equation A-8.

$$[R]\{\ddot{p}\} + [\bar{c}][R]^{-1}\{\dot{p}\} + [\bar{k}][R]^{-1}\{p\} = 0 \qquad (A-11)$$

Premultiply Equation A-11 by $[R]^{-1}$.

$$[R]^{-1}[R]\{\ddot{p}\} + [R]^{-1}[\bar{c}][R]^{-1}\{\dot{p}\}$$
$$+ [R]^{-1}[\bar{k}][R]^{-1}\{p\} = 0 \qquad (A-12)$$

Define

$$[I] = [R]^{-1}[R] \text{ Identity matrix}$$

$$[A] = [R]^{-1}[\bar{c}][R]^{-1}$$

$$[B] = [R]^{-1}[\bar{k}][R]^{-1} \qquad (A-13)$$

Substitute Equations A-13 into Equation A-12.

$$[I]\{\ddot{p}\} + [A]\{\dot{p}\} + [B]\{p\} = 0 \qquad (A-14)$$

[A] and [B] are positive definite and symmetric matrices and according to Hildebrand (38) may be diagonalized simultaneously by a single transformation if and only if the two matrices [A] and [B] commute. See Bellman (39). Let [V] be the transformation such that

$$[V]^T[A][V] = [a] \text{ is a diagonal matrix} \qquad (A-15)$$

and

$$[V]^T[B][V] = [b] \text{ is a diagonal matrix} \qquad (A-16)$$

Define

$$\{p\} = [V]\{n\} \qquad (A-17)$$

and substitute Equation A-17 into Equation A-14.

$$[V]\{\ddot{n}\} + [A][V]\{\dot{n}\} + [B][V]\{n\} = 0 \qquad (A-18)$$

Premultiply by $[V]^T$.

$$[V]^T [V] \{\ddot{n}\} + [V]^T [A] [V] \{\dot{n}\}$$
$$+ [V]^T [B] [V] \{n\} = 0 \qquad (A-19)$$

Substitute Equations A-15 and A-16 into A-19.

$$[V]^T [V] \{\ddot{n}\} + [a] \{\dot{n}\} + [b] \{n\} = 0 \qquad (A-20)$$

Equation A-20 represents the damped uncoupled system if and only if $[V]^T [V]$ is a diagonal matrix. If $[V]$ is normalized, this requirement becomes

$$[V]^T [V] = I \qquad (A-21)$$

Equation A-21 restricts the transformation described by Equation A-17 to be orthogonal.

It is noted that if the above transformations described by Equations A-4, A-9, and A-17 were applied to the undamped system described by Equation A-3, the required transformation would be the same as the above orthogonal transformation. It therefore follows that, if a damped system possesses classical normal modes, these modes are identical with the normal modes for the undamped system. The transformation matrix which uncouples the undamped system is composed of columns which are the eigenvectors of the system. The eigenvectors of the undamped system are, therefore, the proper transformation for uncoupling the equations of motion for the damped system described above.

APPENDIX B

INTEGRATION OF THE TRANSFER FUNCTION
SQUARED BY THE THEOREM OF RESIDUES

The transfer function (H) squared is defined as

$$|H(\omega)|^2 = \frac{1}{M^2 [(\omega_o^2 - \omega^2)^2 + (2 \xi\omega\omega_o)^2]} \qquad (B-1)$$

where

ξ = damping ratio
ω = frequency
ω_o = natural frequency
M = mass

The integral (I) of this function from $-\infty$ to $+\infty$ will be determined
by the theorem of residues. See James (15).

$$I = \int_{-\infty}^{\infty} |H(\omega)|^2 d\omega \qquad (B-2)$$

$$I = \int_{-\infty}^{\infty} \frac{d\omega}{M^2 [(\omega_o^2 - \omega^2)^2 + (2 \xi\omega\omega_o)^2]} \qquad (B-3)$$

The integrand of Equation B-3 which is a function of the real vari-
able ω is treated as a function of the complex variable z. The complex
function f (z) is defined to be

$$f(z) = \frac{1}{M^2 [(\omega_o^2 - z^2)^2 + (2 \xi\omega_o z)^2]} \qquad (B-4)$$

The complex function described by Equation B-4 has two simple poles
in the upper half complex plane and are determined by solving for the
zeroes of the expression enclosed by brackets in Equation B-4. These

91

poles are found to be

$$z_1 = \sqrt{1 - \xi^2} \, \omega_o + i\xi\omega_o$$

$$z_2 = \sqrt{1 - \xi^2} \, \omega_o + i\xi\omega_o \qquad\qquad (B-5)$$

The integral (I) of Equation B-3 is given by the theorem to be

I = 2 π i { The sum of the residues of f(z) in the upper complex plane}

The residues R_1 and R_2 in the upper complex plane are determined by

$$R_1 = (z - z_1) \, |f(z)|_{z = z_1} \qquad\qquad (B-7)$$

$$R_2 = (z = z_2) \, |f(z)|_{z = z_2} \qquad\qquad (B-8)$$

Equation B-6 can be represented as

$$I = 2 \pi i \, (R_1 + R_2) \qquad\qquad (B-9)$$

$$I = \frac{2 \pi i}{M^2} \left\{ \frac{z - \sqrt{1 - \xi^2} \, \omega_o - i \xi \, \omega_o}{\left[\omega_o - \left(\sqrt{1-\xi^2}\omega_o + i\xi\omega_o\right)^2\right]^2 + \left[2\xi\omega_o \left(\sqrt{1-\xi^2} \, \omega_o + i\xi\omega_o\right)\right]^2} \right.$$

$$\left. + \frac{z + \sqrt{1 - \xi^2} \, \omega_o - i \xi \, \omega_o}{\left[\omega_o^2 - \left(-\sqrt{1-\xi^2}\omega_o + i\xi\omega_o\right)^2\right]^2 + \left[2\xi\omega_o\left(-\sqrt{1-\xi^2}\omega_o + i\xi\omega_o\right)\right]^2} \right\} \quad (B-10)$$

Equation B-10 is reduced to

$$I = \frac{2\pi i}{M^2\omega_o^4} \left(\frac{\omega_o}{4i\xi} \right) = \frac{\pi}{2M^2\omega_o^3 \, \xi} \qquad\qquad (B-11)$$

92

Equation B-11 represents the integral of the transfer function squared from $-\infty$ to $+\infty$.

$$\int_{-\infty}^{\infty} H^2(\omega) = \frac{\pi}{2M^2 \omega_o^3 \xi} \qquad (B-12)$$

For the purpose of practical application the range of integration is reduced to 0 to ∞. Since the integrand of Equation B-12 is an even function the integral may be represented by

$$\int_{-\infty}^{\infty} H^2(\omega) = 2 \int_{o}^{\infty} H^2(\omega) = \frac{\pi}{2 M^2 \omega_o^3 \xi} \qquad (B-13)$$

thus

$$\int_{o}^{\infty} H^2(\omega) = \frac{\pi}{4 M^2 \omega_o^3 \xi}$$

APPENDIX C

COMPUTER PROGRAM

Preceding page blank |

```
****PROGRAM RANDOM****

THIS PROGRAM TAKES AN INFLUENCE COEFFICIENT MATRIX, DECOMPOSES IT INTO AN
UPPER TRI-DIAGONAL MATRIX, INVERTS IT AND PRODUCES THE STIFFNESS
COEFFICIENT MATRIX. THE MASS MATRIX IS COMBINED WITH THE STIFF MATRIX AND
USED TO COMPUTE THE EIGENVALUES AND EIGENVECTORS OF THE SYSTEM.
THE EIGENVECTORS ARE CONVERTED INTO A NORMALIZED FORM IN THE REAL SPACE
AND USED TO CALCULATE THE MODAL PARTICIPATION FACTORS. THE PROGRAM THEN
READS THE MODAL DAMPENING RATIO MATRIX AND THE EXCITATION POWER SPECTRAL
DENSITY. THE RMS DISPLACEMENT(IN.) FOR EACH LUMPED MASS IS DETERMINED
BY EXCITING EACH MASS AND SUPERIMPOSING THE DISPLACEMENTS DUE TO ALL
EXCITATIONS. THE POWER SPECTRAL DENSITY OF THE OUTPUT RESPONSE AT EACH
LUMPED MASS IS PLOTTED FOR THE FREQUENCY BANDWITH OF 6 TO 500 HZ.

PREPARED BY DENNIS J. BILYEU

K  = NO. OF CASES
NA = DIMENSION SIZE
N  = DEGREES OF FREEDOM
A  = INFLUENCE COEFFICIENT MATRIX
D  = DIAGONAL OF INFLUENCE COEFFICIENT MATRIX
AMASS = MASS MATRIX
E  = NATURAL FREQUENCIES(HZ)
F  = NATURAL FREQUENCIES(RAD/SEC)
V  = EIGENVECTORS
P  = MODAL PARTICIPATION FACTORS
HZ = FREQUENCY SPECTRUM (6-500HZ)
Z  = MODAL DAMPENING RATIO
W  = AVERAGE VALUE OF EXCITATION PSD (VOLTS**2/HZ)
X  = RMS DISPLACEMENT ASSOCIATED WITH W (IN)
WO = PSD OF RESPONSE (POUNDS FORCE**2/HZ)
XI = RMS DISPLACEMENT ASSOCIATED WITH WI (IN)
FA = AREA OVER WHICH FORCE IS APPLIED FOR EACH MASS
```

```
      DIMENSION A(14,14),Q(14,14),E(14),AMASS(14),SMASS(14),XMASS(14)
      DIMENSION P(14),F(14),X(14),Z(14),V(14,14),WO(502),HZ(502)
      DIMENSION IAT1(18),IAE1(18),WI(530),XD(500),IAX1(18),IAX2(18)
      DIMENSION IAX3(18),IAT2(18),IAT3(18),IAE2(18),IAE3(18)
      DIMENSION D(14),FA(14),FOR(14)
      COMMON ID9(15),BUF(3000),ID8(15)
      LOGICAL*1 C
      LOGICAL SKIP
      DATA C/'*'/
      SKIP=.FALSE.
      CALL PLOTS(BUF,3000)
      CALL PLOT(0.,1.5,-3)
      READ(5,2) ID9
      READ(5,2) ID8
    2 FORMAT(15A4)
      READ (5,4) IAT2
      READ (5,4) IAE1
      READ (5,4) IAE2
      READ (5,4) IAE3
    4 FORMAT(18A4)
      READ(5,3) K,NA
    3 FORMAT(2I3)
      READ(5,5) N
    5 FORMAT(I3)
      READ(5,30) (AMASS(I),I=1,N)
   30 FORMAT (8F10.6)
      READ(5,31) (FA(I),I = 1,N)
   31 FORMAT(14F5.1)
      WRITE(6,32)(FA(I),I = 1,N)
   32 FORMAT(F14.7)
      READ(5,130) (Z(J),J=1,N)
  130 FORMAT(10F7.4)
      READ(5,131) W
  131 FORMAT (F10.6)
      READ(5,250) (WI(M),M = 1,495)
  250 FORMAT(15F5.1)
```

```
      WRITE (6,13)
   13 FORMAT (1H1,20X,'MASS MATRIX',////)
      DO 35 I=1,N
      AMASS(I) = AMASS(I)/386.4
      WRITE (6,14) I,(AMASS(I))
      SMASS(I) = (SQRT(AMASS(I)))
      XMASS(I) = 1.0/SMASS(I)
   35 CONTINUE
   14 FORMAT (10X,I2,10X,F13.6,/)
      WRITE (6,15)
   15 FORMAT(1H1,15X,'DAMPING RATIOS',////)
      WRITE(6,14) (J,Z(J),J=1,N)
      DO 255 M = 1,495
      IF(WI(M).LT.0.0) GO TO 260
  255 WI(M) = WI(M)*10.**(-5)
      GO TO 1
  260 SKIP=.TRUE.
    1 DO 1000 L=1,K
      READ(5,10)((A(I,J),J=1,N),I=1,N)
   10 FORMAT(8E10.3)
      DO 310 I = 1,14
  310 D(I) = A(I,I)
      WRITE (6,11)
   11 FORMAT(1H1,20X,'INFLUENCE COEFFICIENT MATRIX',////)
      WRITE (6,12) ((A(I,J),J=1,N),I=1,N)
   12 FORMAT(10E12.3,/)
      CALL DECMPS(N,NA,A,EXIT)
      IF(EXIT.EQ.1.0) GO TO 100
      CALL INVERT(N,NA,A)
      GO TO 300
  100 WRITE(6,200)
  200 FORMAT(//,10X,'A ZERO OR NEGATIVE APPEARED ON THE DIAGONAL',////)
      GO TO 500
  300 WRITE(6,400)
  400 FORMAT(1H1,20X,'STIFFNESS MATRIX',///)
      WRITE(6,12)((A(I,J),J=1,N),I=1,N)
```

```
C       PRE-MULTIPLY AND POST-MULTIPLY THE STIFFNESS MATRIX BY
C       THE INVERSE OF THE SQUARE ROOT OF THE MASS MATRIX
C
        DO 40 I=1,N
        DO 40 J=1,N
        A(I,J)=A(I,J)*XMASS(I)*XMASS(J)
40      CONTINUE
        CALL JACOB(E,Q,NA,A,NA,N,+1)
C
C       TRANSFORM EIGENVALUES INTO FREQUENCIES AND EIGENVECTORS INTO
C       ORIGINAL COORDINATE SYSTEM
C
        WRITE (6,55)
55      FORMAT(1H1,20X,'NATURAL FREQUENCIES (HZ)       ',////)
        DO 60 I=1,N
        F(I) = SQRT(E(I))
        E(I) = F(I)/(2o0*3o1415927)
60      WRITE (6,65) I,E(I)
65      FORMAT(10X,I2,10X,F13o7,/)
        DO 80 J=1,N
        DO 80 I=1,N
        V(I,J) = Q(I,J)*XMASS(I)
80      CONTINUE
        AREA =0o
        DO 81 I = 1,N
81      AREA = AREA+FA(I)
        WRITE (6,86) AREA
86      FORMAT(10X,'TOTAL AREA OF STRUCTURE   =',2X,F8o3,2X,'INCHES**2')
C
C       CALCULATION OF MODAL PARTICIPATION FACTORS AND GENERALIZED FORCE
C
        NN = 13
        DO 82 I = 1,NN
        SUM = 0o
        DUM = 0o
```

```fortran
      DO 83 J = 1,N
      SUM = SUM+FA(J)*V(J,I)
   83 DUM = DUM+AMASS(J)*V(J,I)**2
      FOR(I) = SUM
   82 P(I) = 100/DUM
      WRITE (6,101) (I,FOR(I),I = 1,NN)
  101 FORMAT(10X,I2,10X,E14.7,/)
      WRITE (6,105)
  105 FORMAT(1H1,10X,'MODAL PARTICIPATION FACTORS',////)
      DO 120 J=1,NN
  120 WRITE (6,125) J,P(J)
  125 FORMAT(10X,I2,10X,F14.7,/)
C
C
C     REFERENCE PLATE DISPLACEMENT TO THE FRAME
C
      DO 85 J = 1,N
      DO 85 I = 1,N
      V(I,J) = V(I,J) - V(14,J)
   85 CONTINUE
C
   90 FORMAT (10X,I2,5X,I2,10X,F13.7,/)
      WRITE (6,91)
   91 FORMAT(1H1,10X,'NORMALIZED EIGENVECTORS IN O. C. S.',////)
C
C     CALCULATION OF RMS AMPLITUDE OF VIBRATION
C
      CALL GRAND(WI,495,10,EXIC)
      EXIC = EXIC/495.
      WRITE(6,128)
  128 FORMAT(1H1,10X,'RMS AMPLITUDE OF VIBRATION(IN.)',////)
      WRITE(6,270) EXIC
  270 FORMAT(///,50X,'WAV(V**2/HZ) = ',2X,E12.5,/////)
      IF (W.GT.0.0) GO TO 135
      W = EXIC
  135 DO 150 I=1,NN
      SUM = 0.
```

101

```
      DO 140 J=1,NN
      XNUM = 3.1415927*(P(J)**2)*(V(I,J)**2)*(FOR(J)**2)
      DENUM = 4*Z(J)*(F(J)**3)
      FRAC = XNUM/DENUM
140   SUM = SUM+FRAC
      RMSS = W*SUM/(2.*3.141592)
      X(I) = SQRT( RMSS)
      X(I) = X(I)*165.5/AREA
150   WRITE(6,155) I,X(I)
155   FORMAT(10X,I2,10X,E14.7,/)
C
C     CALCULATION OF OUTPUT POWER SPECTRAL DENSITY
C
C     I=N IS REFERENCE FROM WHICH DISPLACEMENTS ARE MEASURED.
      DO 195 I=1,NN
      WRITE(6,180) I
180   FORMAT(1H1,50X,'MASS=',2X,I2,////)
      IF(SKIP) GO TO 100?
      DO 191 M=6,500
      HZM= FLOAT(M)
      SUM =0.
      DO 185 J=1,NN
      XNUM=(V(I,J)**2)*(P(J)**2)*(FOR(J)**2)
      RA = HZM/E(J)
      A1 =(1.-RA**2)**2
      A2 =(2.*Z(J)*RA)**2
      DENUM = (A1+A2)*(F(J)**4)
      FRAC =XNUM/DENUM
185   SUM = SUM+FRAC
      WO(M) = WI(M-5)*SUM/(2.*3.141592)
190   HZ(M-5)    = HZM
      WO(M-5)=    WO(M)*(165.5/AREA)**2
191   CONTINUE
      WRITE(6,12)   (WO(M),M=1,495)
      CALL GRAND(WO,495,1.,DUM)
      XI = SQRT(DUM)
```

```fortran
      WRITE(6,215) XI
  215 FORMAT(///,50X,.'XI(IN) =',2X,E12.5)
      READ (5,4) IAT1
      READ (5,4) IAT3
  195 CONTINUE
      CALL WEBAL(HZ,WI,497,.5,.0,.5,.0,.4,.5,7,.1,.0,.0,IAE1,5.,IAE2,5.,
     1IAE3,50)
      D(2) = (D(2)+D(3)+D(4)+D(5))/4.
      D(3) = (D(6)+D(7)+D(8)+D(9))/4.
      DO 1000 M1= 1.3
      READ(5,250) (XD(M),M = 1,495)
      WRITE(6,250)(XD(M),M = 1,495)
      DO 261 I = 1,495
      XD(I) = XD(I)*1.0.**(-6)*(165.5*D(M1))**2
      HZ(I) = FLOAT(I)+5.
  261 CONTINUE
      READ (5,4) IAX1
      READ (5,4) IAX2
      READ (5,4) IAX3
      CALL WEBAL(HZ,XD,497,.5,.0,.5,.0,.4,.5,7,.1,.0,.0,IAX1,5.,IAX2,5.,
     1IAX3,50)
 1000 CONTINUE
      CALL PLOT(0.,0.,999)
  500 STOP
      END
```

103

```
C       SUBROUTINE DECMPS (N, NA, A, EXIT)
        C------------------------------------
        C     N    =   SQUARE MATRIX SIZE
        C     NA  =ACTUAL MATRIX SIZE
        C     A    =   SQUARE MATRIX
        C     EXIT =   ERROR MESSAGE NUMBER
        C
              DIMENSION A(NA,NA)
              REAL*8 SUM, DBLE
              EXIT = 0.0
              DO 6 I = 1,N
              IM1 = I - 1
              DO 6 J = I,N
              SUM = A(I,J)
              IF (I .LT. 2) GO TO 2
              DO 1 K = 1,IM1
        1     SUM = SUM - DBLE(A(K,I)) * DBLE(A(K,J))
        2     IF (J .NE. I) GO TO 3
              GO TO 4
        3     A(I,J) = SUM * TEMP
              GO TO 6
        4     IF (SUM) 7, 7, 5
        5     DUM = SUM
              TEMP = 1.0 / SQRT(DUM)
              A(I,J) = TEMP
        6     CONTINUE
              RETURN
        7     EXIT = 1.0
              WRITE(6,12)
        12    FORMAT(1X,'SCREWED UP',///)
              WRITE(6,10) I,J,SUM
        10    FORMAT(10X,I2,5X,I2,5X,E14.7,/)
              RETURN
              END
```

```
      SUBROUTINE INVERT (N, NA, U)
C     -------------------------------
C
      DIMENSION U(NA,NA)
      REAL*8 SUM, DBLE
C
C     U  =   UPPER TRIANGULAR MATRIX (FROM DECMPS)
C     N  =   SQUARE MATRIX SIZE
      DO 2 I = 1,N
      IP1 = I + 1
      IF (IP1 .GT. N) GO TO 22
      DO 2 J = IP1, N
      JM1 = J - 1
      SUM = 0.0
      DO 1 K = I,JM1
    1 SUM = SUM - DBLE(U(K,I)) * DBLE(U(K,J))
    2 U(J,I) = SUM * U(J,J)
   22 DO 4 I = 1,N
      DO 4 J = I,N
      SUM = 0.0
      DO 3 K = J,N
    3 SUM = SUM + DBLE(U(K,I)) * DBLE(U(K,J))
      U(J,I) = SUM
    4 U(I,J) = U(J,I)
      RETURN
      END
```

```
      SUBROUTINE GRAND(A,NA,DELTA,AREA)
C     --------------------------------------
C
      DIMENSION A(NA)
      AREA = 0.
      H = DELTA/3.
      N = NA-2
      DO 1 I = 1,N,2
    1 AREA = AREA+H*(A(I)+4.*A(I+1)+A(I+2))
      RETURN
      END
```

```
      SUBROUTINE WEBAL(X,Y,NP2,XO,YO,XB,YB,XL,YL,K,J,KHAR,TIT1,I1,
     1TIT2,I2,TIT3,I3)
C
C -----------------------------------------------------
C
      DIMENSION X(NP2),Y(NP2),TIT1(I1),TIT2(I2),TIT3(I3)
      COMMON ID9(15),BUF(3000)
      CALL PLOT(-.5,-.5,3)
      CALL PLOT(-.5,8.,5,2)
      CALL PLOT(5.5,8.,5,2)
      CALL PLOT(5.5,-.5,2)
      CALL PLOT(-.5,-.5,2)
      N = NP2-2
      CALL SCALE(X,XL,N,K)
      CALL SCALOG(Y,YL,N,K)
      CALL AXIS(XO,YO,ID9,-35,XL,0.,X(N+1),X(N+2))
      CALL LGAXIS(XB,YB,1H ,1,YL,90.,Y(N+1),Y(N+2))
      CALL LGLINE(X,Y,N,K,J,KHAR,1)
      CALL SYMBOL(0.,8.2,.14,TIT1,0.,I1)
      CALL SYMBOL(0.,8.,.14,TIT2,0.,I2)
      CALL SYMBOL(0.,7.8,.14,TIT3,0.,I3)
      CALL PLOT(-.5,7.,5,3)
      CALL PLOT(5.5,7.,5,2)
      CALL PLOT(12.+XO,YO,-3)
      RETURN
      END
```

```
      SUBROUTINE JACOB( D,QT,NQ,A,NA,N,IORD )
C     --------------------------------------------
      DIMENSION A(NA,N),QT(NQ,N),D(N)
      DATA EPS/1.E-8/
      DO 310 K=1,N
      D(K)=A(K,K)
      DO 311 M=1,N
  311 QT(K,M)=0.0
  310 QT(K,K)=1.
      IT=0
      SUM=0.0
      DO 505 I=1,N
      DO 505 J=1,N
  505 SUM = SUM + ABS(A(I,J))
  500 IF(IT-1)510,511,512
  510 TH=SUM/(N*N)
      GO TO 515
  511 TH=TH/N
      GO TO 515
  512 TH =0.0
  515 IT=IT+1
      E=0.0
      NM1=N-1
      DO 10 J=1,NM1
      JM=J+1
      DO 10 I=JM,N
      IF(ABS(A(I,J)).LT.TH) GO TO 10
      L=I
      M=J
      IF(ABS(A(L,M)).LE.EPS*(ABS(D(L))+ABS(D(M)))) GO TO 50
      BETA=(D(L)-D(M))*.5/A(L,M)
      T=1./(BETA+SIGN(SQRT(BETA**2+1.),BETA))
      C2=1./(1.+T*T)
      C=SQRT(C2)
      S=T*C
```

```
      TAU=S/(1.+C)
      T=T*A(L,M)
      E=E+ABS(A(L,M))
      MM=M-1
      MP=M+1
      LM=L-1
      LP=L+1
      IF(MM.LE.0) GO TO 101
      DO 100 K=1,MM
      DUM1=A(M,K)
      DUM2=A(L,K)
      A(M,K)=DUM1-S*(DUM2+DUM1*TAU)
  100 A(L,K)=DUM2+S*(DUM1-DUM2*TAU)
  101 IF(MP.GT.LM) GO TO 202
      DO 200 K=MP,LM
      DUM1=A(K,M)
      DUM2=A(L,K)
      A(K,M)=DUM1-S*(DUM2+DUM1*TAU)
  200 A(L,K)=DUM2+S*(DUM1-DUM2*TAU)
  202 IF(LP.GT.N) GO TO 303
      DO 300 K=LP,N
      DUM1=A(K,M)
      DUM2=A(K,L)
      A(K,M)=DUM1-S*(DUM2+DUM1*TAU)
  300 A(K,L)=DUM2+S*(DUM1-DUM2*TAU)
  303 D(M)=D(M)-T
      D(L)= D(L)+T
      DO 400 K=1,N
      DUM1=QT(K,M)
      DUM2=QT(K,L)
      QT(K,M)=DUM1-S*(DUM2+DUM1*TAU)
  400 QT(K,L)=DUM2+S*(DUM1-DUM2*TAU)
   50 A(L,M)=0.0
   10 CONTINUE
      IF(E.GT.0.0) GO TO 500
      IF(IT.LE.2) GO TO 512
```

```
      DO 306 I=1,N
      DO 306 J=1,N
  306 A(J,I)=A(I,J)
      IF( IORD .EQ. 00 )    RETURN
      FORD = FLOAT(IORD)
      DO 410 I=1,NM1
      IP1=I+1
      IMIN=I
      DO 405 J=IP1,N
  405 IF( (D(IMIN)-D(J))*FORD .GT. 0.0 ) IMIN = J
      IF(IMIN.EQ.I) GO TO 410
      TEMP=D(IMIN)
      D(IMIN)=D(I)
      D(I)=TEMP
      DO 415 J=1,N
      TEMP=QT(J,IMIN)
      QT(J,IMIN)= QT(J,I)
  415 QT(J,I)= TEMP
  410 CONTINUE
      RETURN
      END
```

110

SAMPLE CALIBRATION CALCULATION

Calculation of Constant $\underline{A}$:

$$\Delta R_5 = R_G - \frac{R_G \, R_P}{R_G + R_P}$$

$$\Delta R_5 = 120.8 - \frac{120.8 \ (50,000)}{120.8 + 50,000}$$

$$\Delta R_5 = 120.8 = 120.51$$

$$\Delta R_5 = .29$$

$$\frac{\Delta R}{V} = \frac{.29 - .07}{1.051 - .254} = \frac{.22}{.797} = .276$$

$$\frac{\Delta R}{V} = \frac{.27 - .07}{1.056 - .246} = \frac{.22}{.810} = .2715$$

$$\frac{\Delta R}{V} = \frac{.29 - .07}{1.041 - .2335} = \frac{.22}{.807} = .273$$

$$A = \frac{\Delta R}{V} \ \Big| \ \text{average} = (.276 + .2715 + .273) \ /3 = .274$$

Calculation of Constant $\underline{B}$:

$$B = \frac{1}{RF} = \frac{1}{120.8 \ (1.98)} = .00418$$

Calculation of Constant $\underline{C}$:

From mass number one, L = 20 pounds force,

$t = 10,000 - 9,876 = 124 \times 10^{-6}$ (in/in)

$$C = \frac{L}{t} = \frac{20}{124 \times 10^{-6}} = .1538 \times 10^{6}$$

From mass number two, L = 20 pounds force,

$t = 10,000 - 9,859 = 141 \times 10^{-6}$ (in/in)

$$C = \frac{L}{t} = \frac{20}{141 \times 10^{-6}} = .142 \times 10^{6}$$

From mass number three, L = 20 pounds force,

$t = 5,000 - 4,856 = 144 \times 10^{-6}$ (in/in)

$$C = \frac{L}{t} = \frac{20}{144 \times 10^{-6}} = .14 \times 10^{6}$$

C average = $(.14 + .142 + .1538) \times 10^{6}/3 = .144 \times 10^{6}$

A x B x C = $.274 \times .00418 \times .144 \times 10^{6} = 165.5$

REFERENCES

1. Van Lear, G. A., Jr., and G. E. Uhlenbeck. "The Brownian Motion of Strings and Elastic Rods." Physics Review, Vol. 38, 1931, pp. 1538-1598.

2. Lyon, R. H. "Response of Strings to Random Noise Fields." Journal of the Acoustical Society of America, Vol. 28, 1956, pp. 391-398.

3. Eringen, A. C. "Response of Beams and Plates to Random Loads." Journal of Applied Mechanics, Vol. 24, 1957, pp. 46-52.

4. Thomson, W. T. and M. V. Barton. "The Response of Mechanical Systems to Random Excitations." Journal of Applied Mechanics, Vol. 24, 1957, pp. 248-251.

5. Powell, A. "On the Fatigue Failure of Structure Due to Vibrations Excited by Random Pressure Fields." Journal of the Acoustical Society of America, Vol. 30, 1958, pp. 1130-1135.

6. Samuels, J. C. and A. C. Eringen. "Response of a Simply Supported Timoshenko Beam to a Purely Random Gaussian Process." Journal of Applied Mechanics, Vol. 25, 1958, pp. 496-500.

7. Dyer, I., "Response of Space Vehicle Structures to Rocket Engine Noise." Random Vibration, The M.I.T. Press, Cambridge, Massachusetts, 1963.

8. Dyer, I., "Response of Plates to a Decaying and Convecting Random Pressure Field." Journal of the Acoustical Society of America, Vol. 27, 1959, pp. 922-928.

9. Bogdanoff, J. L., and J. E. Goldberg. "On the Bernoulli-Euler Beam Theory with Random Excitation." Journal of Aerospace Science, Vol. 27, 1960, pp. 371-376.

10. Lin, Y. K., "Nonstationary Response of Continuous Structures to Random Loading." Journal of the Acoustical Society of America, Vol. 35, 1963, pp. 222-227.

11. Lin, Y. K., Probabilistic Theory of Structural Dynamics, McGraw-Hill Book Company, New York, New York, 1967.

12. Barnoski, R. L., "The Maximum Response of Rectangular Plates to Random Excitation." The National Aeronautics and Space Administration, N67-37031, Washington, D. C., 1967.

13. Seireg, A., Mechanical Systems Analysis, International Textbook Company, Scranton, Pennsylvania, 1969.

14. Miles, J. W., "On Structural Fatigue Under Random Loading." Journal of the Aeronautical Sciences, Vol. 21, No. 11, November, 1954, pp. 753-762.

15. James, H. M., "Theory of Servomechanisms." M.I.T. Radiation Laboratory Series, Vol. 25, McGraw-Hill, New York, 1947.

16. Weaver, W., Jr., Computer Programs for Structural Analysis, D. Van Nostrand Company, Inc., Princeton, New Jersey, 1967.

17. Bruel and Kjaer, "Peak Distributions of Random Signals." Technical Review, No. 3, K. Larsen and Son, Naerum, Denmark, 1963.

18. Wilkinson, J. H., The Algebraic Eigenvalue Problem, Oxford University Press, 1965.

19. Tse, F.S., I. E. Morse, and R. T. Hinkle, Mechanical Vibrations, Allyn and Bacon, Inc., Boston, Massachusetts, 1964.

20. Rutishauser, H., "The Jacobi Method for Real Symmetric Matrices." Numerische Mathematik 9, Springer-Verlag, New York, New York, 1966, pp. 1-10.

21. Seto, W. W., "Schaum's Outline of Theory and Problems of Mechanical Vibrations." Schaum's Outline Series, McGraw-Hill Book Company, New York, 1964.

22. Mix, D. F., Random Signal Analysis, Addison-Wesley Publishing Company, Reading, Massachusetts, 1969.

23. Morse, P. M., Vibration and Sound, McGraw-Hill, 1948.

24. Plunkett, R., "Damping Definitions and Classifications." Lecture presented at the meeting of the Acoustical Society of America, Cleveland, Ohio, November, 1968.

114

25. Brüel and Kjaer, "Measurement of Modulus of Elasticity and Loss
    Factor for Solid Materials." Technical Review, No. 2,
    K. Larsen and Son, Naerum, Denmark, April, 1958.

26. Lin, Y. K., "Response of Multi-Spanned Beam and Panel Systems
    Under Noise Excitation." Air Force Materials Laboratory
    Research and Technology Division Air Force Systems Command,
    Wright-Patterson Air Force Base, Ohio, February, 1965.

27. McDaniel, T. J. and B. K. Donaldson, "Free Vibration of Continuous
    Skin-Stringer Panels with Non-Uniform Stringer Spacing and
    Panel Thickness." Air Force Materials Laboratory Research
    and Technology Division, Air Force Systems Command, Wright-
    Patterson Air Force Base, Ohio, February, 1965.

28. Crandall, S. H. and W. D. Mark, Random Vibration in Mechanical
    Systems, New York Academic Press, 1963.

29. Roberts, J. B., "The Response of a Simple Oscillator to Band-
    Limited White Noise." Report No. 65/3, University College
    London, England, Department of Mechanical Engineering, London,
    W.C.T., May, 1965.

30. Seireg, A. and L. Howard, "An Approximate Normal Mode Method
    for Damped Lumped Parameter Systems." Journal of Engineering
    for Industry, Transactions of the ASME, November, 1967.

31. Lord Rayleigh, Theory of Sound, Vol. 1, Dover Publications,
    New York, New York, 1945.

32. Caughey, T. K., "Classical Normal Modes in Damped Linear
    Dynamic Systems." Journal of Applied Mechanics, Vol.
    27, Transactions of the ASME, Vol. 82, Series E, 1960,
    p. 269.

33. Foss, K. A., "Coordinates Which Uncouple the Equations of Motion
    of Damped Linear Dynamic Systems." Journal of Applied
    Mechanics, Vol. 25, Transactions of the ASME, Vol. 80, 1958,
    p. 361.

Page intentionally left blank

Page intentionally left blank

Page intentionally left blank

Page intentionally left blank